University of Stavanger

Faculty of Science and Technology

MASTER'S THESIS

Study program/ Specialization: MSc. Petroleum Technology / Drilling Engineering	Spring semester, 2014. ~~Open~~ / Restricted access
Writer: Muhammad Jahanzeb Hashmi	………………………………………… (Writer's signature)
Faculty supervisor: Dan Sui External supervisor(s): Seyed Ahmad Mirhaj (Aker Solutions)	
Thesis title: Sensitivity Analysis of Factors Affecting Torque and Drag Modelling.	
Credits (ECTS): 30	
Key words: Sensitivity analysis, torque and drag, viscous drag, hydrodynamic viscous drag.	Pages: 83 + enclosure: 2CDs Stavanger, 16 June 2014 Date/year

Abstract

As the modern day extended reached wells are getting longer and more complex, the torque and drag is one of the restraining aspects for achieving the target depth. Torque and drag becomes a precarious issue, for example it can be difficult to land the long completion string. Therefore, understanding the friction in the wellbore and how it affects hook load and torque is essential for well path design in planning phase as well as for real time monitoring analysis and post analysis. In planning phase the offset well torque and drag profiles will be used to better well planning. In real time monitoring the torque and drag roadmaps will be used as the well is drilling in order to warn us about upcoming potential drilling problems. In post analysis the torque and drag profiles will be analyzed in order to optimize the well path and drillstring design of new wells in the same area.

There are some confusion about torque and drag software and validity of models that are used to characterize drilling operation, especially as the well trajectory is getting more complex.

The objective of this study is to perform a sensitivity analysis on different parameters that affect torque and drag in drilling wellbores. The parameters that will be investigated in this project are those which are place of negotiation among individuals; in a way that some of them believe the effect of such parameters are negligible whereas some have opinion that effects of these parameters must be taken into account. These parameters are:

Extra friction due to sheave

Friction due to hydrodynamic viscous drag force

Effect of weight on bit (WOB) on torque

In order to carry out this study Landmark WellPlan software has been used. For the effect of viscous drag forces Kristian Gjesrstad's medium-order flow model for dynamic pressure surges (Gjerstad, March 2013) was used to compare the results obtained from WellPlan. The Gjerstad's model takes into account the effects of combined axial and rotational movement of pipe as well as the flow regimes.

Table of Contents

Acknowledgement

List of figures

List of tables

Nomenclature

A_i = Inner cross sectional area

A_o = Outer cross sectional area

BHA = Bottomhole Assembly

e = Sheave efficiency

ERD = Extended Reach Drilling

ERW = Extended Reach Well

D_s = Diameter of string

D_w = Diameter of wellbore

DL = Dogleg

DLS = Dolgleg severity

F_D = Drag force

F_f = Friction force

F_N = Normal or Side force

F_t = Axial tension acting at lower end of string

ΔF_t = increase in tension over length of element

M = Torsion at the lower end of element

r = Characteristic radius of drillstring element

ΔL = Length of segment

W = Weight of element

W_b = Buoyed weight of element

β = Buoyancy factor

μ = Friction coefficient

ρ = Density

α = Azimuth

τ_w = Wall shear stress

Θ = Inclination

σ = Tension

1 Introduction

As the modern day drilling is getting longer and longer, the drillstring torque and drag is one of the restraining aspects for achieving the target depth. Torque and drag models are used in the planning phase but also in real time drilling to evaluate the problems if any encountered during drilling. For this purpose it is very important to use the models that are accurate and to know their limitations. There are number of parameters that can affect the torque and drag profiles. The hydrodynamic viscous drag effect is one of the important factors which affect the torque and drag. The torque and drag models that are currently used in industry are mostly based on Johancsik's model (Johancsik, 1984), presented in 1984. There might be no robust model available that can determine the exact effects of hydrodynamic viscous drag on torque and drag. In a planning and ERW there is need of determining the exact amount of friction that can encounter during the course of drilling. The effects of following factors on torque and drag have been analyzed in this thesis:

1. Sheave friction
2. Hydrodynamic viscous drag force
3. Weight on Bit.

The simplified model was used which is based on Kristian Gjerstad's medium-order flow model for dynamic pressure surges, (Gjerstad, March 2013) for analyzing viscous drag effects on hook load, for the comparing the results for hydrodynamic viscous drag forces obtained from WellPlan.

2 Torque and drag fundamentals

This chapter deals with the basic theory behind the torque and drag and various parameters that affects torque and drag modelling. In this section deliberation on existing torque and drag models along with literature review will be given.

2.1 Torque and drag theory

The general theories of torque and drag modelling will be discussed here, including the fundamental physics and explanations of factors that affect the torque and drag.

2.1.1 Drag

Drag refers to the force difference between the free rotating weight and the force required to axially move the drillstring up or down in the wellbore. For deviated wells the pick-up drag is higher and slack off drag normally lower than the free rotating weight. In vertical wellbores pick-up, slack off and free rotating weight are all normally the same. Figure 2-1 shows the schematics of friction in deviated wellbore.
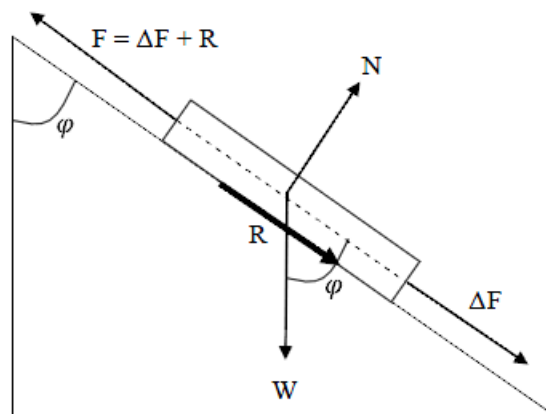
Figure 2-1 Friction in a deviated well

2.1.2 Torque

Torque is moment or moment of force to rotate drillstring. The moment is used to overcome the rotational friction in the well and on the bit. In deviated wellbores there is a significant reduction in the magnitude from the rotating string so that less amount of torque is available on bit for crushing the rock. In perfect vertical wells there is almost zero torque loss, apart from minor

torque loss due to viscous forces from drilling fluid. Figure 2-2 shows the schematics for torque to rotate the drillstring.
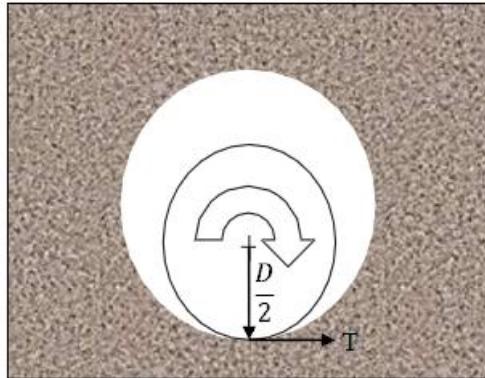
Figure 2-2 Torque to rotate the drillstring

2.2 Factors affecting torque and drag

There are number of parameters/effects that influence torque and drag. Some of them can be modelled while others cannot. The effects that cannot be modelled are lumped together into a fudge factor commonly known as friction factors. The friction factors varies from openhole to cased hole and from region to region. Below is the detailed explanation of these effects and parameters.

2.2.1 Drillstring and BHA

Drag is directly related to drillstring weight. Therefore use of low weight pipes in a long ERW is beneficial. In the other hand the low weight pipes might not weight enough to overcome the friction and drill further in long ERW. As a result an optimum evaluation of drillstring design should be considered. Stiff BHA and stabilizers can interact with formation resulting in higher friction particularly in a high dogleg section. If the surface of drillstring is rough it will add in the friction hence higher torque and drag.

2.2.2 Well path and profile

Well path and profile have major effects of torque and drag. The factors that affect the torque and drag because of well path are explained below.

2.2.2.1 **Dogleg severity:** Dogleg severity is a measure of the amount of change in the inclination and/or azimuth of borehole, is usually measured in degrees per 100 feet or degrees per 30 meters. If dogleg severity is high one can expect the higher friction due to BHA and drillstring stiffness. Figure 2-3 shows the effects of dogleg.

$$DL = \frac{180\,|\theta|}{\pi} \qquad\qquad\qquad (2\text{-}1)$$

$$DLS = \frac{DL}{\Delta L} 30 \qquad\qquad\qquad (2\text{-}2)$$

Figure 2-3 Dogleg effect

2.2.2.2 **Contact surface:** Contact surface refers to the interaction of borehole walls with drillstring and BHA. In deviated wellbores while moving up, drillstring interacts with upper wall of the wellbore normally in build sections and while moving down, drillstring slides over the lower wall. In either case it gives rise to the friction.

2.2.3 Drilling fluid

Drilling fluid can effect torque and drag in many ways depending on properties of drilling fluid.

2.2.3.1 **Type of drilling fluid:** Generally OBM has more lubricating characteristic than WBM. So using OBM will yield less friction and hence low torque and drag compared with WBM, although some lubricants may cause formation damage and can reduce the well inflow performance.

2.2.3.2 **Rheological properties and hydrodynamic viscous forces:** The rheology of drilling fluid is main factor that creates the hydrodynamic viscous forces. These forces can directly superimpose on torque and drag. Depending upon the well trajectory and rheology, these forces either reduce or increase the magnitude of torque and drag or. The detail explanation about these effects will be discussed in chapter 3 and 4.

2.2.3.3 **Drilling fluid density:** Fluid density differences during tripping in due to pipe filling intervals affects the increase the drag because of buoyancy effects. See section2.3 Buoyancy factor.

2.2.4 Formation effects

2.2.4.1 **Formation Properties:** Different formation lithologies have different lubricating properties due to chemical composition and grain size. The coarse grained formations give high friction when drillstring is moved against their walls as compared to fine grained formations.

2.2.4.2 **Wellbore Stability:** Differential sticking, swelling shale, tight hole and sloughing shale all give rise to frictions in wellbore and hence to torque and drag. Loss of circulation can also increase the friction due to loss of lubricity. Figure 2-4 and Figure 2-5 shows the mechanism of differential sticking and shale formations respectively.
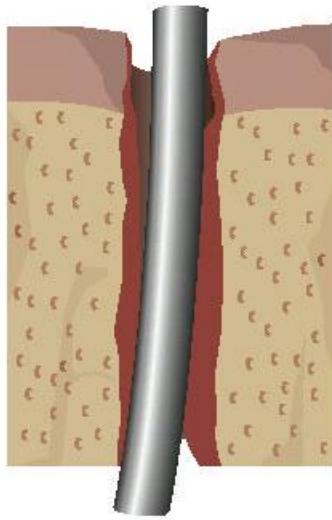
Figure 2-4 Differential Sticking
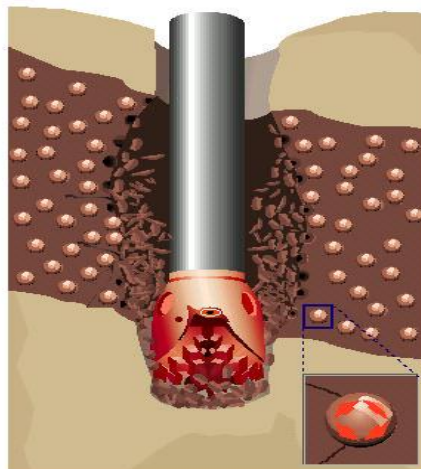
Figure 2-5 Shale formation

2.2.5 Hole cleaning

If the hole is not properly cleaned due to improper cuttings transport and medium to high angle well sections, cuttings bed can be formed in high angle section and cuttings can accumulate in form of dunes at the tip of medium angle section. This could yield in minor to severe pack-off situations which of course cause high drag and torque. The presence of cuttings in fluid flow system also gives rise to in friction. Figure 2-6 shows the cuttings accumulation behavior in ERWs.
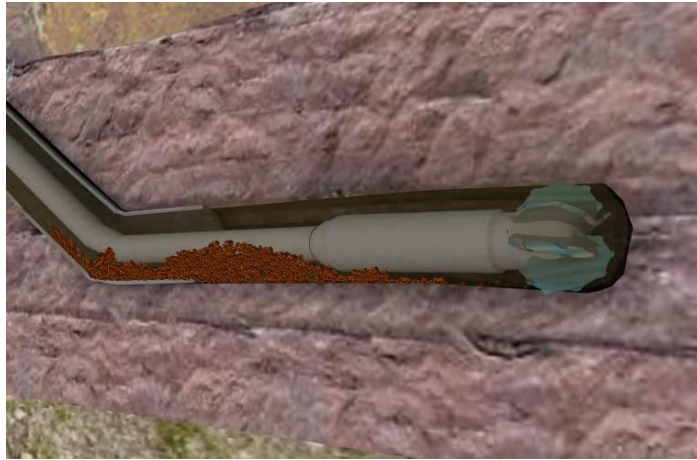
Figure 2-6 Cuttings accumulation in ERW

2.3 Buoyancy factor

Buoyancy is an upward force exerted by a fluid that opposes the weight of an immersed object. In a fluid column, pressure increases with depth as a result of the weight of the overlying fluid. Thus a column of fluid, or an object submerged in the fluid, experiences greater pressure at the bottom of the column as of at the top. The figure below shows the concept of buoyancy on for an immersed object in fluid.
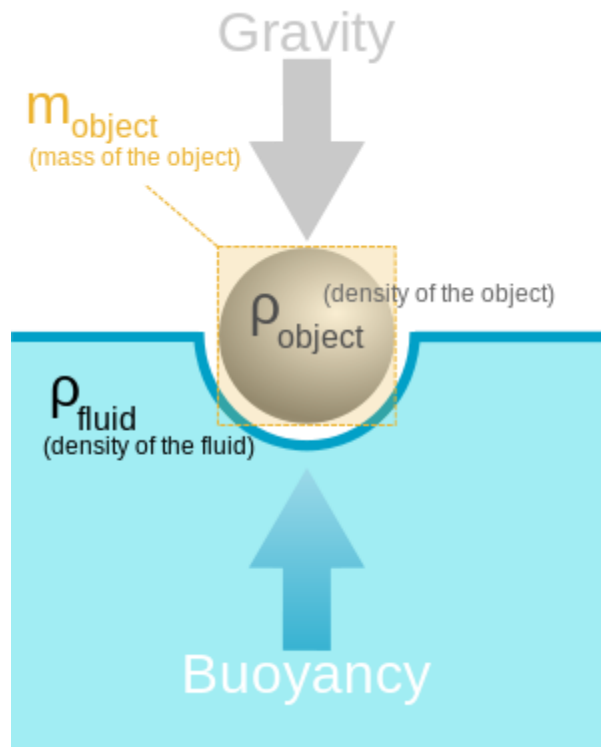
Figure 2-7 Buoyancy effects

In the well filled with drilling fluid/mud, the weight of drillstring is the weight in air minus the mud weight that the steel in the string displaces, this phenomenon is Archimedes principle. The buoyancy factor can be defined conveniently as:

$$\beta = 1 - \frac{\rho_{mud}}{\rho_{string}} \tag{2-3}$$

If there is different densities of fluid inside and outside the pipe for example during tripping in, during displacement of mud to new mud and while cementing, the buoyancy factor can define as:

$$\beta = 1 - \frac{\rho_o A_o - \rho_i A_i}{\rho_{string} (A_o - A_i)} \tag{2-4}$$

Where:

β = Buoyancy factor

ρ_{mud} = Density of drilling mud/fluid

ρ_{string} = Density of drillstring normally density of steel

ρ_o = Density of fluid outside the pipe

ρ_i = Density of fluid inside the pipe

A_o = Outer cross sectional area

A_i = Inner cross sectional area

A heavy mud will decrease the effective weight of the drillstring, and thus decrease side force and the load from friction and torque. However a heavy mud has more weighing particles which could lead to less lubricity and therefore higher friction.

2.4 Friction

Contact friction as when two relatively smooth solid bodies slide against each other will be independent of the speed the two bodies slide against, and independent of the contact area, only for soft string model being under consideration but friction force will be proportional to the contact force of which the surfaces are slided against. A friction coefficient, μ is the ratio of friction force to normal force. In order to find the normal force in an inclined plane consider the schematics shown in Figure 2-8.

$$\mu = \frac{F_f}{F_N} \tag{2-5}$$
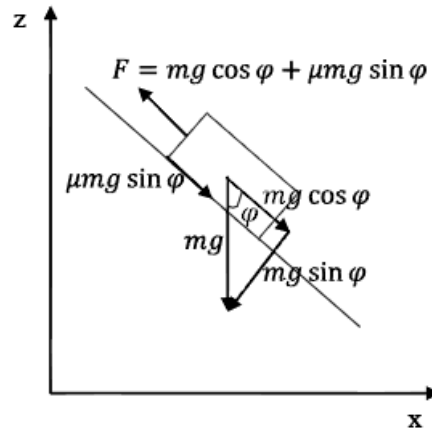
Figure 2-8 Forces on a block sliding on an inclined plane

Where

μ= friction coefficient

F_f = Friction force

F_N = Normal force

The friction coefficient gives friction force as percentage of the normal force. The direction of friction is always opposite the direction of movement.
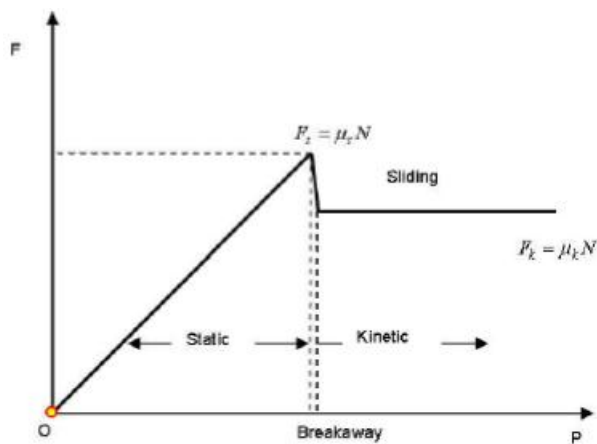
Figure 2-9 Static and dynamic friction

When the two bodies are at rest we have static friction, which normally is higher than sliding friction. This is shown in Figure 2-9. This is due to interlocking of irregularities of the two surfaces. Static friction will resist motion and counteract any applied force up to a certain maximum where friction is overcome and motion begins. Once the object is in motion, the dynamic friction will

resist motion. Coefficients for static and dynamic friction are not equal. Torque and drag models use only dynamic friction effects.

The friction factor is a key parameter in torque and drag modeling because it characterizes the surface to surface interaction which is the heart of model. The friction factor applicable to any situation is a function of many things, including fluid type, composition and lubricity, formation type, casing and tool joint material and roughness. When significant portions of both cased and open hole exists, it may be necessary to use more than one friction factors, normally two one for openhole and one for cased hole. Generally the friction factors selected are 0.2 and 0.3 for cased and openhole respectively. But in real time operations these friction factors are calibrated regularly during the operations.

3 Torque and drag models

Commonly used torque and drag models will be discussed together with historical evolution of these models. Since most of work for this thesis has been done using Halliburton Landmark WellPlan software, the theories and calculations that are used in WellPlan will also be discussed. Also model for hydrodynamic viscous forces will be discussed here.

3.1 Johancsik torque and drag model

In 1984 C.A. Johancsik presented the pioneer friction analysis model. In his model both torque and drag were assumed to be caused entirely by sliding friction between drillstring and borehole wall. Other sources of torque and drag like friction due to fluid and cuttings, static friction and piston forces were not considered. [1]

The sliding friction coefficient is the ratio of friction force to the normal contact force. The following set of equations represent the mathematical model and steps for determining the torque and drag forces.

$$F_N = [(F_t \, \Delta \alpha \, sin\theta)^2 + (F_t \, \Delta\theta + W \, sin\theta)^2]^{1/2} \qquad \text{(3-1)}$$

The normal force leads to the equation for tension increments.

$$\Delta F_t = W \, cos\theta \, \pm \, \mu F_N \qquad \text{(3-2)}$$

Torsion increment:

$$\Delta M = \, \mu F_N \, r \qquad \text{(3-3)}$$

In Equation (3-2) plus and minus signs are for tripping out and tripping in respectively. Figure 3-1 shows the forces acting on drillstring element.
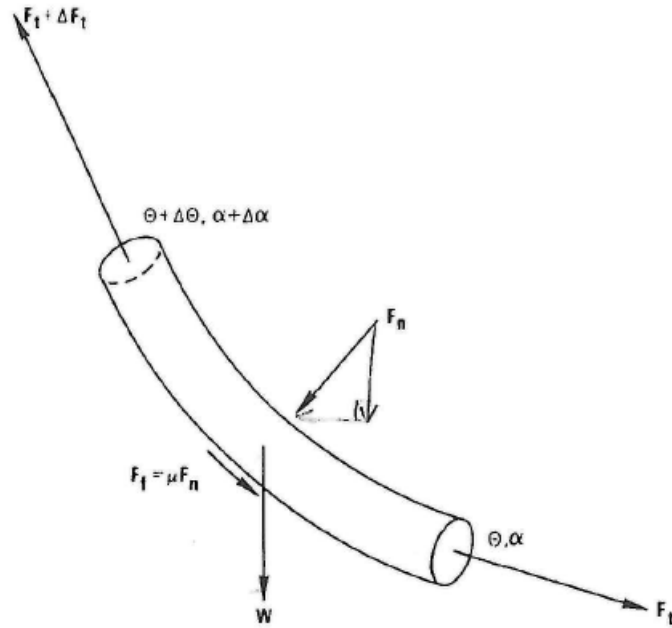
Figure 3-1 Forces acting on drillstring element during pickup.

3.2 Sheppard model

In 1987 Sheppard et al. put the Johancsik model into standard differential form and also took the mud pressure into account that acts upward so instead of using true tension he used effective tension. [2]

He presented the friction model in order to estimate the torque and drag in different well geometries. This model was based on assumption that the drag force on the drillstring at any location is proportional to side force acting there. The coefficient of proportionality, K is the sliding friction coefficient in the model.

He proposed the use of effective tension $\sigma_e(S)$, which is the sum of true tension $\sigma(S)$, and product of mud pressure acting at S and the cross-sectional area of the pipe. S is the distance along the well path from the bit.

$$\sigma_e(S) = \delta(S) + P(S)A(S) \tag{3-4}$$

The tension profile can be derived from σ_e profile, which is given by

$$\frac{\partial \sigma_e}{\partial S} = W_b \cos\theta(S) \pm K \left\{ \left[\sigma\frac{\partial\theta}{\partial S} + W_b \sin\theta(S)\right]^2 + \left[\sigma_e \frac{\partial\beta}{\partial S}\sin\theta(S)\right]^2 \right\}^{1/2} \tag{3-5}$$

In Equation (3-5) W_b is the buoyed weight per unit of the drillstring. The + K applies for tripping out, while – K for tripping in.

From Equation (3-4), the drag profile F(S) can be derived as.

$$F(S) = K\{[\sigma_e(S)\frac{\partial \theta}{\partial S} + W_b \sin \theta(S)]^2 + [\sigma_e(S)\frac{\partial \beta}{\partial S}\sin \theta(S)]^2\}^{1/2} \tag{3-6}$$

In case of rotation the drag is considered to act at an appropriate radius giving rise to a local torque loss. The total torque loss is the sum of these contributions.

3.3 Review summary of works

After Sheppard et al. (1987) drag model, Maidla and Wojtanowicz (1987) [3], Lesage et al. (1988) [4], Brett et al. (1989) [5], Lesso er al. (1989) [6], Aarrestad (1990) [7], Wilson et al. (1992) [8], Alfsen et al. (1993) [9], and Rae et al. (2005) [10], all performed a field case study on torque and drag analysis with Johancsik's model (1984) with the evaluating effects of various parameters.

Luke and Juvkam-Wold (1993) [11], investigated the effect of sheave friction in the block and tackle system of drilling line and they concluded that hook load is also dependent upon deadline tension, number of lines as well as sheave efficiency and block movement direction. They predicted the effect of sheave friction to be as much as 19% on hook load.

Maidla and Wojtanowicz (1987) [12] presented a new procedure for predicting a drag force in wellbore. The model considered the effects of hydrodynamic viscous drag, contact surface and dogleg angle.

Aarrestad (1994) [13] discussed the benefits of using the catenary well profile. This work was the continuation of proposal of catenary profile (Sheppard, 1987).

Aadnøy (2006) [14] derived the mathematical equation for the catenary well profile and applied them in a field case study on an ultra-long well, and compered the results with the results that obtained from conventional well. Based on his study he proposed that 15 KM horizontal departure wells can be drilled using the existing equipment and modern drilling units available at that time.

Aadnøy (2008) [15] developed a generalized model for torque and drag which accounted for torque and drag in bends.

3.4 Models that are used in WellPlan

Landmark WellPlan (Halliburton) software had been used for analyzing torque and drag behavior, hence it is important to give the overview of the models [16].

3.4.1 Axial force calculations

WellPlan uses two methods for calculating axial force, buoyancy method and pressure area method.

3.4.1.1 Buoyancy method

$$F_{axial} = \sum[LW_{air} \cos(inc) + F_D + \Delta F_{area}] - F_{bottom} - W_{WOB} + F_{BS} \qquad (3\text{-}7)$$

3.4.1.2 Pressure area method

$$F_{axial} = \sum[LW_{air} \cos(inc) + F_D + \Delta F_{area}] - F_{bottom} - W_{WOB} \qquad (3\text{-}8)$$

Where:

L = Length of drillstring hanging below point (ft)

W_{air} = weight per foot of the drillstring in air (lb/ft)

inc = Inclination (deg)

F_{bottom} = Bottom pressure force, a compression force due to fluid pressure applied over the cross sectional area of the bottom component

F_{area} = Change in force due to a change in area at junction between two components of different cross sectional areas, such as the junction between drill pipe and heavy weight or heavy weight and drill collar. If the area of the bottom component is larger the force is a tension, if the top component is large the force is compression.

W_{WOB} = Weight on bit (lb), (0 for tripping in and out)

F_D = Drag force (lb)

F_{BS} = Buckling Stability Force = External Pressure x External Area – Internal pressure x Internal Area

3.4.2 Buoyed weight calculations

The buoyed weight is used to determine the forces and stresses acting on the work string in the analysis.

$$W_{buoy} = W_{air} - W_{fluid} \qquad (3\text{-}9)$$

$$W_{fluid} = (MW_{annular} x\ A_{external}) - (MW_{internal}\ x\ A_{internal}) \qquad (3\text{-}10)$$

Where:

$A_{external}$ = External area of the component

$A_{internal}$ = Internal area of the component

W_{fluid} = Weight per foot of displace fluid

W_{buoy} = Buoyed weight of per foot of the component

$MW_{annular}$ = Annular mud weight at component depth in the wellbore

$MW_{internal}$ = Internal mud weight at component depth inside the component.

3.4.3 Curvilinear model

For a torque and drag analysis, the work string is divided into 30-feet section. The straight model assumes each section is of constant inclination. The curvilinear model takes into account the inclination (build or drop) change within each 30-feet section.

In hole sections where there is an angle change, compression in the pipe through the doglegs causes extra side force. The additional side force acts to stabilize the pipe against buckling. The exception to this is where the pipe is dropping angle.

$$F_c > 2 \left(\sqrt{\frac{EIW_c}{v}} \right) \qquad (3\text{-}11)$$

$$W_c = 2 \sqrt{((W\ \sin(inc) + F\ \varphi')^2\ ) + F\ \sin^2(inc)\varphi'^2\ )} \qquad (3\text{-}12)$$

Where:

F = Compressive axial force

F_c = Critical buckling force

I = Moment of inertial component

E = Young's modulus of elasticity

W = Tubular weight in mud

inc = Wellbore inclination

φ' = Radial clearance between the wellbore and component

W_c = Contact load

3.4.4 Drag force calculations

Drag force is calculated using the following equation:

$$F_D = F_N \mu \frac{|T|}{|V|}$$ (3-13)

Where:

$|T|$ = Tripping speed

$|V|$ = Resultant velocity = $\sqrt{(T^2 + A^2)}$

A = Angular speed

F_N = Side or normal force

μ = Coefficient of friction

F_D = Drag force

3.4.5 Sheave friction correction calculations

Sheave friction correction calculation is given below

$$L_r = \frac{n\,(e-1)\,(H_r + W_{tb})}{e\left(1 - \frac{1}{e^n}\right)}$$ (3-14)

$$L_l = \frac{n\,(1-e)(H_l + W_{tb})}{(1 - e^n)}$$ (3-15)

Where:

L_r = Weight indicator reading while raising

L_l = Weight indicator reading while lowering

H_r = Hook load while raising, calculated in analysis

H_l = Hook load while lowering, calculated in analysis

W_{tb} = Weight of travelling block, user input

n = Number of lines between the blocks

e = individual sheave efficiency

3.4.6 Side force calculations for soft string model

The following equation is used for side force calculation, this known as Johansik's model, (Johancsik, 1984).

$$F_N = \sqrt{(F_T \, \Delta\alpha sin\varphi)^2 + (F_T \, \Delta\theta + WL \sin\varphi)^2} \tag{3-16}$$

Where:

F_N = Normal or side force

F_T = Axial force at bottom of section calculated using buoyancy method

$\Delta\alpha$ = Change in azimuth over section length

φ = Average inclination of the section

$\Delta\theta$ = Change in inclination over the section length

L = Section length

W = Buoyed weight of the section

3.4.7 Torque calculations

The following equation is used for calculating torque

$$T = F_N r \mu \frac{|A|}{|V|} \tag{3-17}$$

Where

T = Torque

$|A|$ = Angular speed

$|V|$ = Resultant velocity

F_N = Slide or normal force

μ = Coefficient of friction

r = Radius of component

F_D = Drag force

3.4.8 Viscous drag

The additional drag force due to hydraulic effects while tripping or rotating, that acts on drillstring is known as viscous drag force, sometimes also refers to hydrodynamic viscous forces. Viscous drag force is calculated as follows:

$$\Delta Force = \frac{\Delta P \pi \left(D_h^2 - D_p^2\right). \, D_p}{4.\left(D_h - D_p\right)} \tag{3-18}$$

Shear stress is calculated using shear rate using various rheological models for non-Newtonian fluid such as Bingham plastic, Power law and Herschel-Bulkley.

This model has taken the following assumptions into account:

1. No direct computations of drag due to pipe rotation.

2. No consideration to flow regime is given.

3. Combined hydraulic effects of axial and rotational movement were ignored.

The following equation is used for additional torque losses due to viscous drag:

$$\Delta Torque = \frac{\tau_t \, 2\pi L \left(\frac{D_p}{24}\right)^2}{100} \tag{3-19}$$

3.5 Hydrodynamic viscous friction

Gjerstad, Kristian (2013) developed very simple but dynamic model that predicts the piston forces in well during tripping operation. The drilling mud is described as Herschel-Bulkley fluid. Continuous flow equations were used for the estimation of frictional pressure gradient [17].

3.5.1 Wall shear stress in annulus/wellbore

The friction forces on the fluid from the walls in a wellbore volume may be expressed by, (Gjerstad, March 2013)

$$F_{f(j)} = A_{u1(j)}\tau_{w1(j)} + A_{u2(j)}\tau_{w2(j)}, j = 1, \dots n_s \tag{3-20}$$

Where A_u is the contact layer area between the drilling fluid and the walls, (annulus and drillstring inner and outer). τ_w is the average value of the wall shear stress over the area A_u. Equation (3-20) forms the basis of hydrodynamic viscous drag forces. The viscous drag force that is calculated from this equation can be superimposed in torque and drag values obtained without the effect of

viscous drag, (that can be obtained by simple WellPlan analysis). In this thesis the same approach has been used for evaluating the true effect of viscous drag forces (see chapter 4). The further set of computational equations for this model (Gjerstad, March 2013) will be discussed which had been used for estimating the wall shear stress considering the various flow regimes and simultaneous effect of pipe axial and rotational motion.

Here shear stress is defined as function of effective velocity v_e, which can be computed as:

$$v_e = \bar{v} + K_c v_s \qquad (3\text{-}21)$$

$\bar{v}$ is the average fluid velocity, v_s is the string or tripping velocity and Kc is the clinging factor, which determines the amount of fluid which follows the moving wall. The clinging factor is generally dependent on flowrate and the diameter ratio α, between string and wellbore.

$$\alpha = \frac{D_s}{D_w} \qquad (3\text{-}22)$$

Where D_s and D_w are the diameters of string and wellbore respectively.

In case of Newtonian fluids in annular geometry, clinging factor is not dependent upon the flow rate and can be estimated as [18]:

$$K_{cl} = \frac{1}{2 \ln \alpha} + \frac{\alpha^2}{1 - \alpha^2} \qquad (3\text{-}23)$$

The following clinging factor is applicable for turbulent flow. [19]

$$K_{ct} = \frac{\alpha^2 - \sqrt{(\alpha^4 + \alpha)/(1 + \alpha)}}{1 - \alpha^2} \qquad (3\text{-}24)$$

3.5.1.1 Laminar flow

The average shear stress in laminar flow based on Herschel-Bulkley model is given by

$$\tau_{xz} = \left(k|\gamma|^{n-1} + \frac{\tau_y}{|\gamma|} \right) \gamma; \; |\tau_{xz}| > \tau_y \qquad (3\text{-}25)$$

$$\gamma = 0; \; |\tau_{xz}| \le \tau_y \qquad (3\text{-}26)$$

Gjerstad, used the simplified continous flow equation derived by Gjerstad and Rune [20], with some modifications. Below is the set of eqautions wall shear stress for laminar flow.

$$\tau_{w,lam} = \tau_w \left(1 - |f_{yco}| \right) + \left(\tau_{wp} + f_{ycpo} \right) f_{yco} \qquad (3\text{-}27)$$

$$\tau_{wL}(\bar{v}_e) = -\frac{6\mu_{1r}}{h} v_e \qquad (3\text{-}28)$$

$$\tau_{wp}(\bar{v}_e) = k \left(\frac{4n+2}{hn} |v_e| \right)^n \qquad (3\text{-}29)$$

3.5.1.2 Turbulent flow

$$\tau_{w,turb} = -\frac{1}{2} f\rho|v_e|v_e \qquad (3\text{-}30)$$

$$f = \frac{a}{(R_{e,eq})^b} \qquad (3\text{-}31)$$

$$R_{e,eq} = \frac{8\rho}{k} \left(\frac{hn}{4n+2}\right)^n |v_e|^{2-n} \qquad (3\text{-}32)$$

3.5.1.3 Transitional flow

$$\tau_w = \tau_{w,lam}f_{tr} + \tau_{w,turb}(1 - f_{tr}) \qquad (3\text{-}33)$$

3.5.2 Wall shear stress inside drillstring

The major friction forces on the fluid from the walls inside the string are expressed as:

$$F_{fI} = A_{uI1}\tau_{wI1} + A_{uI2}\tau_{wI2} \qquad (3\text{-}34)$$

3.5.2.1 Laminar flow

Following is a set of equations for laminar flow:

$$\tau_{wI,lam} = -\tau_y \left(|P_p| + f_{YP}\right)f_0 \qquad (3\text{-}35)$$

3.5.2.2 Turbulent flow

$$\tau_{wI,turb} = -\frac{1}{2} f\rho|\overline{v_{Ir}}|v_{Ir} \qquad (3\text{-}36)$$

3.5.2.3 Transitional flow

$$\tau_{wI} = \tau_{wI,lam}f_{tr} + \tau_{wI,turb}(1 - f_{tr}) \qquad (3\text{-}37)$$

For detail study of this model see the Gjerstad's work [17].

4 Analysis, results and discussions

This chapter deals with the quantitative analysis of various parameters on torque and drag profiles. These parameters include:

1. Effect of sheave friction correction on hook load using WellPlan.

2. Effects of hydrodynamic viscous drag forces on hook load at different flow rates using WellPlan.

3. Effects of hydrodynamic viscous drag forces on hook load at different flow rates using the hydrodynamic viscous drag model (Gjerstad, March 2013).

4. Effects of hydrodynamic viscous drag forces on torque at different flow rates using WellPlan.

5. Effects of weight on bit (WOB) on torque at various WOB.

4.1 Analysis information

4.1.1 Basic well data

For detailed well information please see the appendix 7.1. The general overview of well is given below:

Total well depth = 6266.83 m

Hole diameter = 12.125 inch

Open hole length = 3519.83 m

Casing shoe depth = 2747 m

Casing ID = 13.375 m

Riser ID = 17.75

Riser length = 26 m

Length of BHA = 161 m

Drilling fluid density = 1.6 sg

Fluid rheology model = Herschel-Bulkley

Type	Length [m]	Depth [m]	OD [in]	ID [in]	Weight [Kg/m]
Drill Pipe	3654.83	3654.83	6.625	5.696	44.7
Drill Collar	0.4	3655.23	5.5	4.781	40
Drill Pipe	2468.7	6123.93	5.5	4.656	44.5
Drill Collar	1.04	6124.97	8.312	2.12	150
Heavy Weight Drill Pipe	83.75	6208.72	6.625	5	75
Drill Collar	1.08	6209.8	8.25	2.812	160
Hydraulic Jar	9.47	6219.27	8.25	2.75	240.3
Drill Collar	0.86	6220.13	8.312	2.812	150
Heavy Weight Drill Pipe	17.95	6238.08	6.625	5	75
Non-Mag Drill Collar	0.8	6238.88	8.312	2.812	160
Float Sub	0.91	6239.79	8.125	2.812	164
Integral Blade Stabilizer	2.42	6242.21	8.125	2.812	165.21
MWD Tool	6.94	6249.15	8.125	5	171.1
MWD Tool	8.46	6257.61	8.125	5.906	131.8
Drill Pipe	2.84	6260.45	8.125	5	162.9
Near Bit Stabilizer	1.87	6262.32	8.125	3	160.43
Bent Housing	4.22	6266.54	8.125	3	156
Bit	0.29	6266.83	12.125		517.24

Table 4-1 Drillstring and BHA data
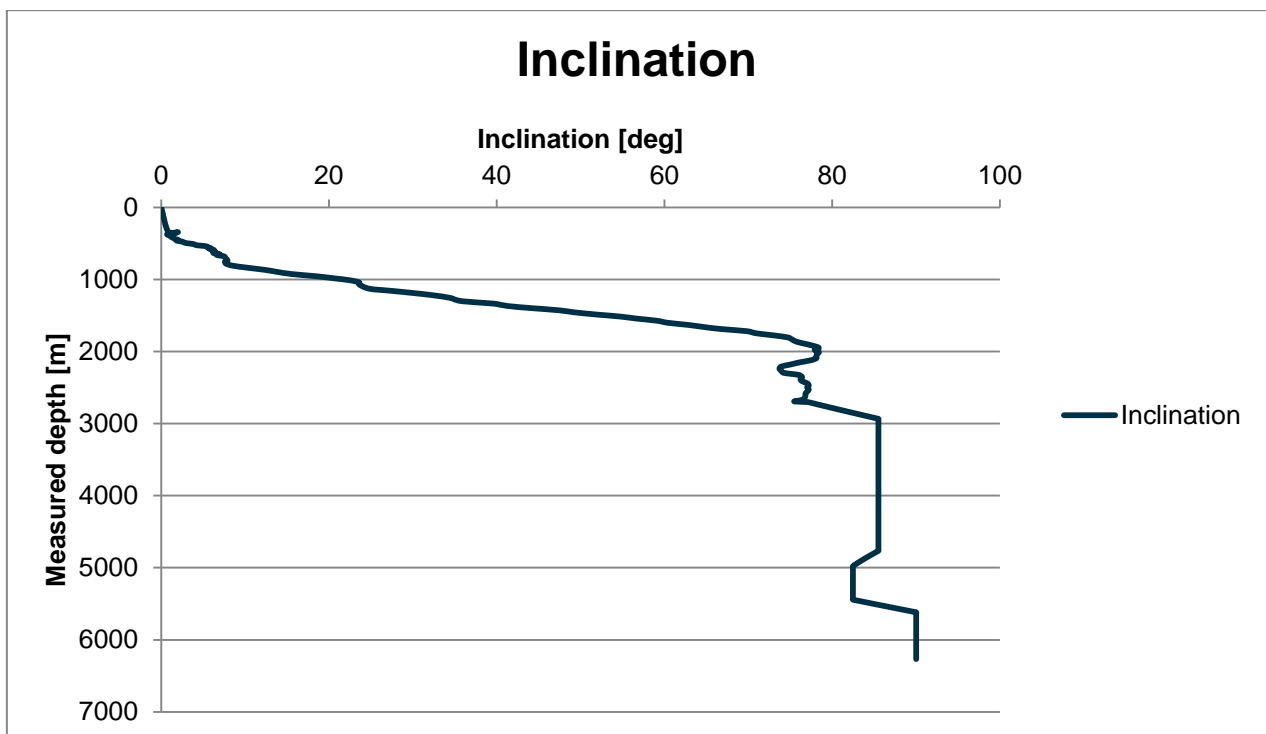
Figure 4-1 Well inclination

4.1.2 WellPlan T&D setup

The details can be found in appendix 7.2, the summary is given below:

Friction factor inside casing and riser = 0.2

Friction factor in openhole = 0.3

Tripping speed = 20m/min

Weight of travelling block = not considered

Torque of bit = 20 KN-m

Weight on bit = 25 Klbf

Drilling	Use	WOB /Overpull (kip)	Torque at Bit (kN-m)
Rotating on Bottom	Yes	25,0	20,0000
Slide Drilling	Yes	25,0	20,0000
Backreaming	Yes	15,0	10,0000
Rotating off Bottom	Yes		
Tripping	Use	Speed (m/min)	RPM (rpm)
Tripping In	Yes	20,00	
Tripping Out	Yes	20,00	
Friction Factors	Hole Section Editor		

Table 4-2 Torque and drag normal analysis setup

4.2 Analysis of hook load

The hook load profiles for tripping out and tripping in were generated using WellPlan. These profiles used 0.2 and 0.3 friction factors in cased and open hole respectively. The tripping speed was set at 20 m/min without the effects of viscous drag and sheave friction. These hook loads were set as standard for the comparison with using different parameters, and refers to normal hook loads. See Figure 4-2 and Figure 4-3.
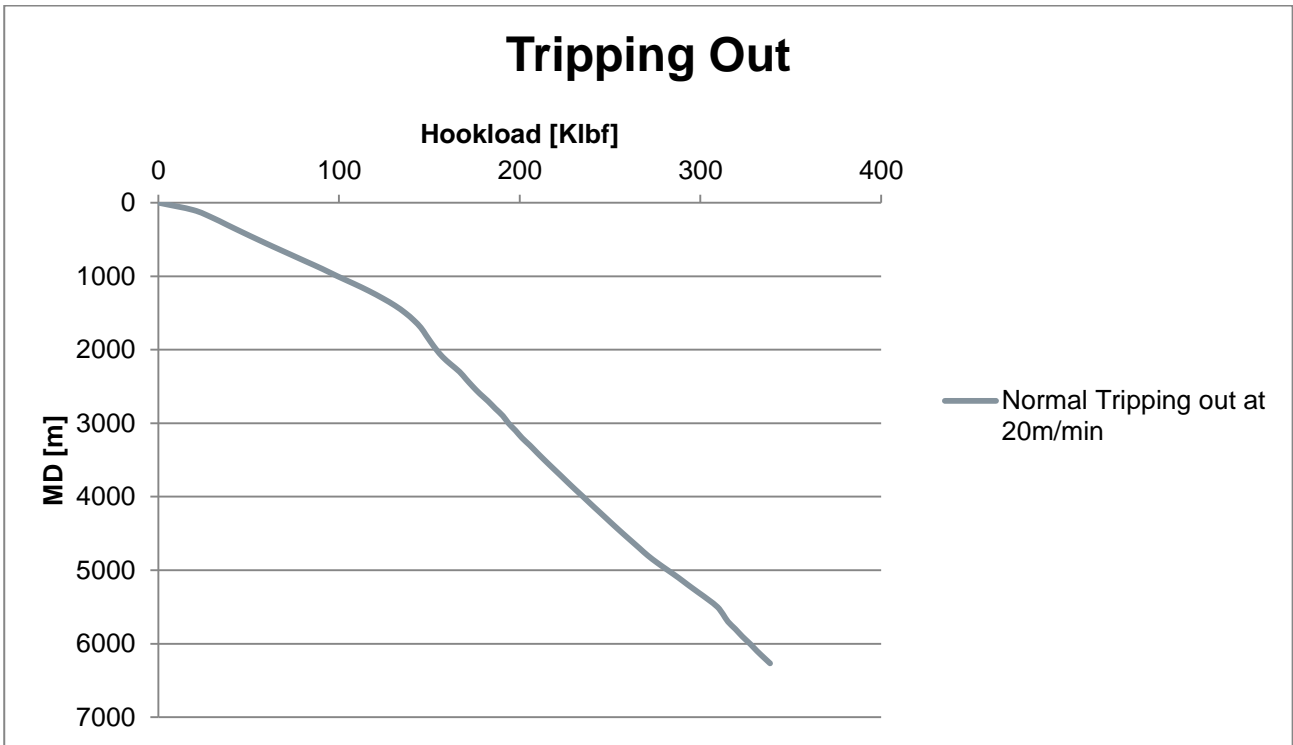
Figure 4-2 Hook load while tripping out
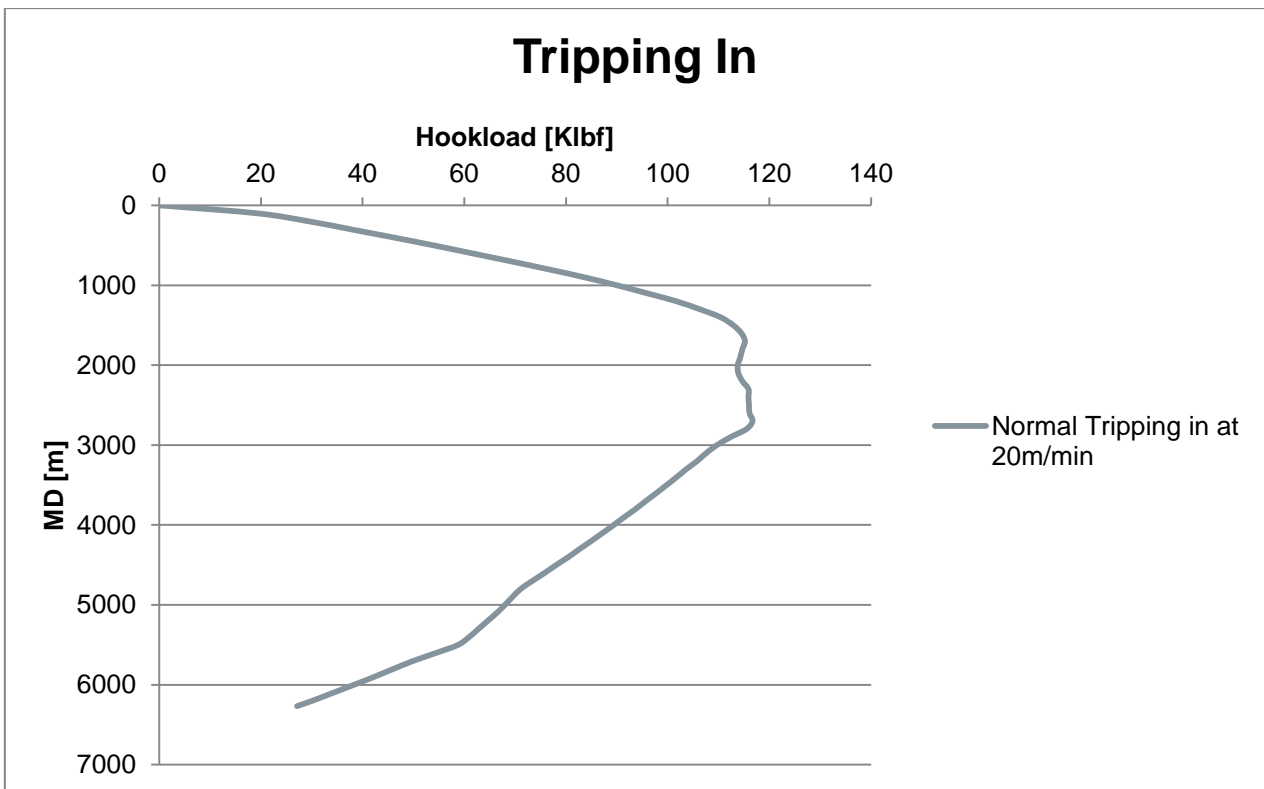
Figure 4-3 Hook load while tripping in

4.2.1 Sheave friction effects

In order to determine the sheave effects, the sheave correction was adjusted to 97% efficiency and 12 lines were used. The drag data obtained after sheave correction is compared with the drag data obtained originally Figure 4-2 and Figure 4-3 without the sheave correction. See Figure 4-4 and Figure 4-5. This must be understood well that in analysis weight of travelling block is not considered.
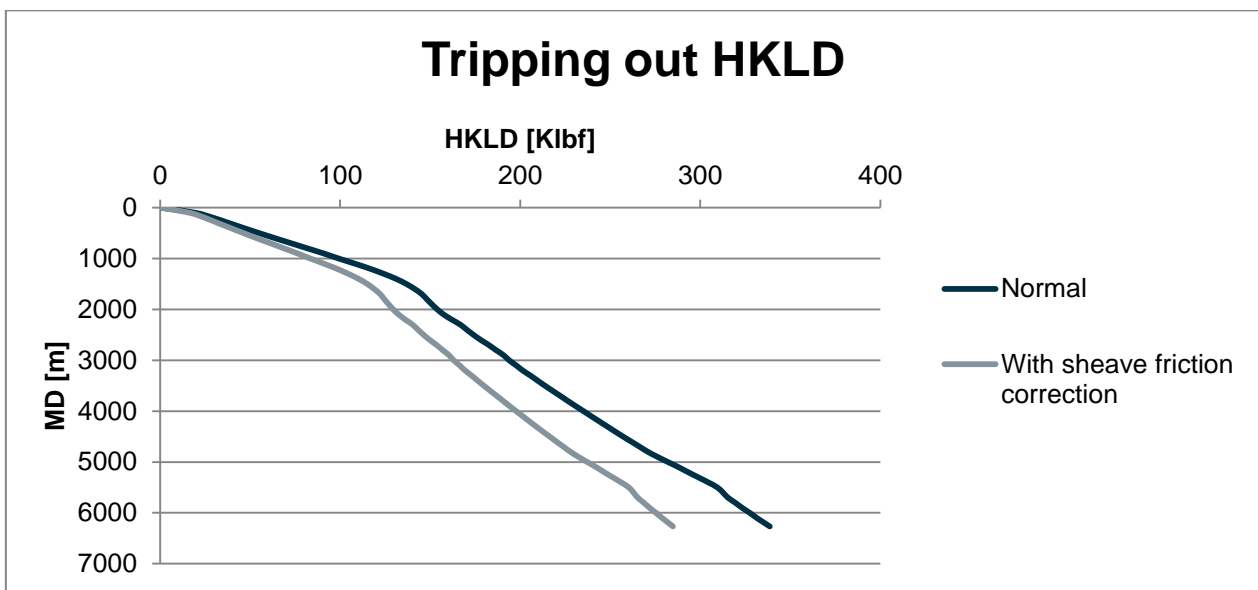

Figure 4-4 Hook load while tripping out with sheave friction correction using 12 lines and 97% efficiency, compared with normal hook load without sheave friction correction.

Tripping In HKLD

HKLD [Klbf]
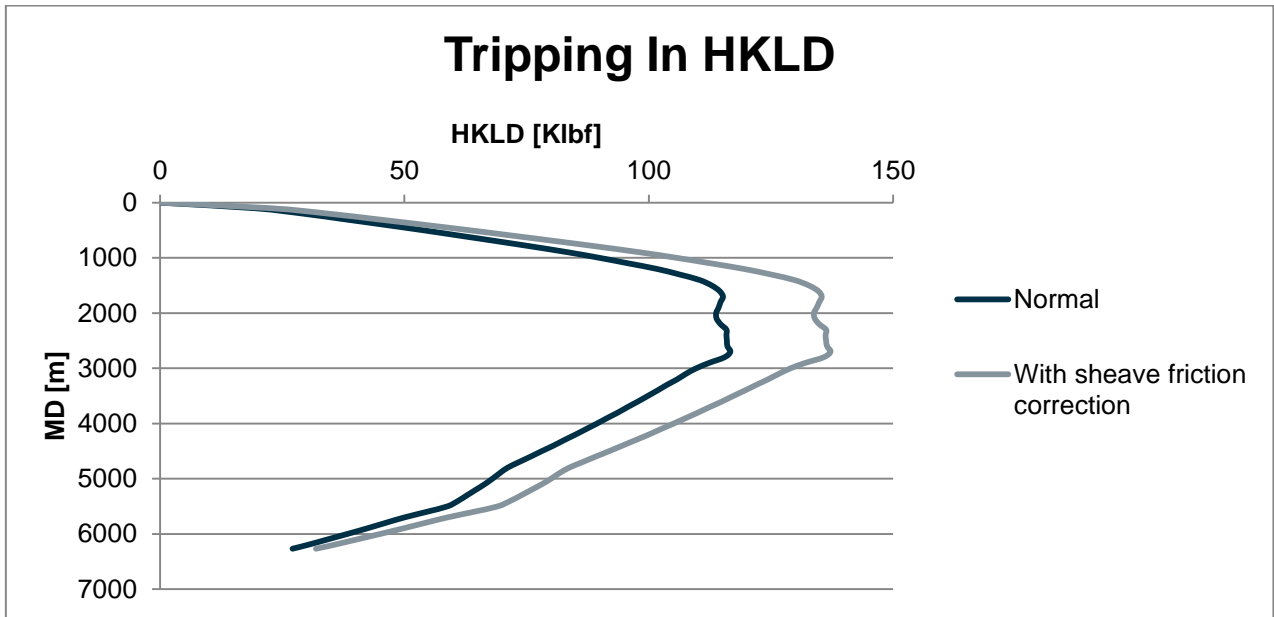
Figure 4-5 Hook load while tripping in with sheave friction correction using 12 lines and 97% efficiency, compared with normal hook load without sheave friction correction.

Percent Difference
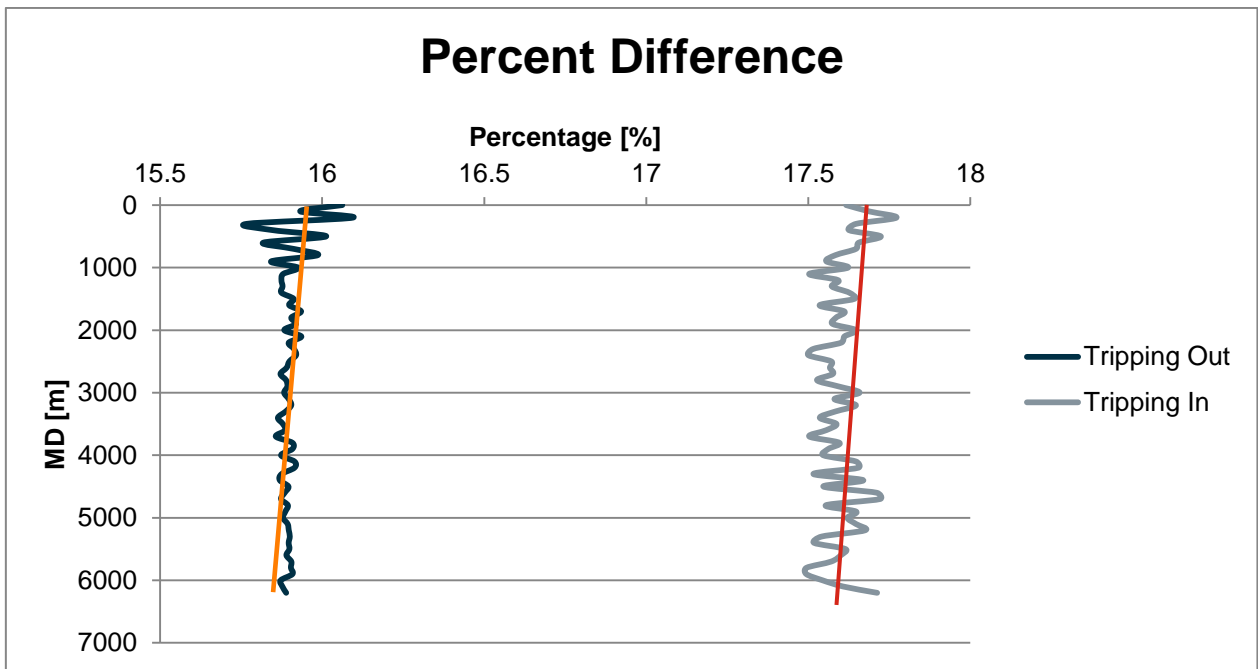
Percentage [%]

Figure 4-6 The percentage differences between hook loads with and without sheave friction correction for tripping out and tripping in.

The effect of sheave friction is very obvious and it is recommended to consider the effects of sheave friction while planning a well and during the torque and drag analysis. As it can be seen in Figure 4-6, the effect of sheave friction while tripping out is almost 16% and for tripping in the effect is up to 17.6%. According to Luke 1993,[11] this effect is almost 19% but here in this case we

did not consider the weight of travelling block, as it can be quite obvious from Equations (3-14) and (3-15) the weight of travelling block is an important parameter for sheave friction.

4.2.2 Effects of viscous drag on hook load using WellPlan

In WellPlan we considered the viscous drag effects and obtained the results for 0, 50, 100, 300, 400, and 500 GPM flowrates, and compared the results with that of what we called normal hook loads.
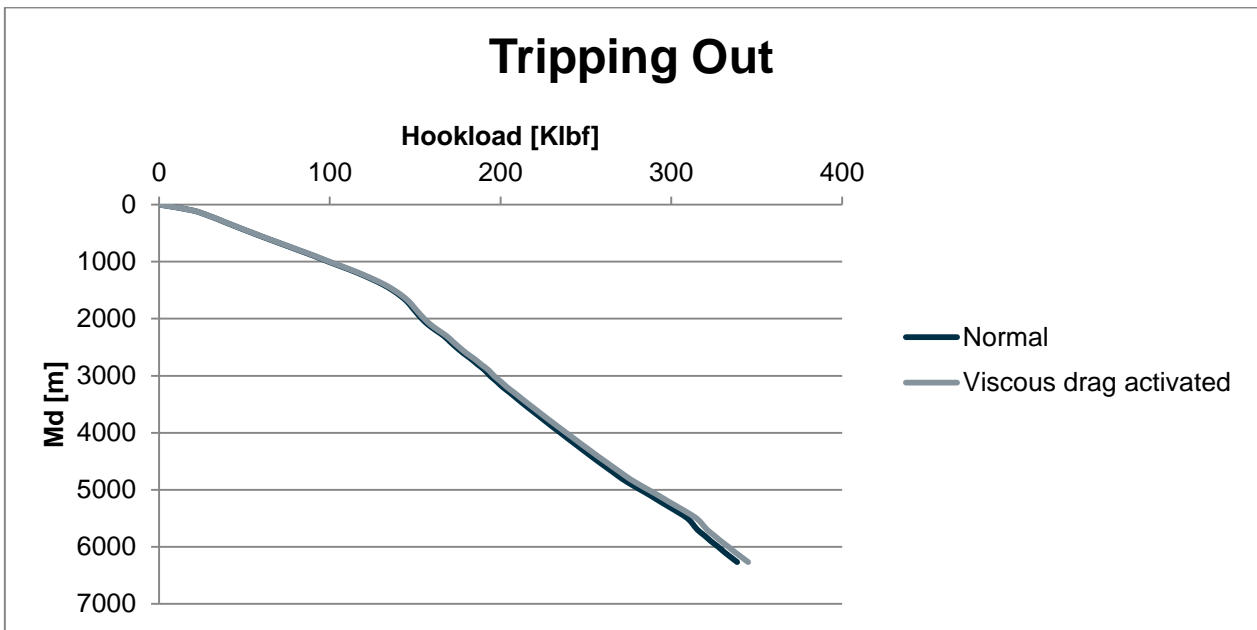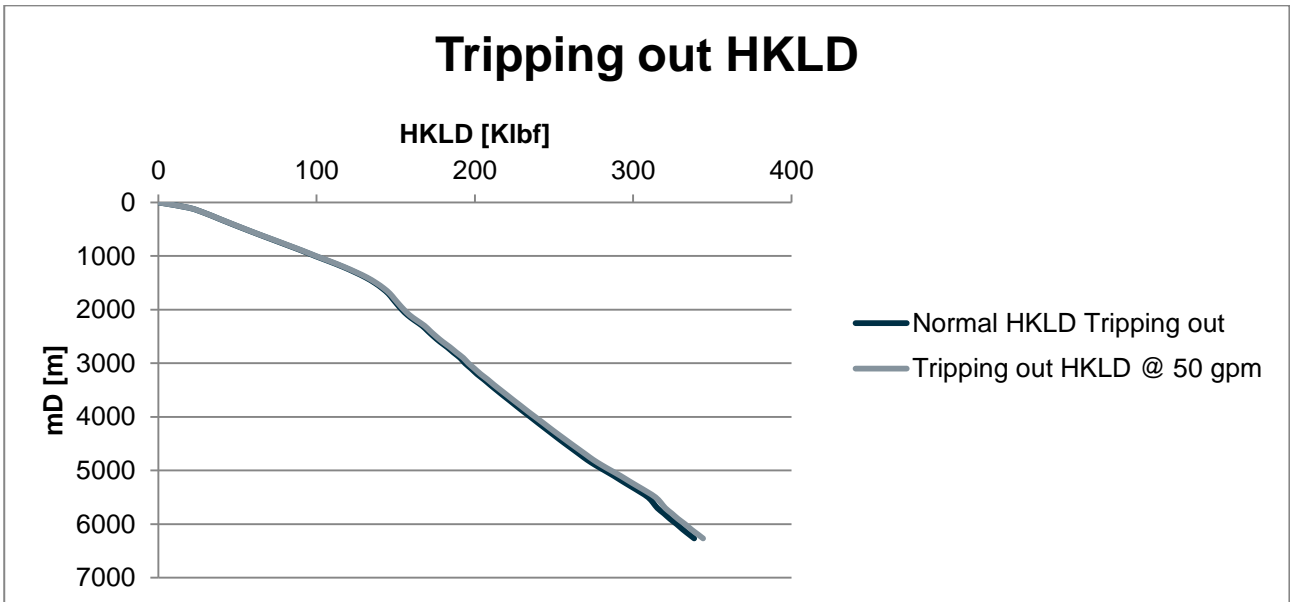

Figure 4-7 Comparison between hook loads while tripping out with and without viscous drag at flow rate of 0 GPM.
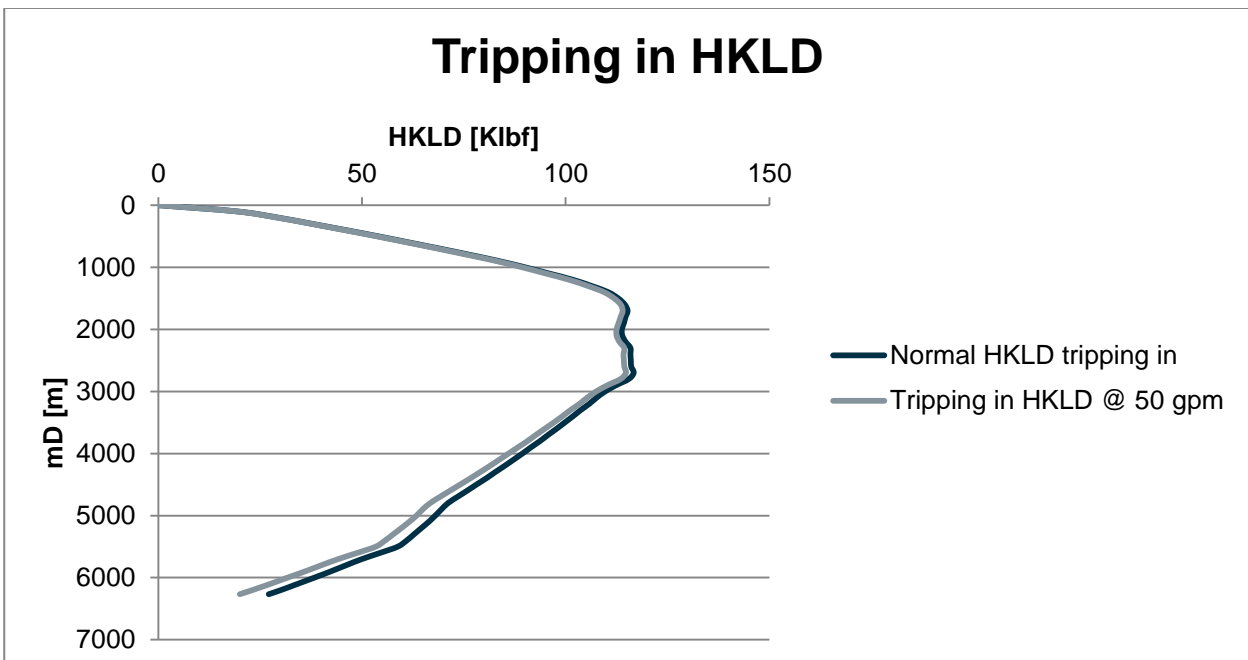
Tripping In

Hookload [Klbf]
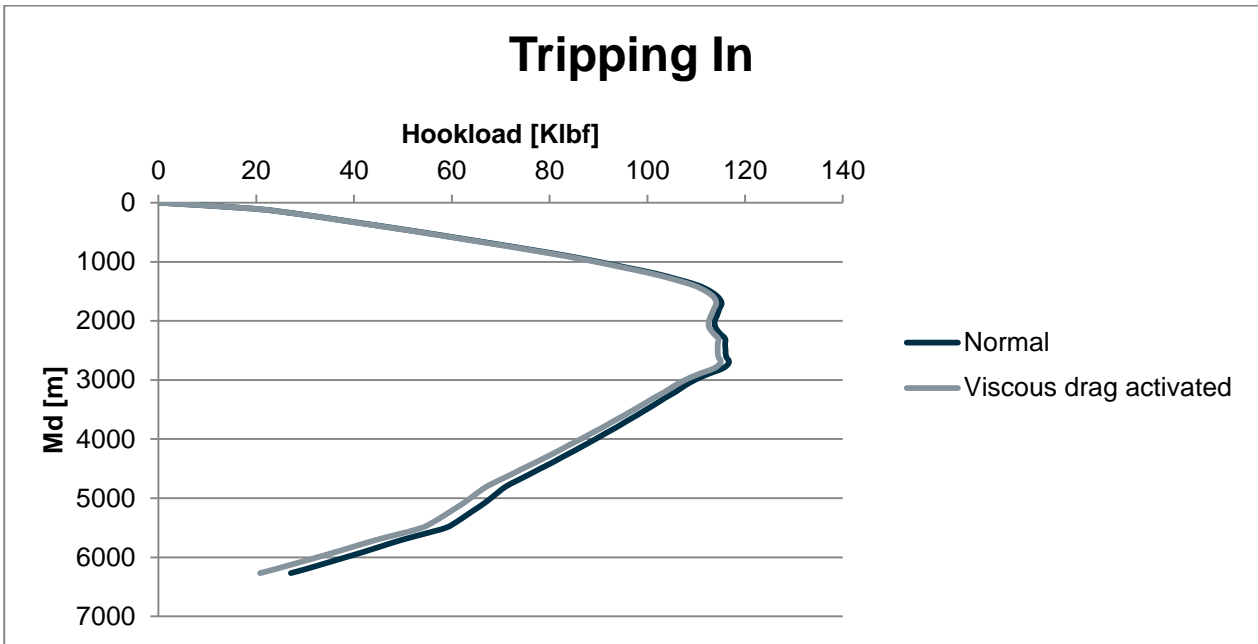
Figure 4-8 Comparison between hook load while tripping in with and without viscous drag at flow rate of 0 GPM
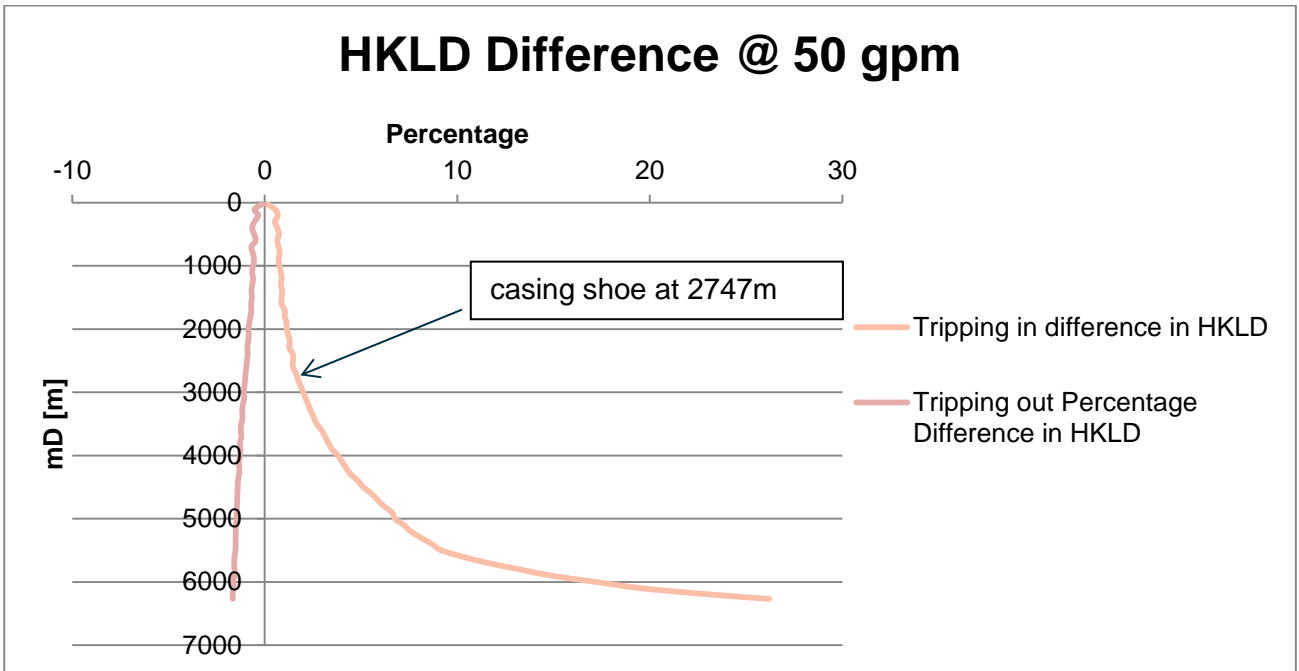
Percent Difference

Percentage [%]

Casing shoe at 2747 m
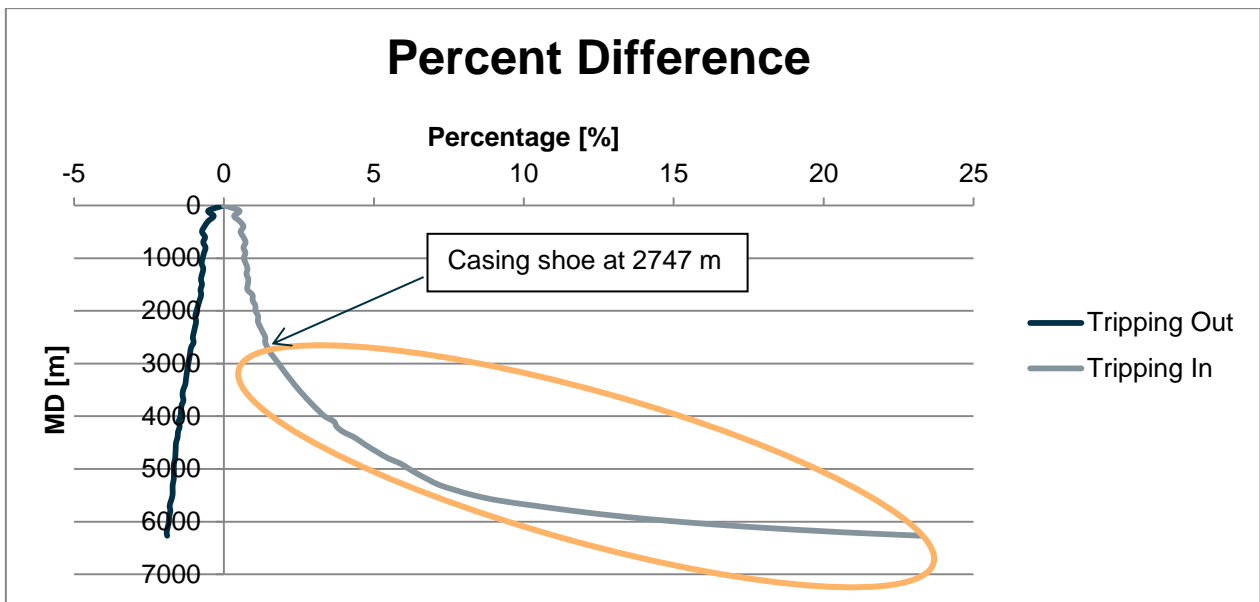
Figure 4-9 Percentage difference between hook loads with and without viscous drags at flow rate of 0 GPM while tripping in and out.

According to Figure 4-7, Figure 4-8 and Figure 4-9 it is obvious that there are no major differences encountered in hook loads while tripping out in upper sections of the well but it is getting higher as it gets deeper i.e. almost 2.5%, whereas while tripping in the difference is not significant in the shallow depths but it becomes drastic at the bottom i.e. up to almost 22%. We can see the effects are getting greater while tripping in as we go below the casing shoe. It is worth mentioning that

the negative differences for tripping out means extra load while positive differences for tripping in means excessive weight loss. We will further investigate this change with evaluating at other flow rates of 50, 100, 300, 400 and 500 GPM.
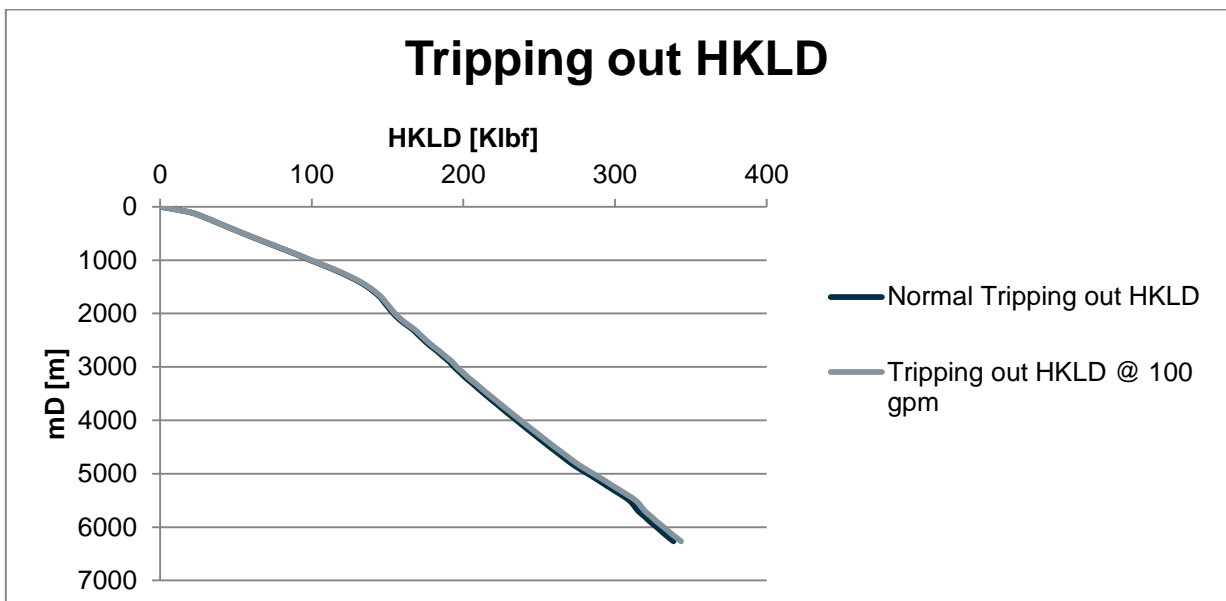

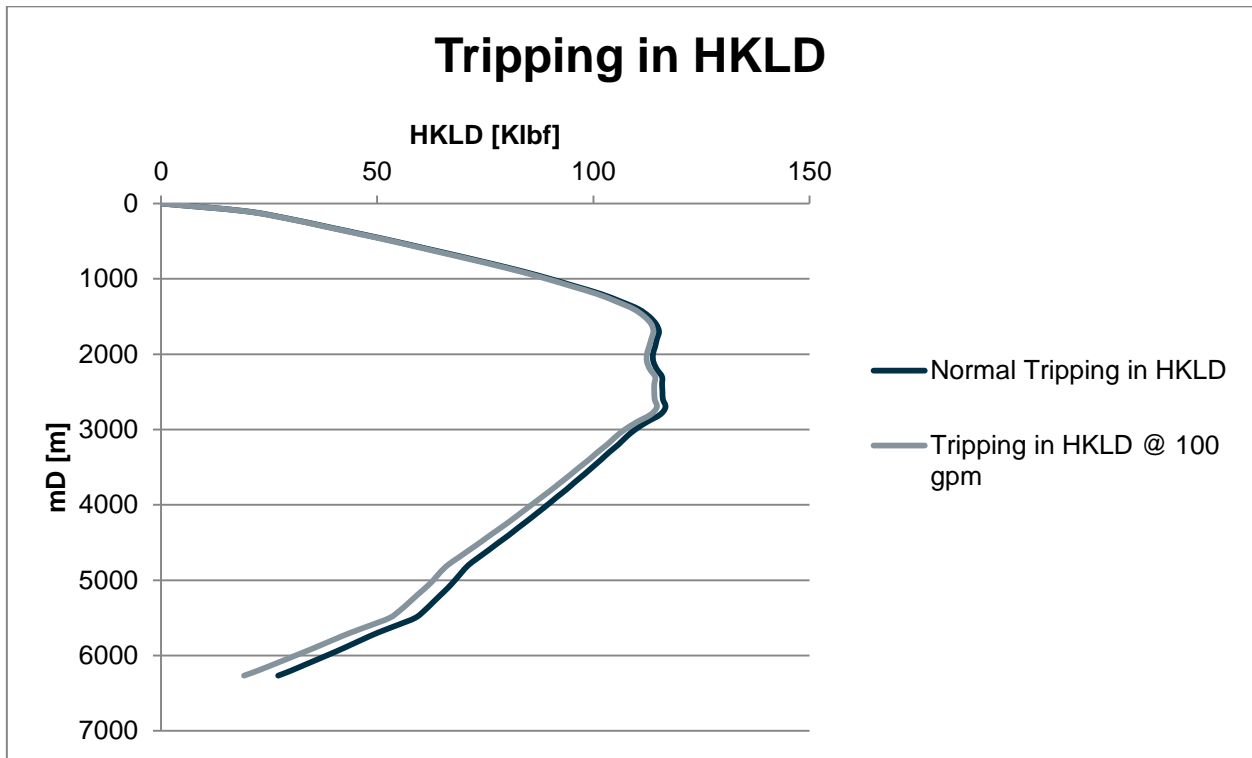**Figure 4-10 Comparison between hook loads while tripping out with and without viscous drag at flow rate of 50 GPM.**

Figure 4-11 Comparison between hook load while tripping in with and without viscous drag at flow rate of 50 GPM
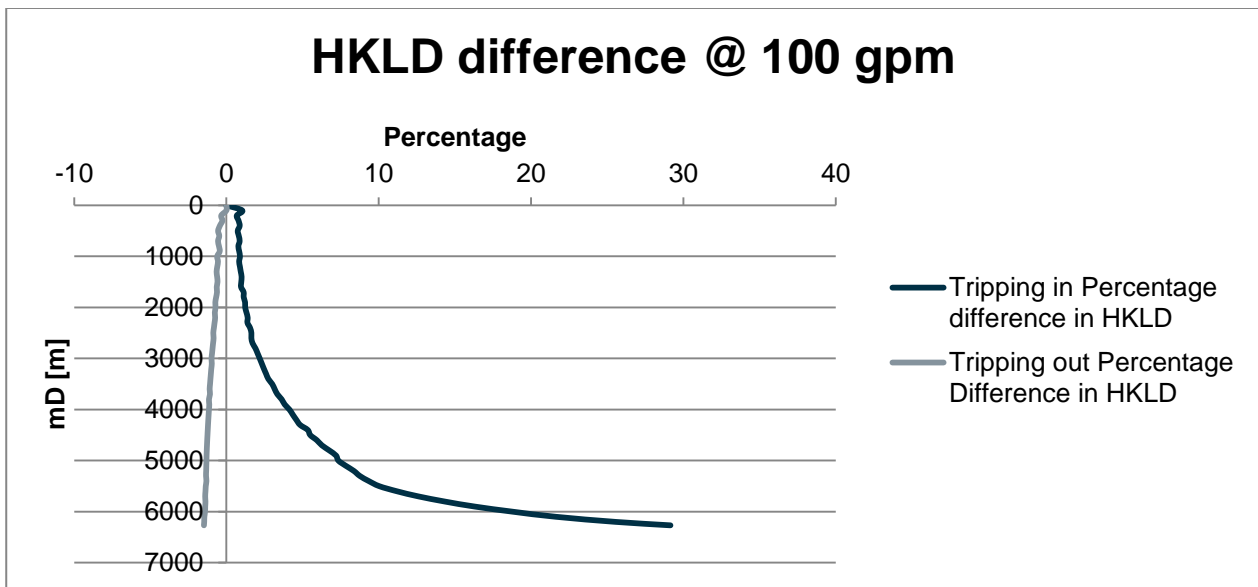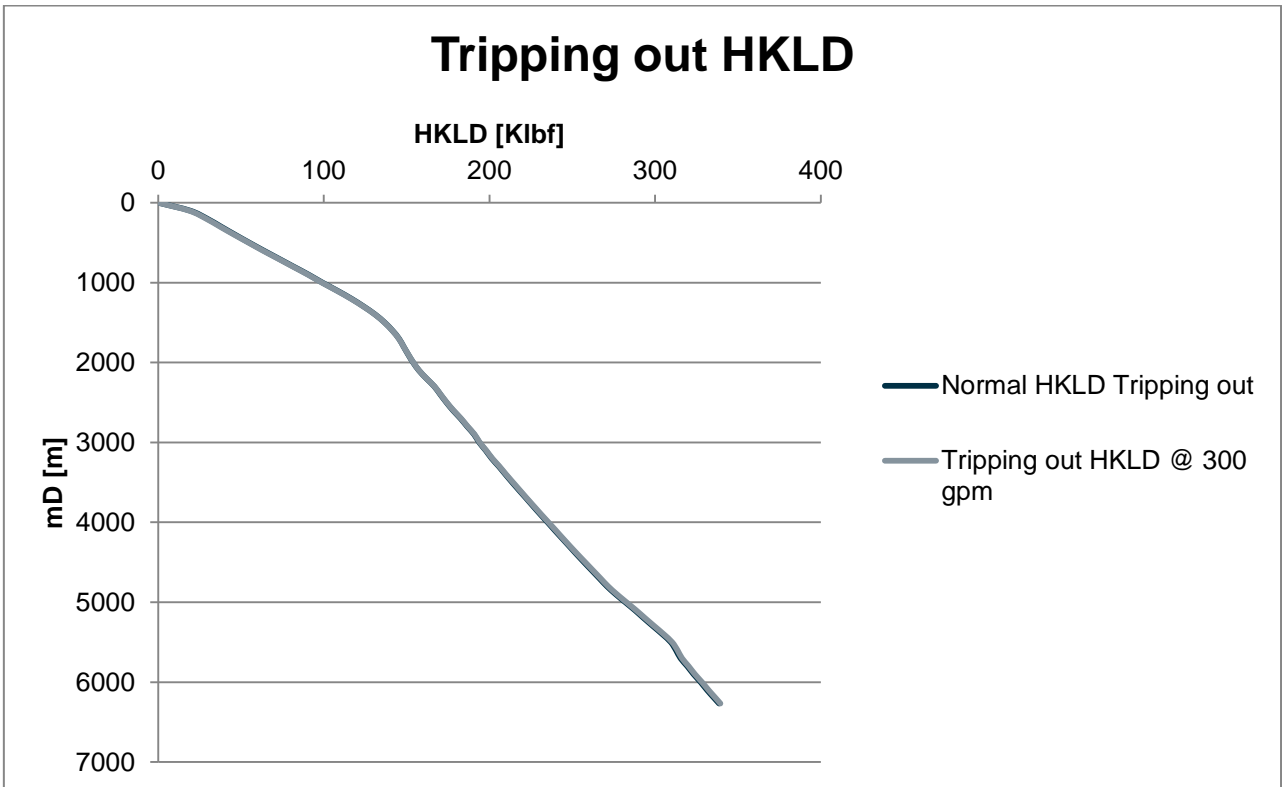
HKLD Difference @ 50 gpm

Figure 4-12 Percentage difference between hook loads with and without viscous drags at flow rate of 50 GPM while tripping in and out

From Figure 4-10, Figure 4-11 and Figure 4-12, we can see that at low flow rate of 50 GPM we observe the difference in hook load while tripping out, although the difference is of only 2 to 3% which is not very significant. But while tripping in the difference is still very high of up to 25%. It is slightly higher as compared with the observations from 0 GPM. See Figure 4-8 and Figure 4-9. We will discuss the reasoning for this behavior of hook load after investigating the trends for other flow rates as well.
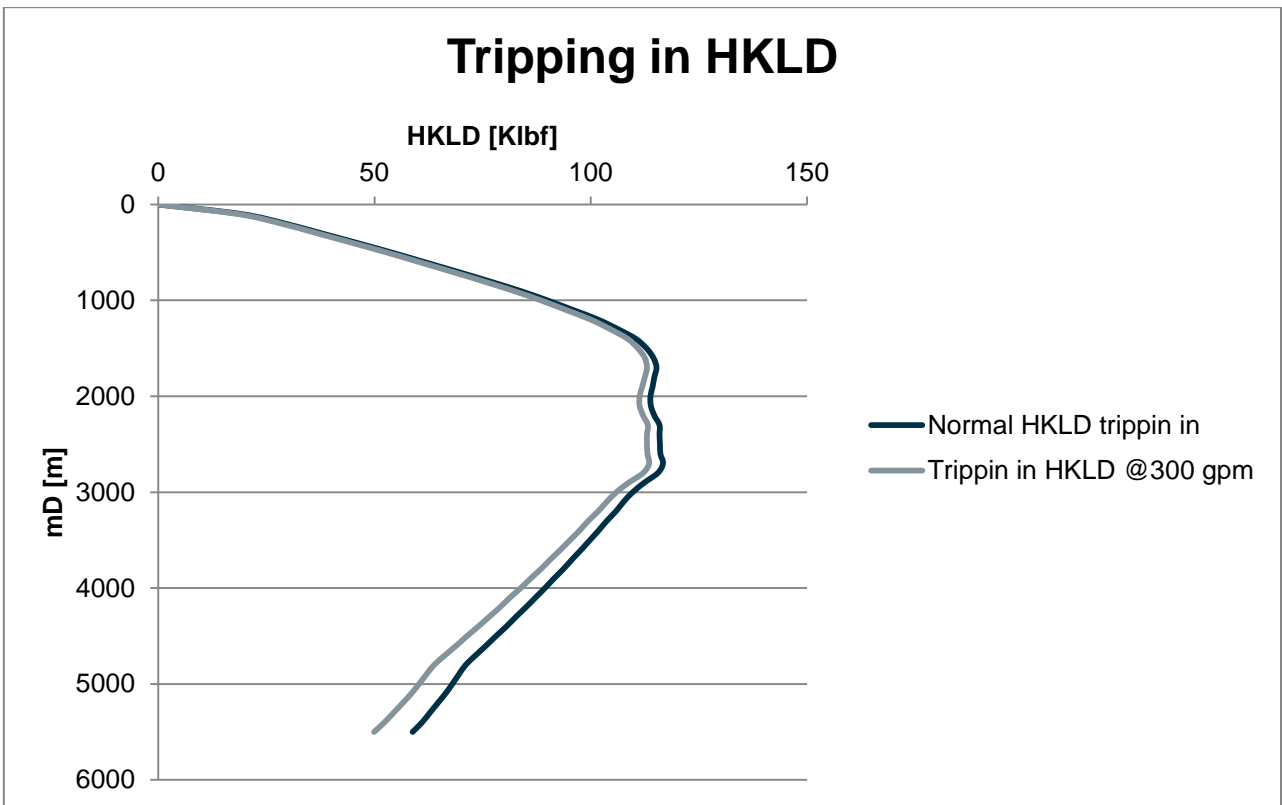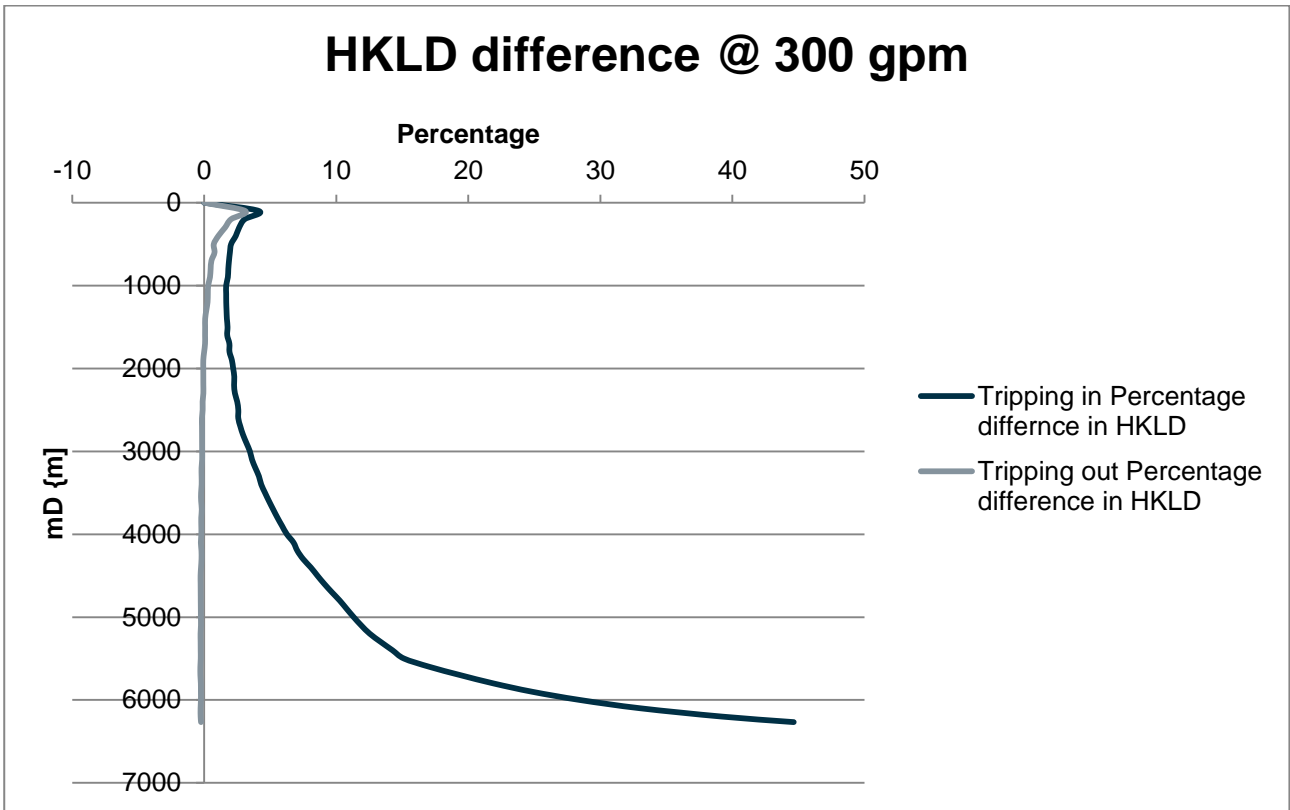

Tripping out HKLD

Figure 4-14 Comparison between hook load while tripping in with and without viscous drag at flow rate of 100 GPM

Figure 4-15 Percentage difference between hook loads with and without viscous drags at flow rate of 100 GPM while tripping in and out

From the Figure 4-13, Figure 4-14 and Figure 4-15 we can see the trends are almost the same but differences are getting slightly higher as expected.

Tripping out HKLD

HKLD [Klbf]

Figure 4-16 Comparison between hook loads while tripping out with and without viscous drag at flow rate of 300 GPM.

Tripping in HKLD

HKLD [Klbf]

Figure 4-17 Comparison between hook load while tripping in with and without viscous drag at flow rate of 300 GPM

Figure 4-18 Percentage difference between hook loads with and without viscous drags at flow rate of 300 GPM while tripping in and out
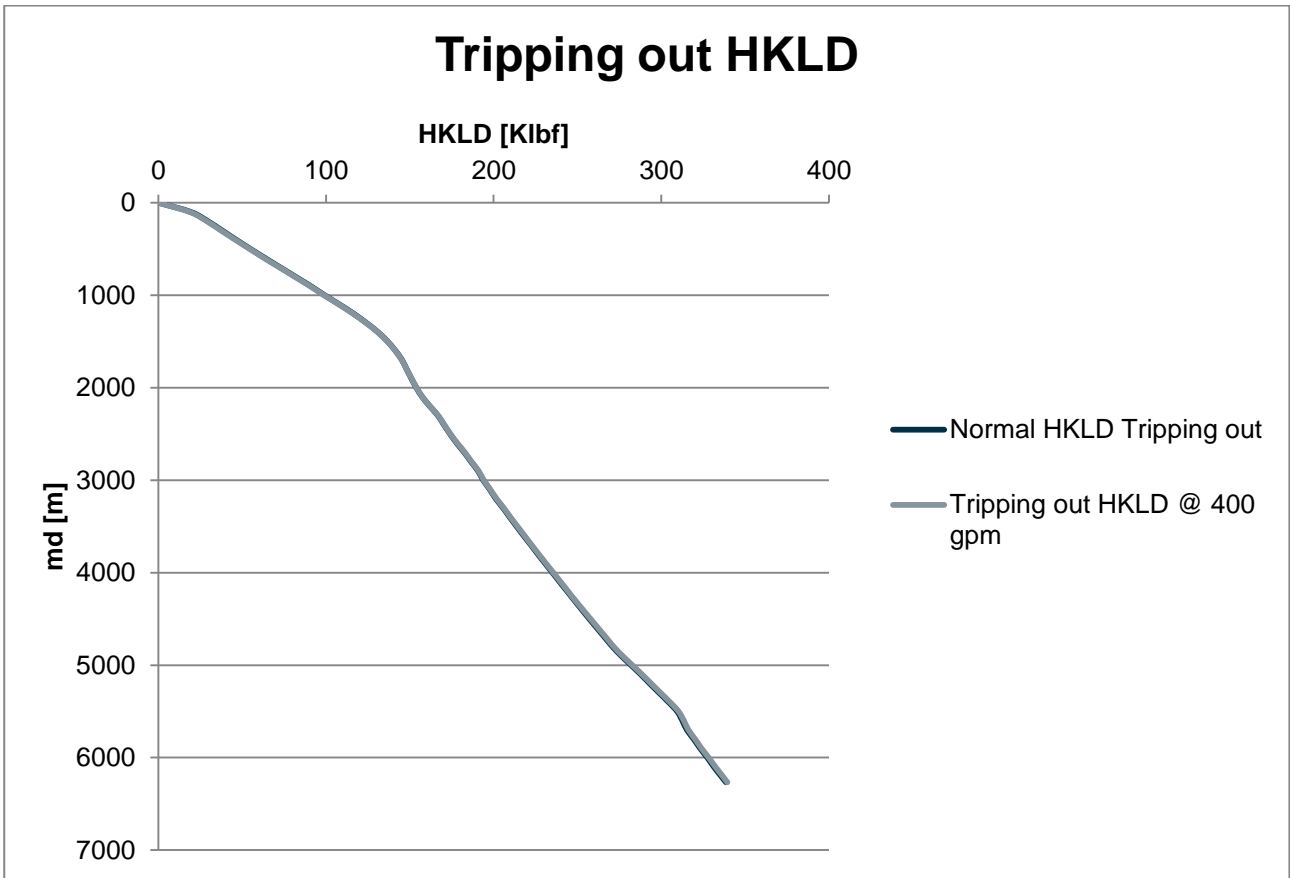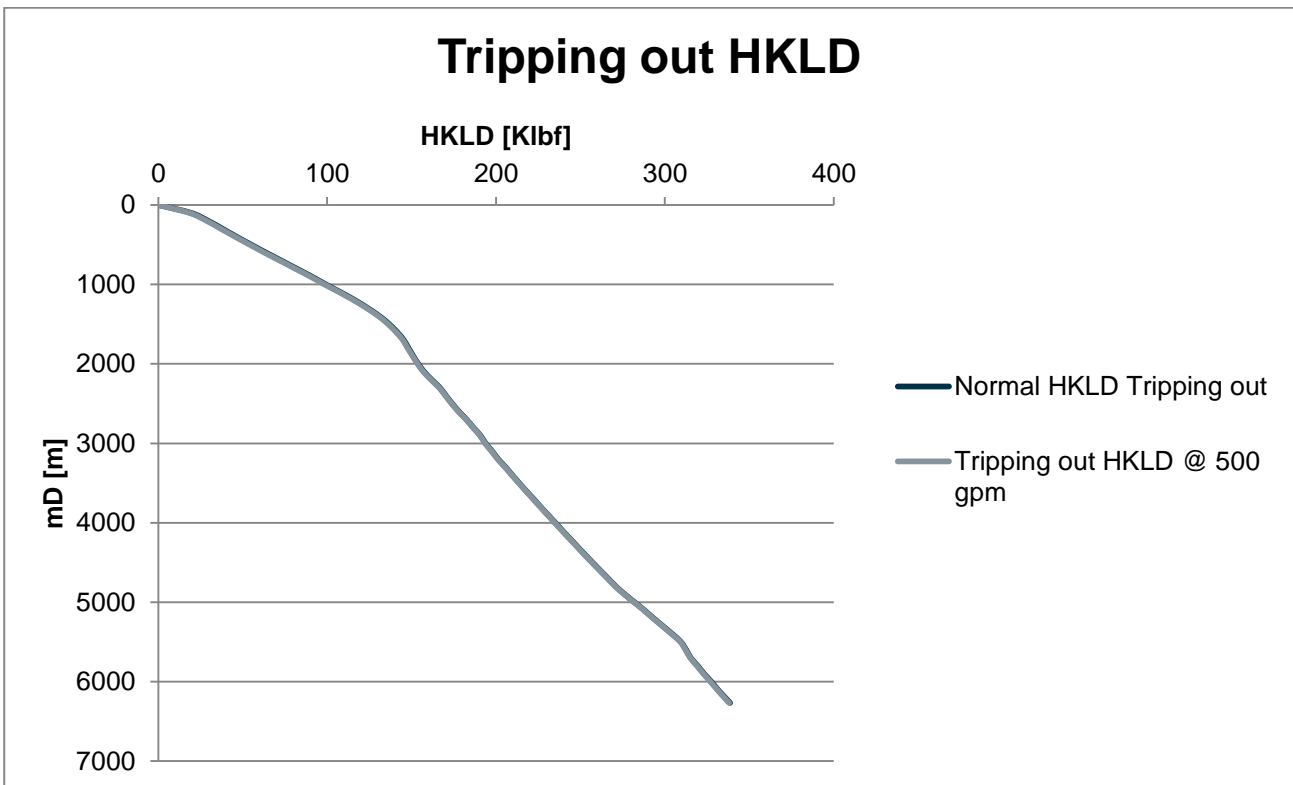
Figure 4-19 Comparison between hook loads while tripping out with and without viscous drag at flow rate of 400 GPM.
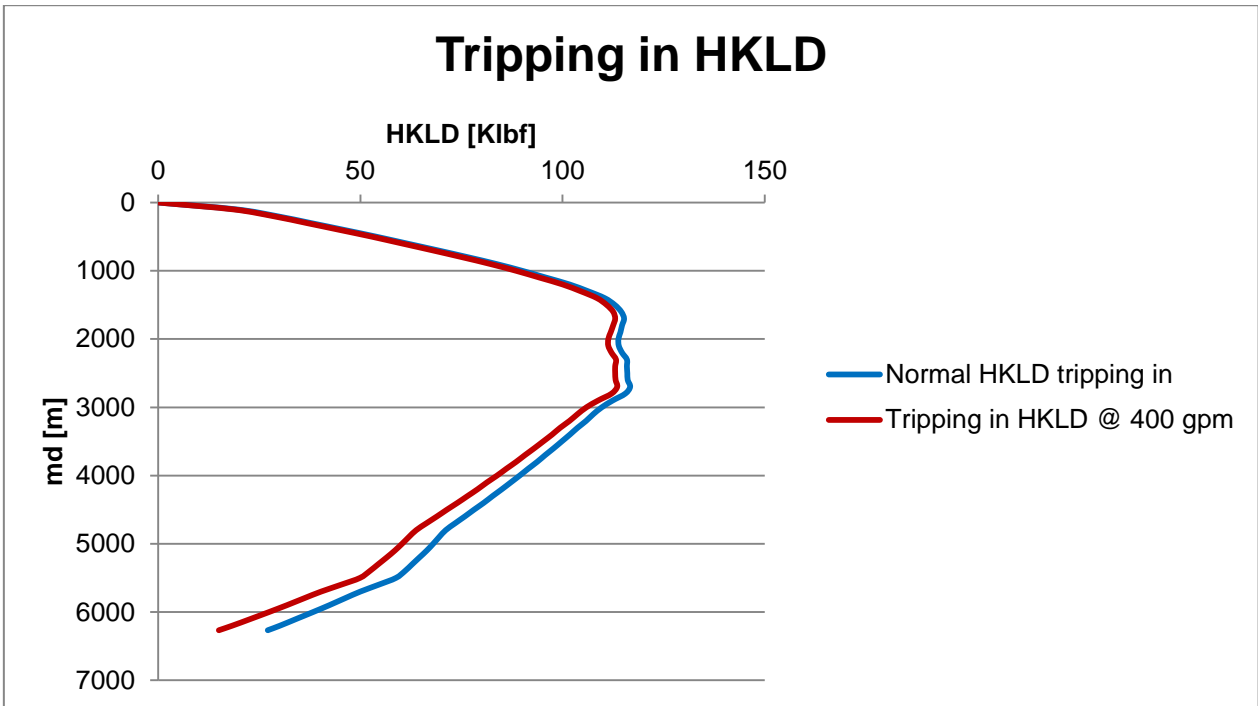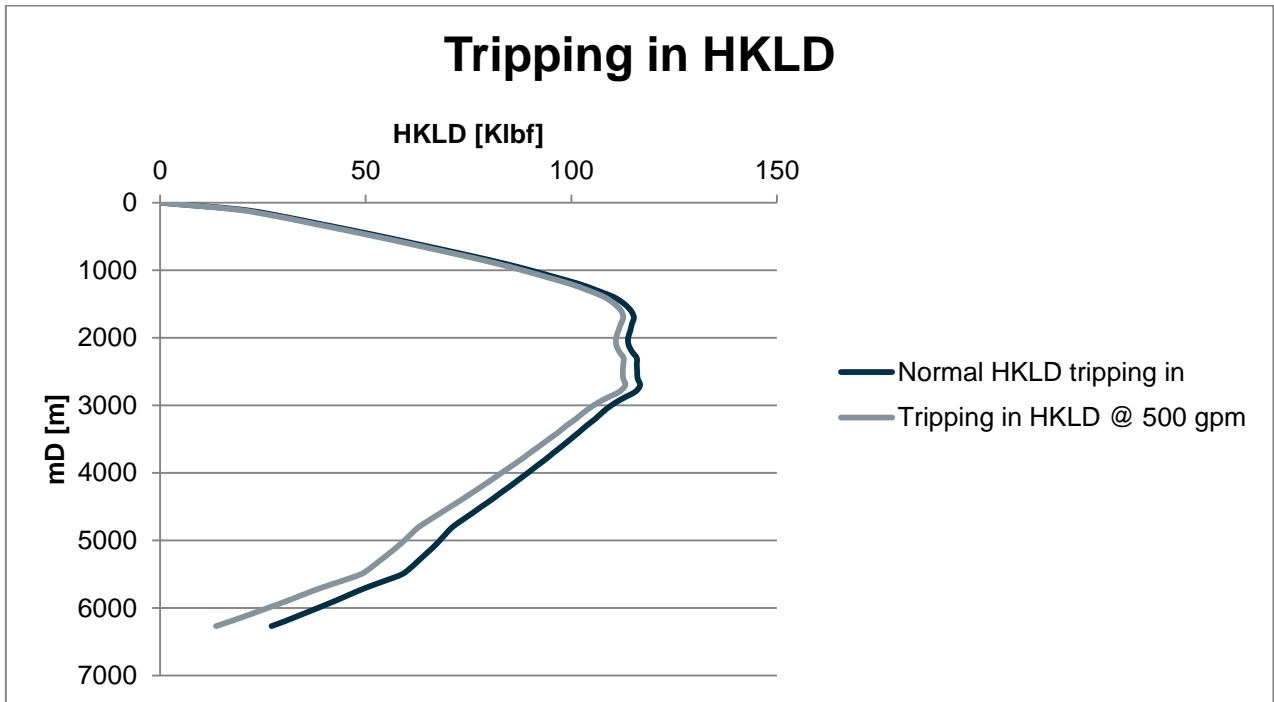

Figure 4-20 Comparison between hook load while tripping in with and without viscous drag at flow rate of 400 GPM
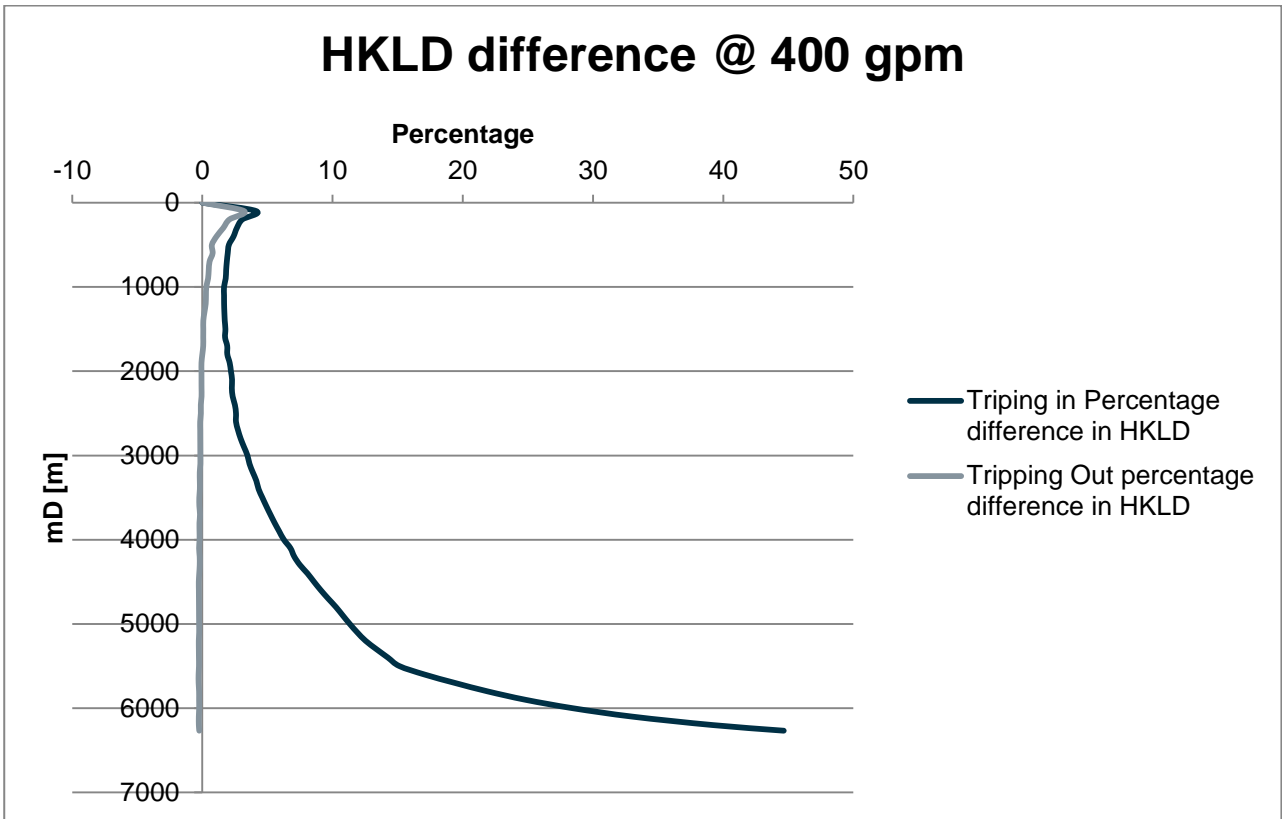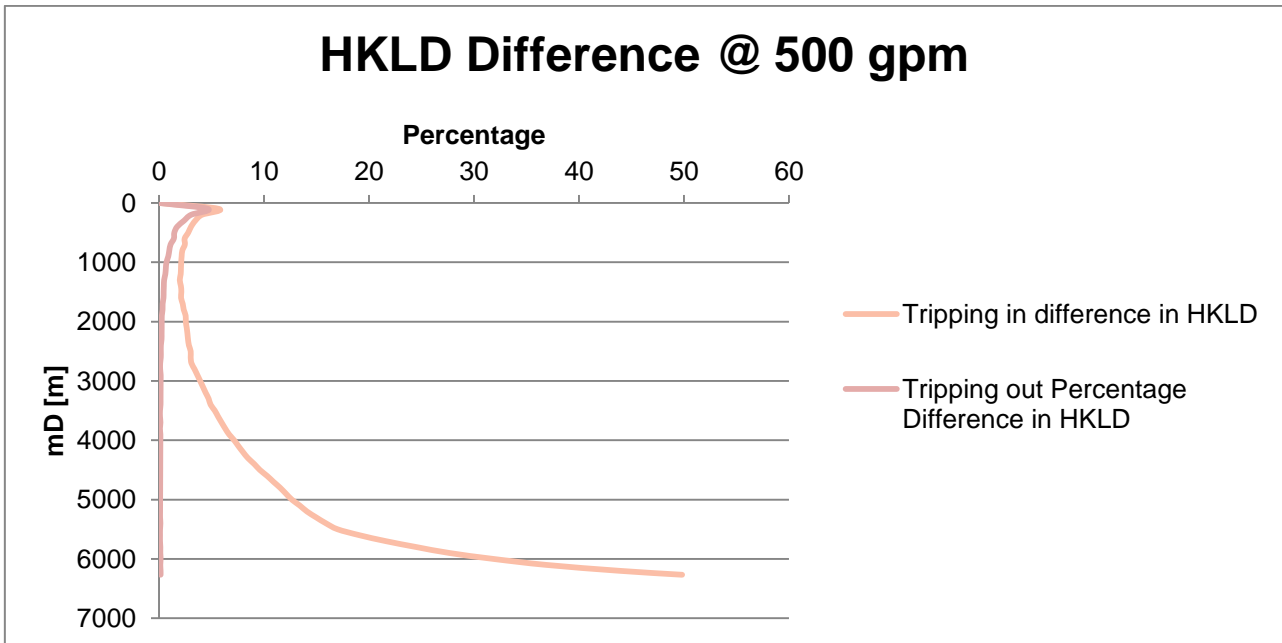
Figure 4-21 Percentage difference between hook loads with and without viscous drags at flow rate of 400 GPM while tripping in and out

Figure 4-22 Comparison between hook loads while tripping out with and without viscous drag at flow rate of 500 GPM.

Figure 4-23 Comparison between hook load while tripping in with and without viscous drag at flow rate of 500 GPM

Figure 4-24 Percentage difference between hook loads with and without viscous drags at flow rate of 400 GPM while tripping in and out

From Figure 4-7 to Figure 4-24 it is becoming obvious that as the flow rates increasing the differences between tripping out hook loads is getting narrower while tripping in hook loads the differences are increasing with increasing flow rate. We will further investigate the effects of hydrodynamic viscous forces in the following section:

4.2.3 Effects of viscous drag on hook load using Gjerstad's model

As it has been mentioned previously the viscous drag model used in WellPlan does not account for flow regimes and the combined effect of axial and rotational motion of pipe. We will further investigate the effect of hydrodynamic viscous drag forces, computed from the model (Gjerstad, March 2013). As described in section 3.5, the wall shear stresses in annulus and inside the drillstring are used to compute the viscous friction forces. Based on Gjerstad's[17], model which is a simple computer program and was designed to calculate the wall shear stresses based on flow regime and considering the effect of axial and rotational motion of drillstring. Viscous friction force will be computed by multiplication of wall shear stresses by the respective circumferential areas of pipes. The viscous friction forces were then superimposed to the hook load values (obtained from WellPlan with the effect of viscous friction) for tripping in and tripping out. The results were obtained as follow:
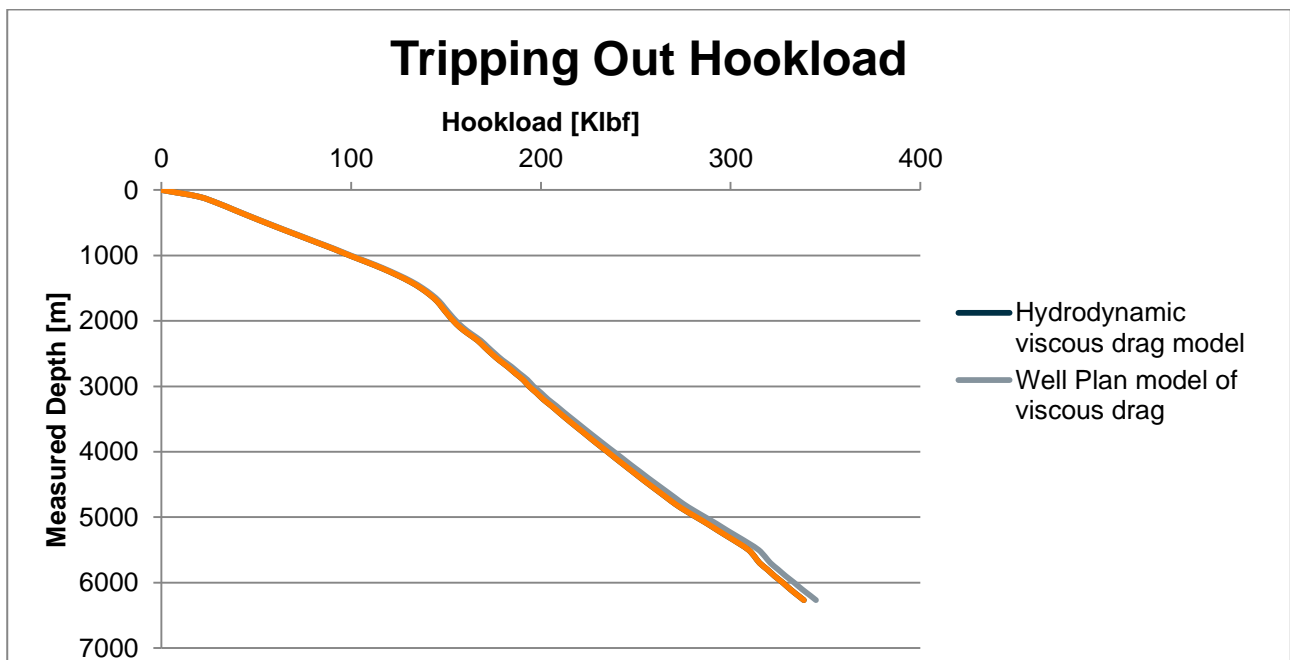

Figure 4-25 The comparison of hook load without the viscous drag effect, WellPlan model of viscous drag and hydrodynamic viscous drag model, for tripping out at 0 GPM of flow.

It is obvious from the Figure 4-25, that there is very close agreement found between the tripping in hook load profiles of WellPlan viscous drag model and the hydrodynamic viscous drag model. Now we will see the effect on tripping out hook loads.
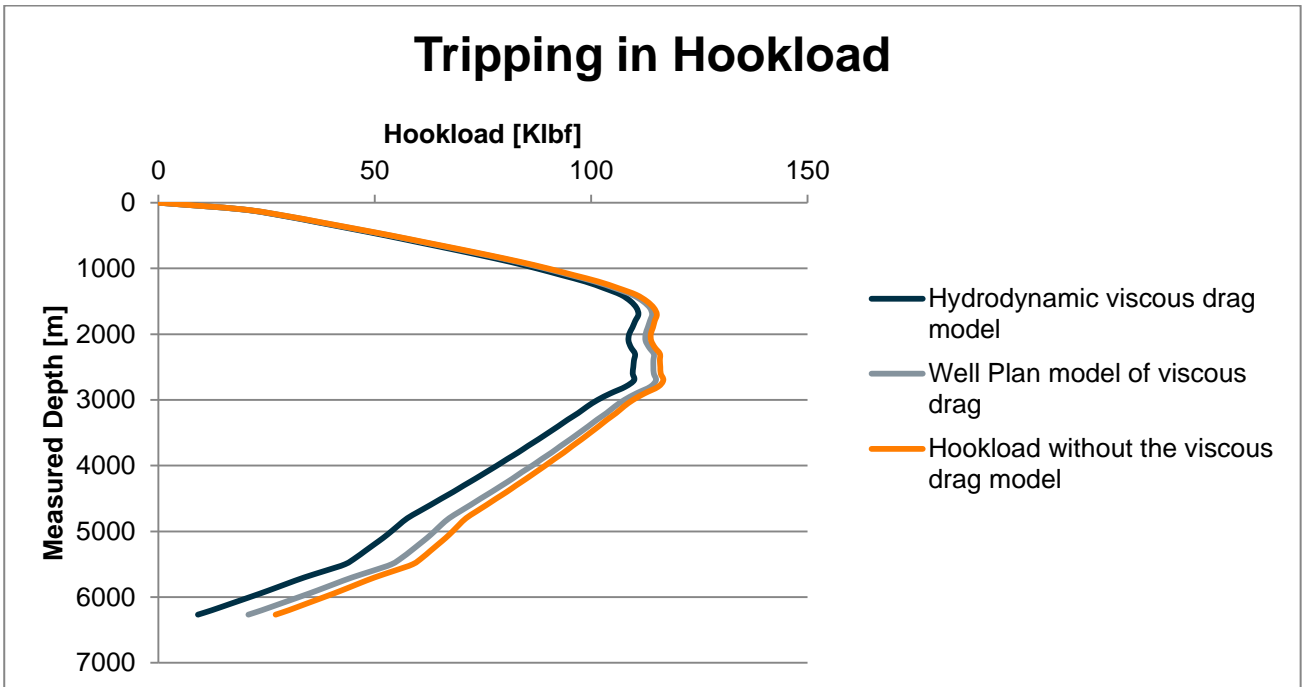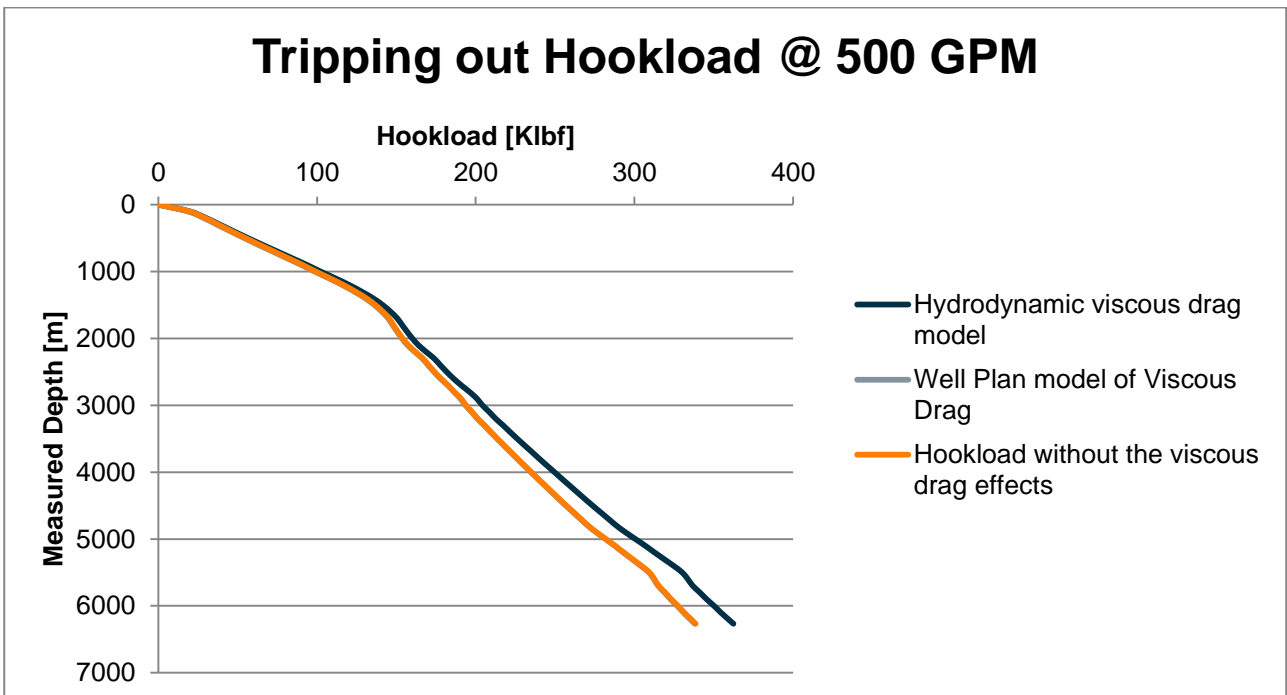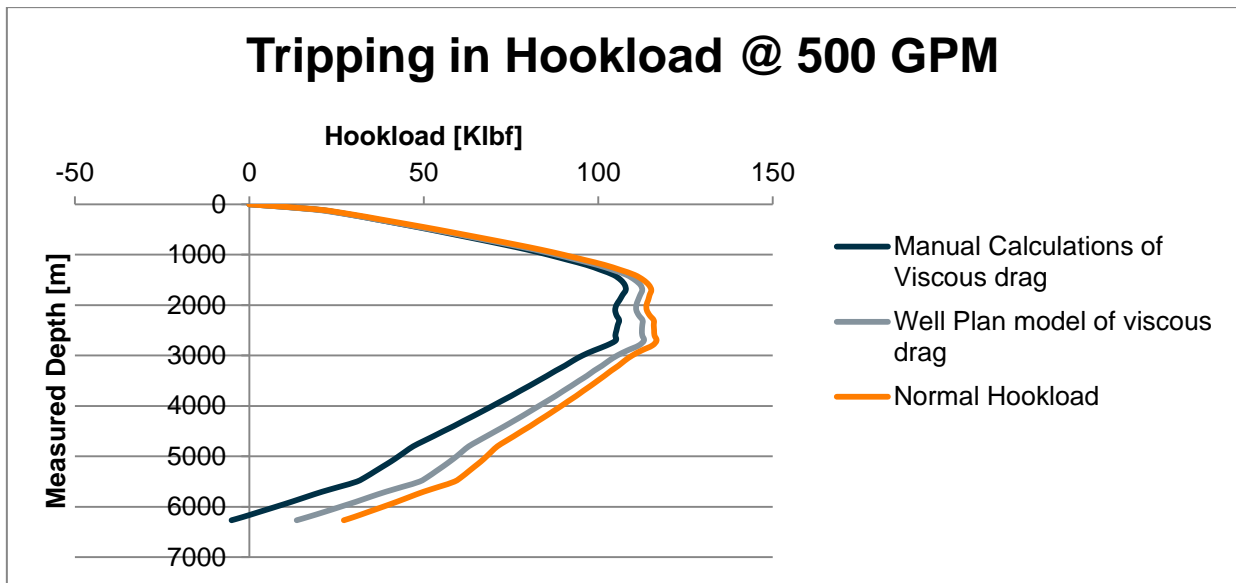
Figure 4-26 The comparison of hook load without the viscous drag effect, WellPlan model of viscous drag and hydrodynamic viscous drag model, for tripping in at 0 GPM of flow.

Figure 4-26, shows the differences in hook loads while tripping in for three models. The results are still the same as expected and the trends for both models are pretty much the same. The main difference is in the lower section. Let us show the trends that were obtained by using the flowrate of 500 GPM.

Figure 4-28 The comparison of hook load without the viscous drag effect, WellPlan model of viscous drag and hydrodynamic viscous drag model, for tripping in at 500 GPM of flow.

Again the Figure 4-27 & Figure 4-28, shows the same results and trends. For tripping out the results from WellPlan and hydrodynamic viscous drag model are overlapping each other. While for tripping in the WellPlan is overestimating the hook load, the reason behind is that it does not consider the effects of flow regime and the combined effect of axial and rotational motion. In Figure 4-28 the hydrodynamic viscous drag model is shown the negative hook load at the bottom of the wellbore. This is because we have not considered the weight of travelling block in our analysis. The zero hook loads at the surface means zero plus the weight of travelling block (which have been neglected).

From Figure 4-7 to Figure 4-28, it can be seen clearly that as the flow rate is increasing the effect of viscous drag is increasing especially for tripping in and below the casing shoe. The reason behind these effects could be different velocity profiles in openhole and in cased hole, as the open hole diameter is 12.125 inch and casing inner diameter is 13.375 inch. The fluid velocity is calculated by:

$$v_f = \frac{Q}{A} \tag{4-1}$$

The effective velocity can be calculated by using $ve = \bar{v} + K_c v_s$. The rotational velocity was set to 0 RPM, and the axial velocity of string was set at 20 m/min (0.333 m/s). The sign convention was used as negative for tripping out and positive for tripping in. The expected velocities for 0, 50, 100,

300, 400 and 500 GPM in cased hole and open hole were computed for BHA, lower drill pipe and upper drill pipe. The results are given in Table 4-3.

	Total effective velcoity [m/min]											
	0 GPM		50 GPM		100 GPM		300 GPM		400 GPM		500 GPM	
Annulus	RIH	POOH	RIH	POOH	RIH	POOH	RIH	POOH	RIH	POOH	RIH	POOH
UDP/Open hole	9.76	9.76	13.38	6.13	17.00	4.73	31.49	11.98	38.73	19.22	45.98	26.46
LDP/Open hole	9.36	9.36	11.87	6.84	14.38	0.69	24.44	5.72	29.46	10.75	34.49	15.77
BHA/ Open hole	9.92	9.92	14.65	5.19	19.39	9.00	38.31	18.46	47.77	27.92	57.23	37.39
UDP/Cased hole	9.64	9.64	12.41	6.87	15.18	1.43	26.24	6.96	31.78	12.49	37.31	18.03
LDP/Cased hole	9.36	9.36	11.87	6.84	14.38	0.69	24.44	5.72	29.46	10.75	34.49	15.77
BHA/Cased hole	9.86	9.86	13.23	6.49	16.60	3.62	30.09	10.36	36.83	17.10	43.57	23.84

Table 4-3 Total effective viscosities in various annuli encountered

It is clearly shown in Table 4-3 that the maximum velocity recorded when BHA is run through open hole section. The velocities are also increasing with increasing flow rate. For a particular flowrate the effective velocity is higher for tripping in as compared with that of tripping out. Flow regime and wall shear stresses are directly dependent upon velocity. This means when the velocity is higher the flow could be turbulent or transitional and in either case giving rise to wall shear stress. Figure 4-29 shows the total viscous drag force acting on the string while tripping in. As it can be seen the viscous force jumps from about 20.3 KN to 23.4 KN just as we moved down to casing shoe. It should be noted that in this context we are not considering any other sort of friction but only viscous friction. The reason for having higher drag forces while tripping in as compared with tripping out is mainly due to the effective velocities differences in annuli. Since the fluid is moving upward in the annulus and for tripping in, pipe is moving downwards the friction is more as compered the case of tripping out where the fluid is moving upward in annulus and pipe is also moving upward. The tripping speed is also an important factor which can affect the hook load. In this model we keep the tripping speed constant at 20 m/min.
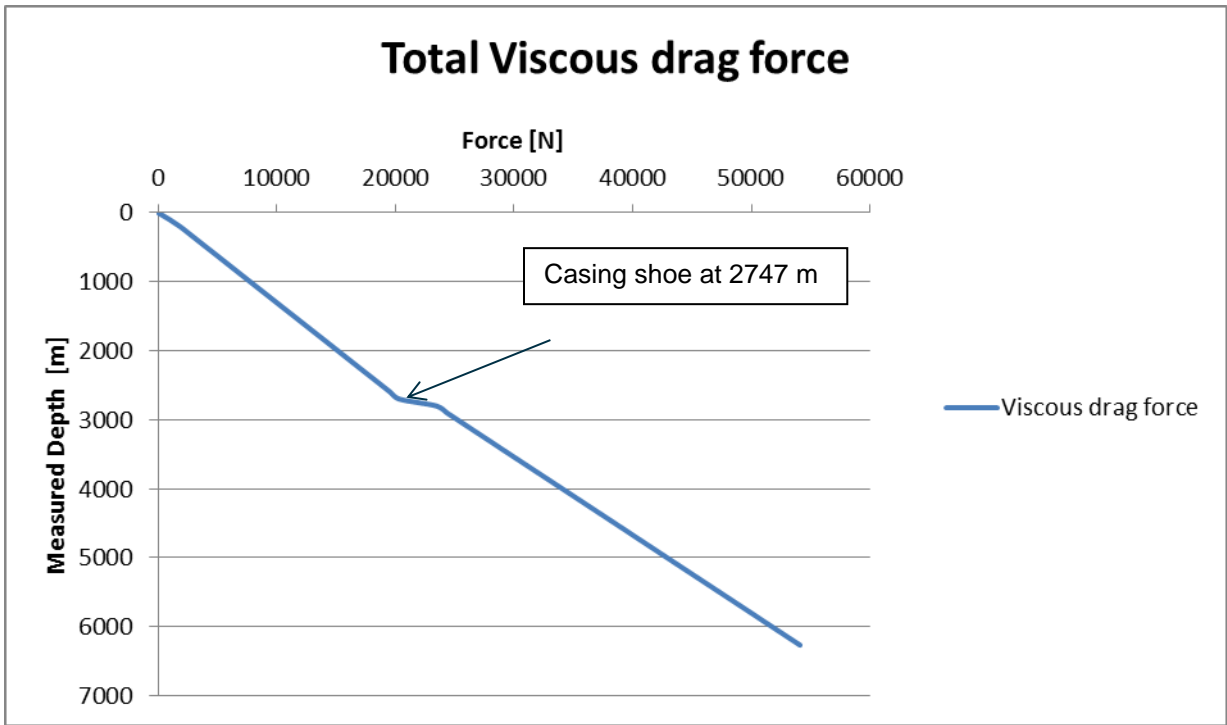
Figure 4-29 Total viscous drag force acting on drillstring while tripping in

4.3 Analysis of Torque

The torque has been analyzed for viscous drag forces and WOB. We have considered the constant torque on bit 20 KN-m. Three torques were recorded, free rotating torque, torque while backreaming and torque while rotating on bottom. The normal torque trends were recorded using 25 Klbf WOB, 0 GPM flowrate and without the effect of viscous drag. The analysis for factors affecting torque is only done by using WellPlan. Here we encountered some ambiguities as the viscous drag model is not taking care of flow regimes and rotational motion together with axial motion.
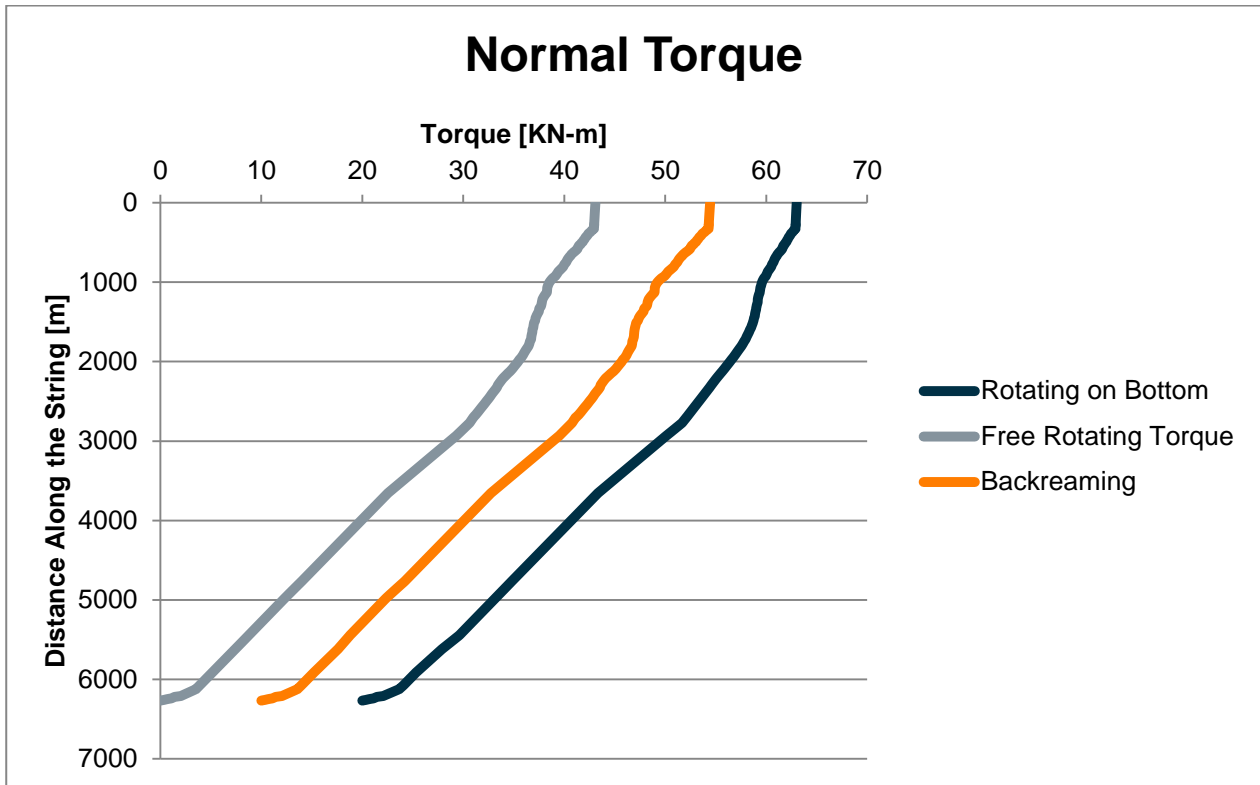
Figure 4-30 Normal torque trends.

4.3.1 Effects of viscous drag on torque.

The torque trends had been evaluated using flow rates 50, 100, 300, 400 and 500 GPM.
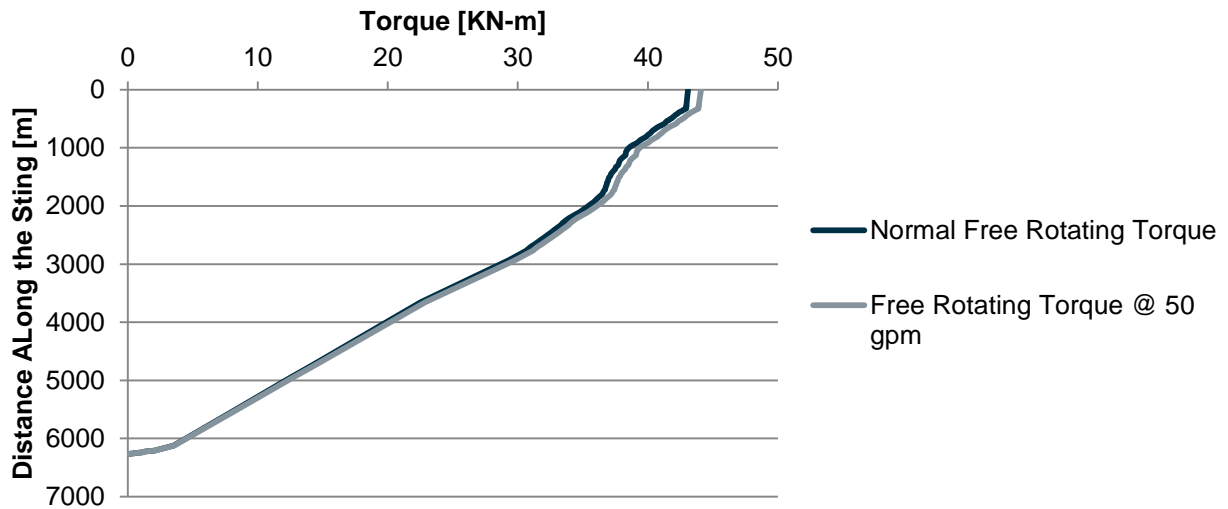
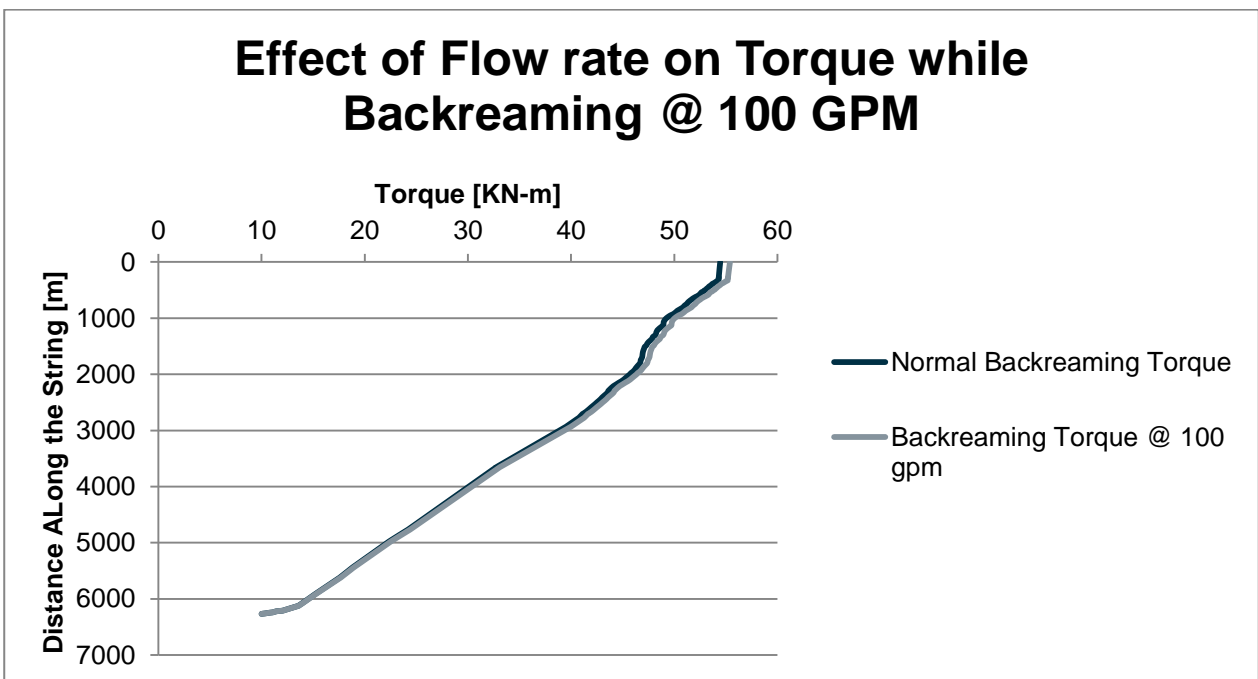**Figure 4-31 Effect of flow rate on free rotating torque at 50 GPM**
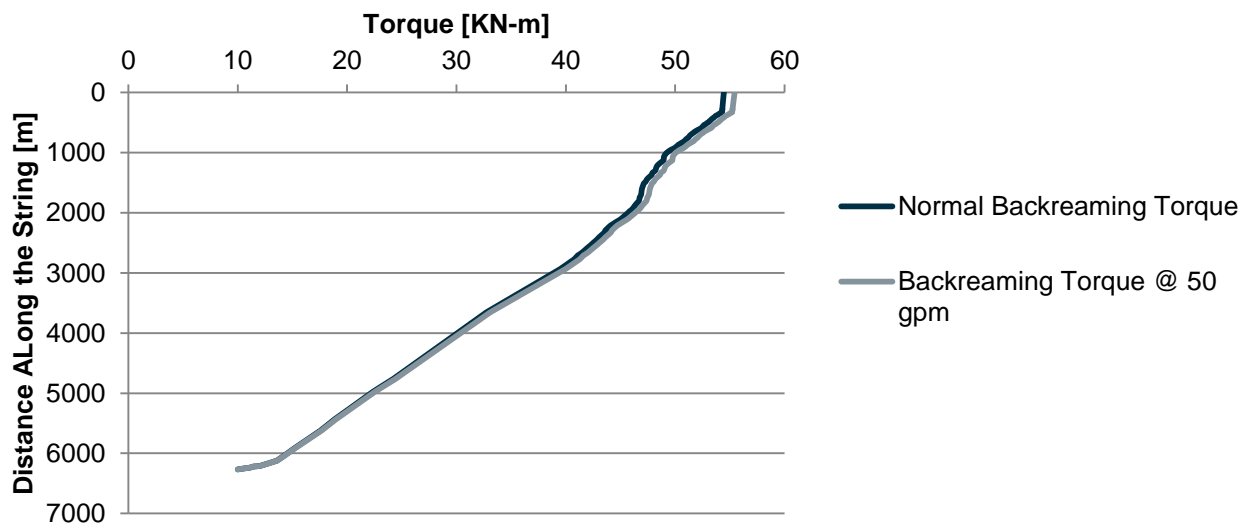
Figure 4-32 Effect of flowrate of backreaming torque at 50 GPM flowrate

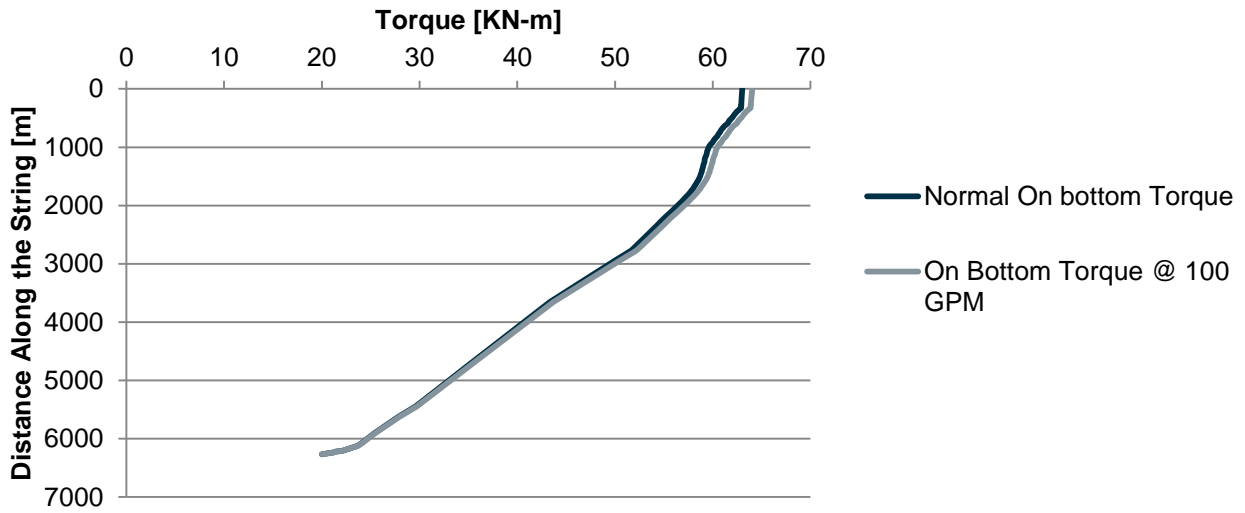Figure 4-33 Effect of flowrate on torque while rotation on bottom at 50 GPM flowrate
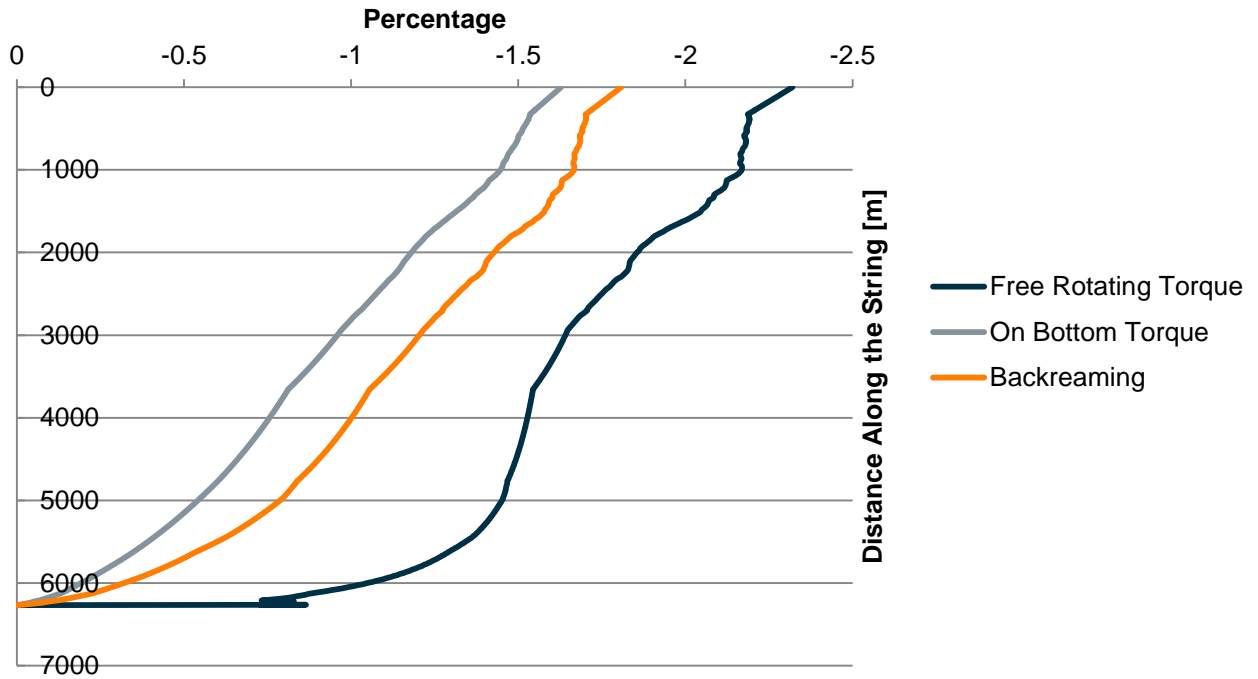
Figure 4-34 Percentage difference in torques at 0 and 50 GPM

Due to the viscous drag friction the torque losses encountered along the string, free rotating torque is the most affected one, while the on bottom torque is the least affected. The differences are not very significant in case of 50 GPM. We can further take the evaluation process to 100 GPM.
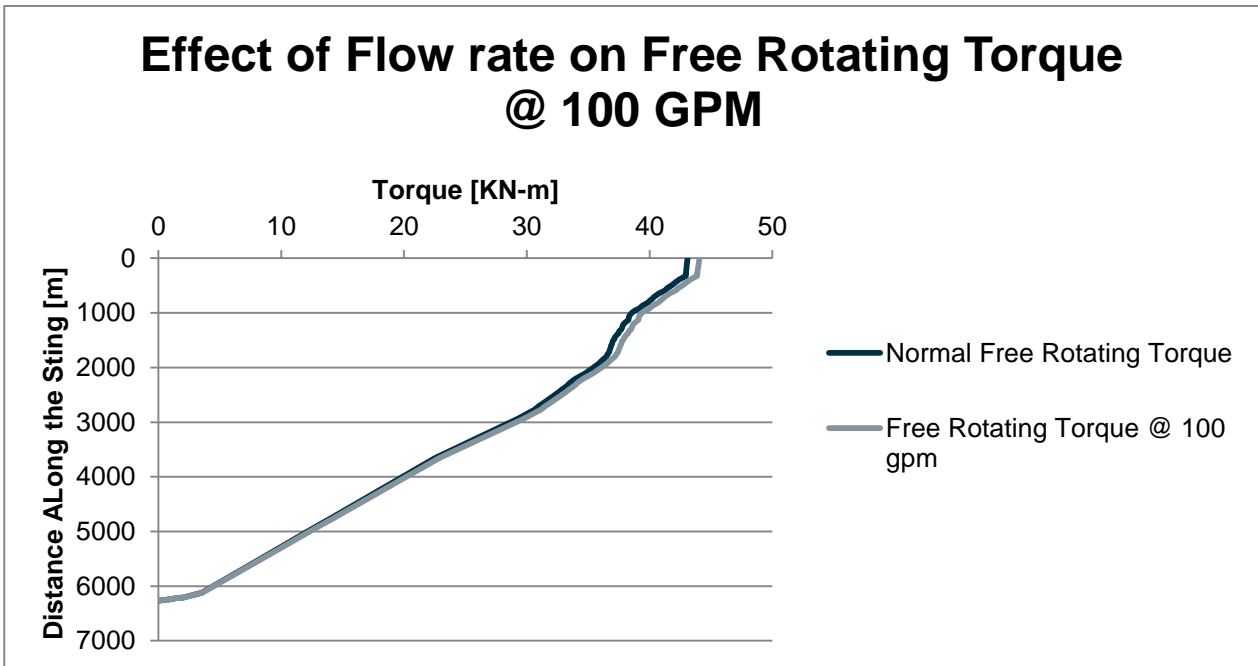
Figure 4-35 Effect of flow rate on free rotating torque at 100 GPM

Figure 4-36 Effect of flowrate of backreaming torque at 100 GPM flowrate

Figure 4-37 Effect of flowrate on torque while rotation on bottom at 100 GPM flowrate
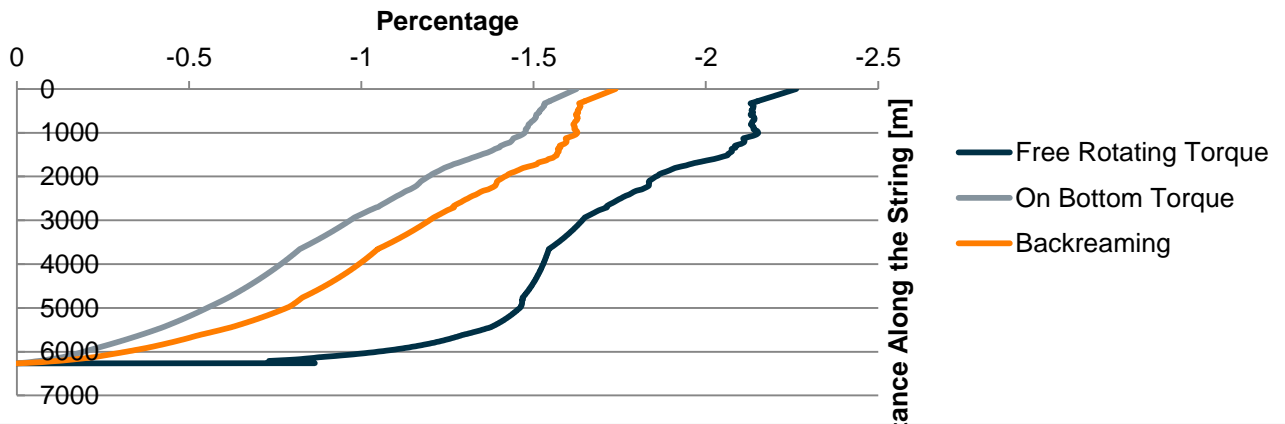
Figure 4-38 Percentage difference in torques at 0 and 100 GPM

In this case also the same trends and results were obtained. The most affected torque is the free rotating torque and the least affected is torque on bottom. The differences are slightly higher. Now we will see the effects of 300 GPM flowrate.
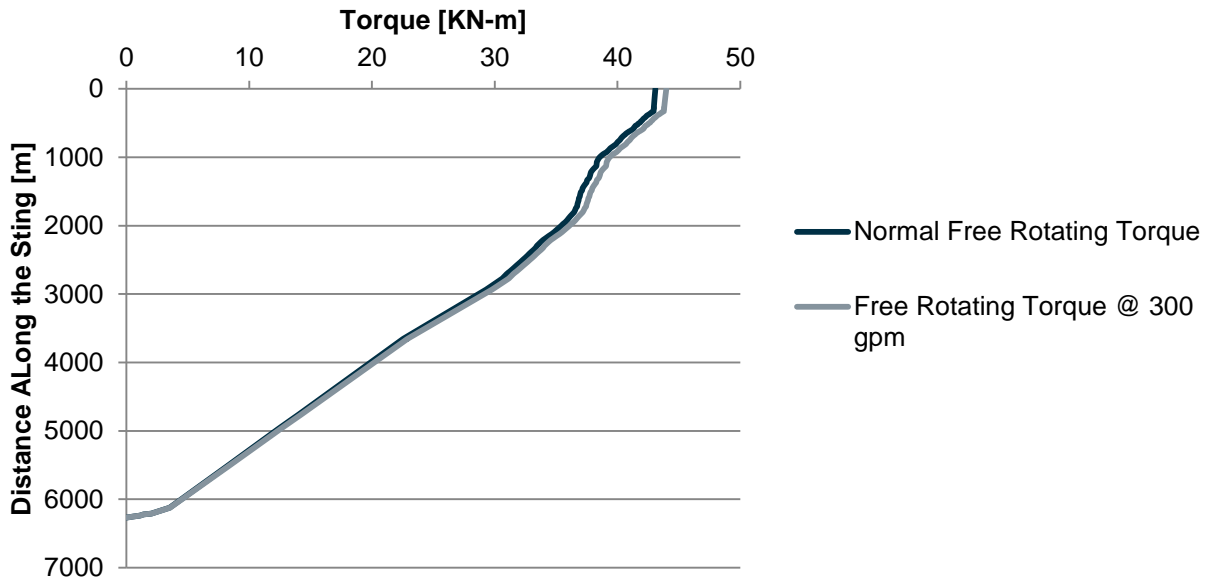
Figure 4-39 Effect of flow rate on free rotating torque at 300 GPM

Figure 4-40 Effect of flowrate of backreaming torque at 300 GPM flowrate

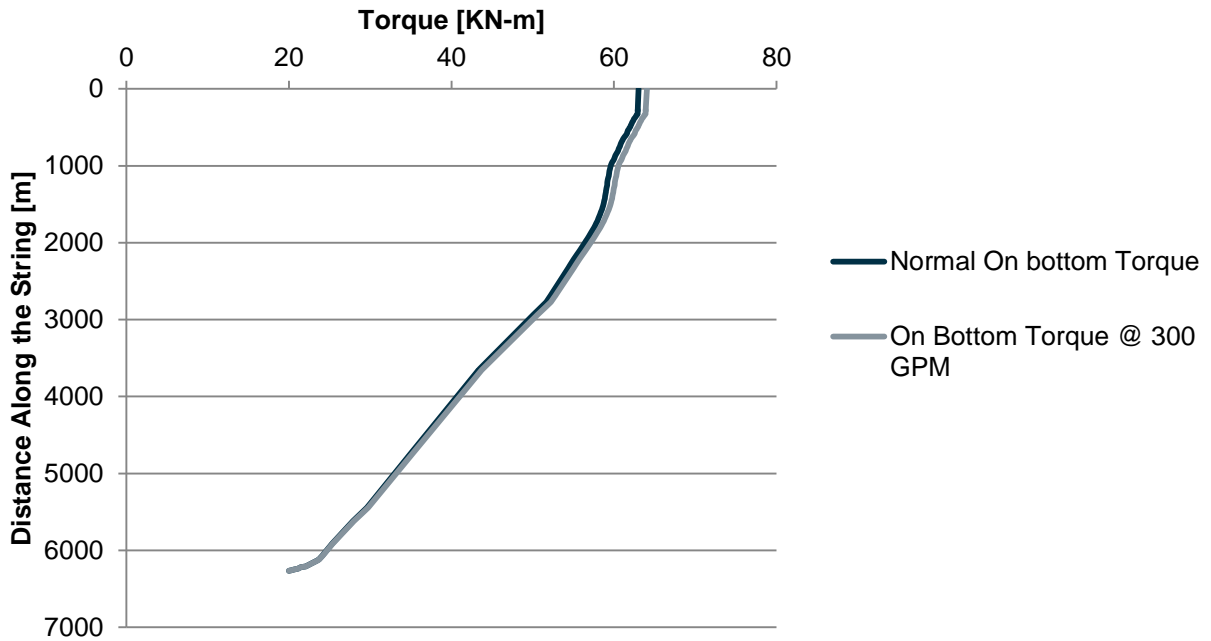**Figure 4-41 Effect of flowrate on torque while rotation on bottom at 300 GPM flowrate**
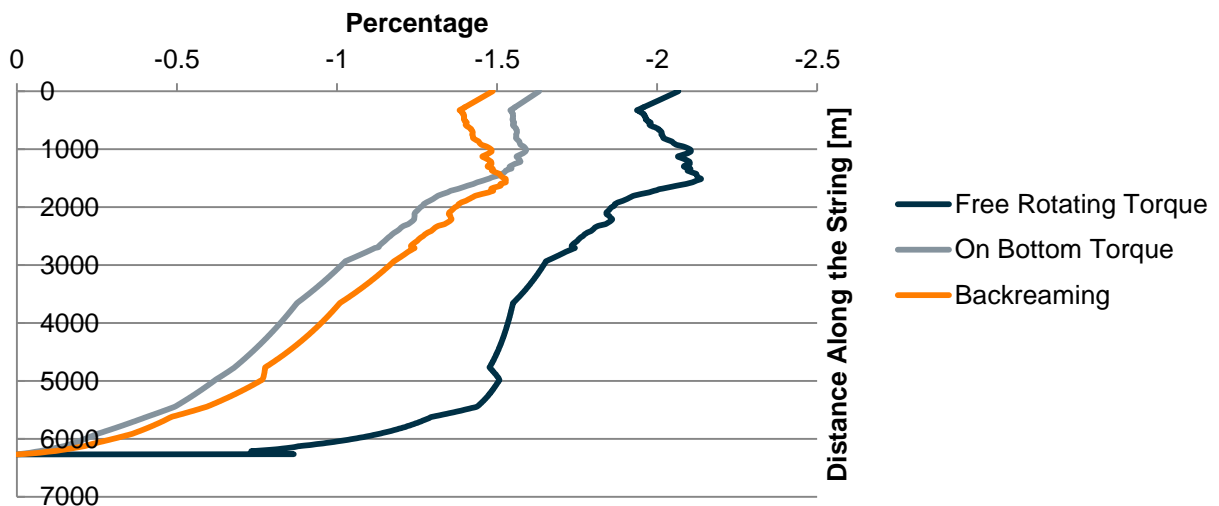

Figure 4-42 Percentage difference in torques at 0 and 300 GPM

In this case the backreaming torque has suspicious behavior the other trends looks normal. As the flow rate increases the torque increases as well due to the increase in friction which is mostly due

to the fact that the velocity of fluid is getting higher with flowrate. Now we see the effects for 400 GPM flowrate.
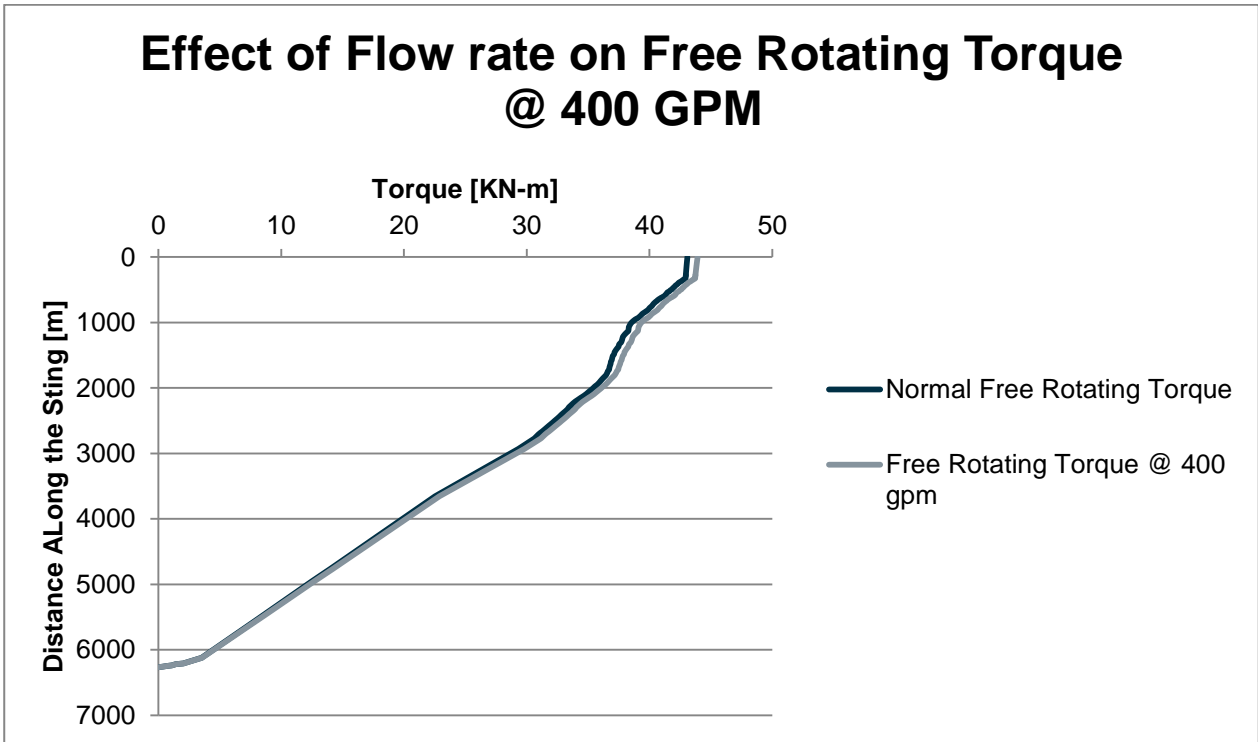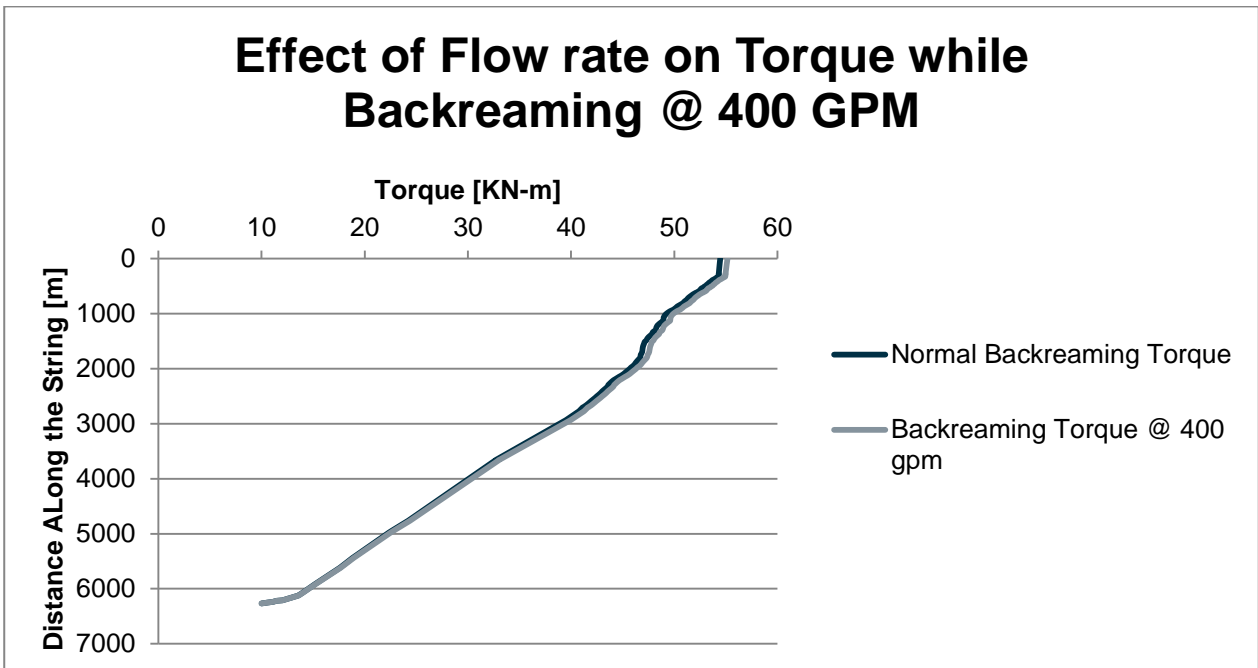
Effect of Flow rate on Free Rotating Torque @ 400 GPM

Torque [KN-m]

— Normal Free Rotating Torque

— Free Rotating Torque @ 400 gpm

Figure 4-43 Effect of flow rate on free rotating torque at 400 GPM

Effect of Flow rate on Torque while Backreaming @ 400 GPM

Torque [KN-m]

— Normal Backreaming Torque

— Backreaming Torque @ 400 gpm

Figure 4-44 Effect of flowrate of backreaming torque at 400 GPM flowrate

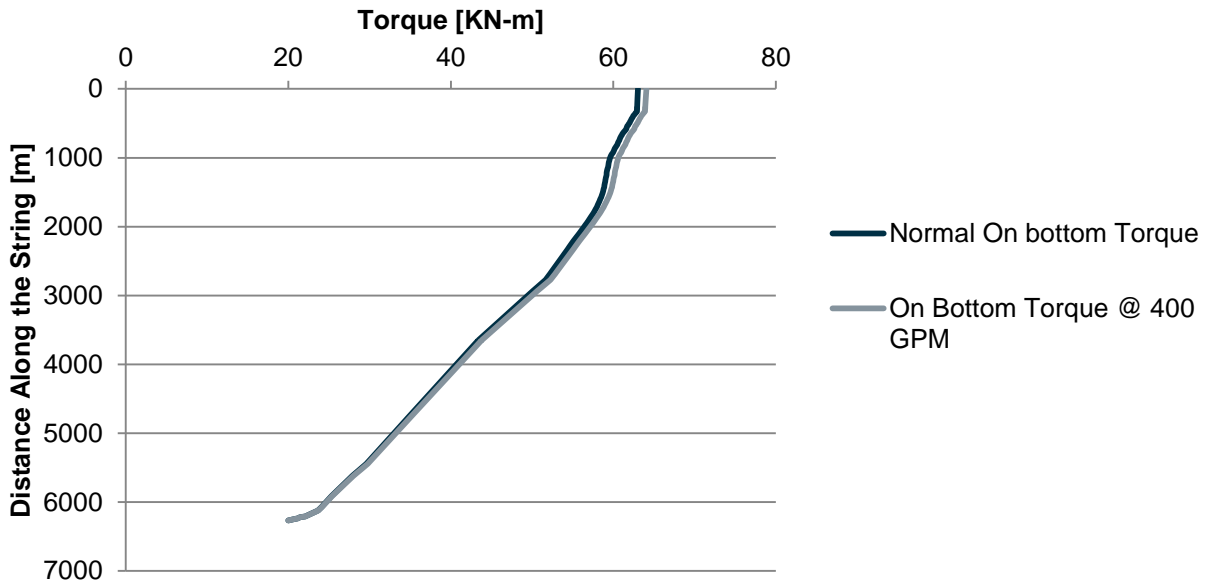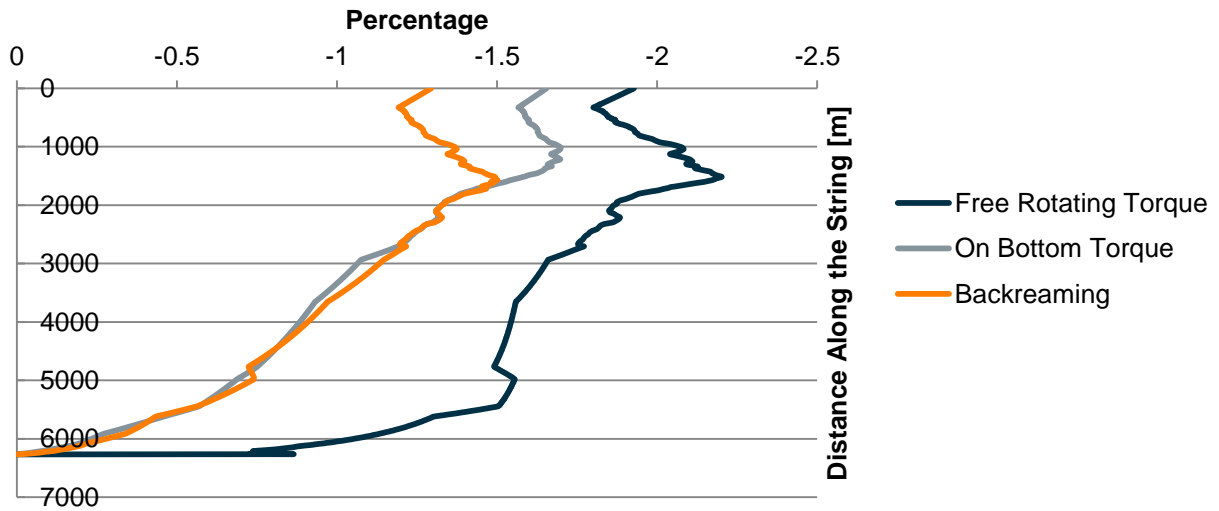**Figure 4-45 Effect of flowrate on torque while rotation on bottom at 400 GPM flowrate**

Figure 4-46 Percentage difference in torques at 0 and 400 GPM

The difference in back-reaming torque reduces abruptly in shallower depths. But again the differences are not very significant. Let see the results for 500 GPM flowrate.

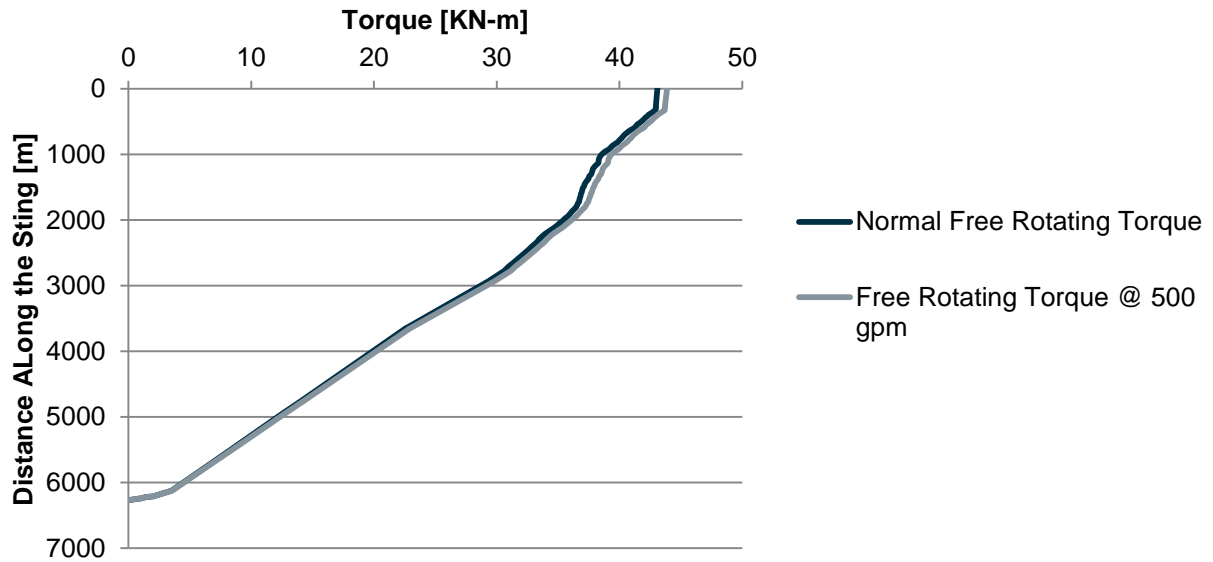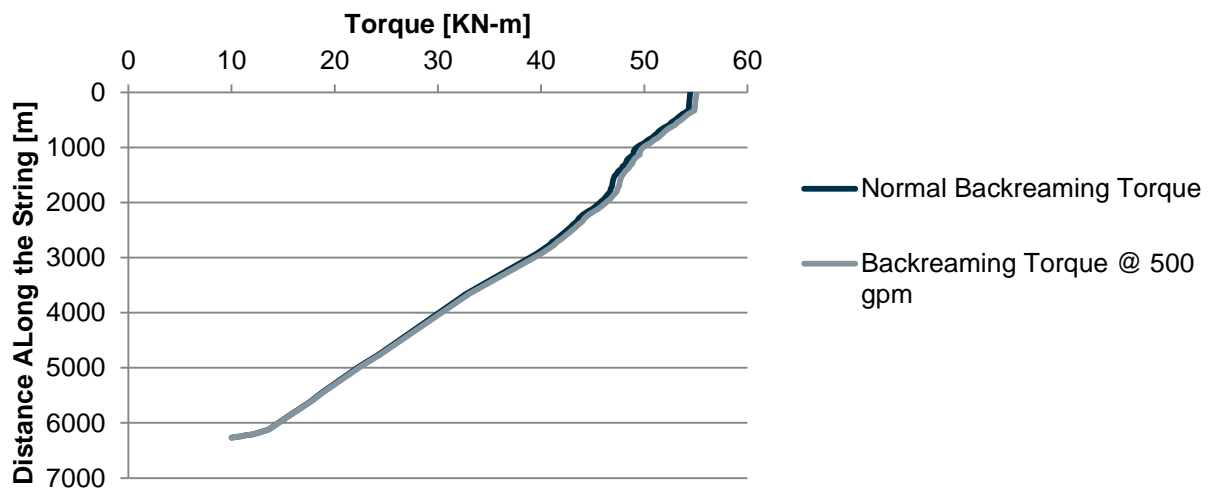**Figure 4-47 Effect of flow rate on free rotating torque at 500 GPM**

Figure 4-48 Effect of flowrate of backreaming torque at 500 GPM flowrate

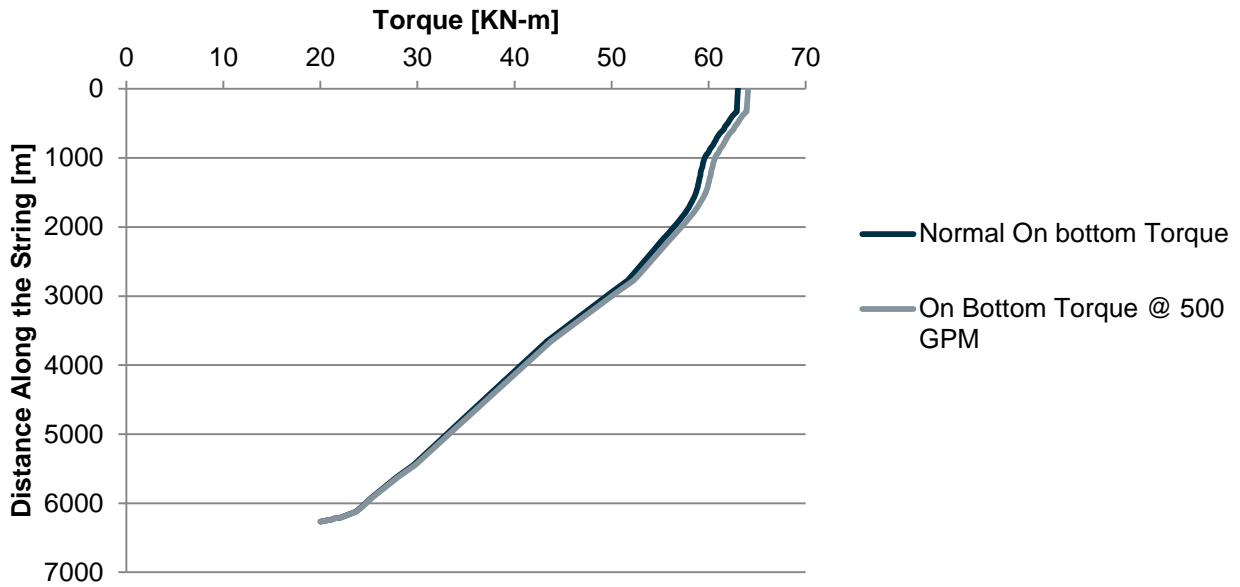**Figure 4-49 Effect of flowrate on torque while rotation on bottom at 500 GPM flowrate**
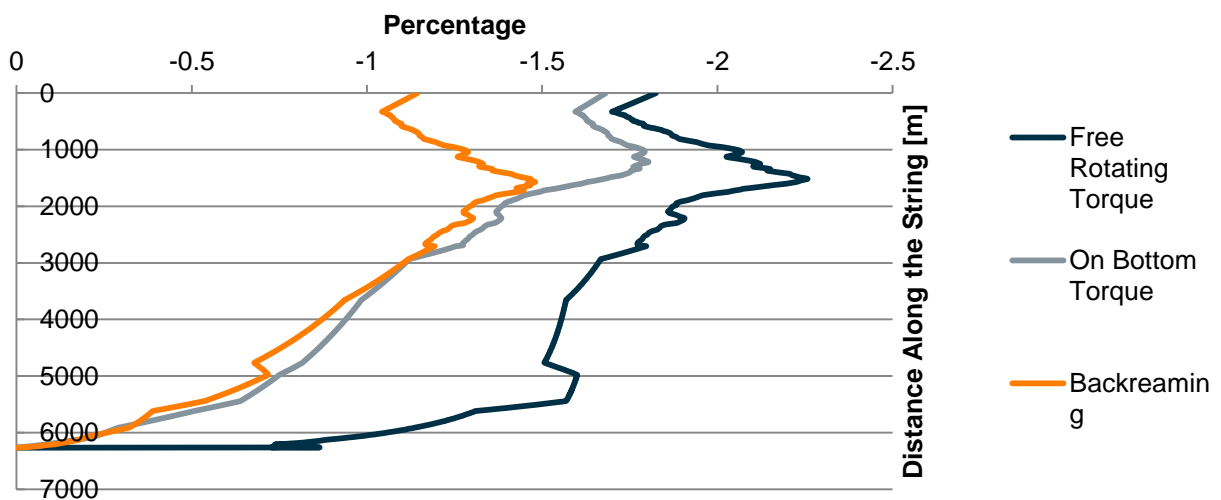

Figure 4-50 Percentage difference in torques at 0 and 500 GPM

From Figure 4-31 to Figure 4-50, it is quite obvious there are not much effects of viscous friction on torque. The torque while backreaming is anyhow affected by viscous drag. This is due to the simultaneous axial and rotational movement of pipe.

Next section deals with the effect of weight on bit on torque.

4.3.2 Effects of WOB on torque

This section deals with the investigation of effects of WOB on torque. For this analysis the 25 Klbf WOB is set as standard and the effects were compared with torques obtained by 30, 35, 40, 45 and 50 Klbf WOB.
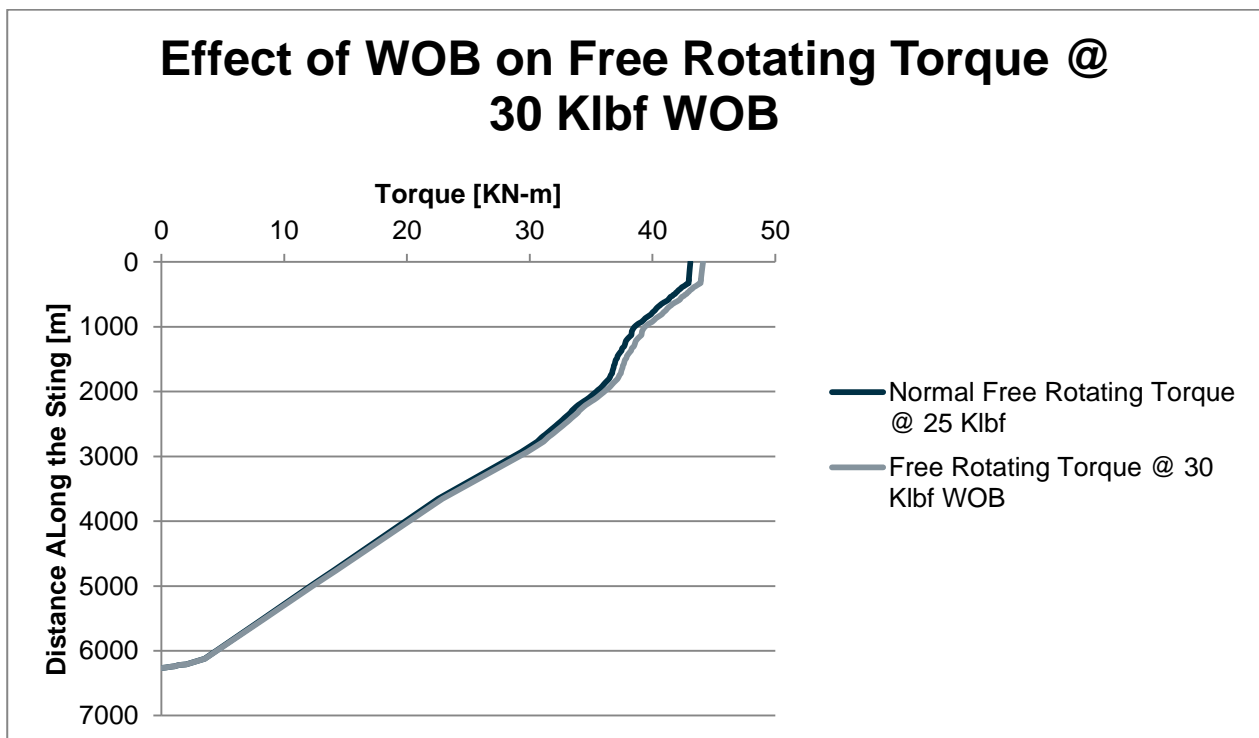

Figure 4-51 Effects of WOB on free rotating torque at 30 Klbf WOB

Figure 4-52 Effect of WOB on torque while backreaming at 30 Klbf WOB

Figure 4-53 Effect of WOB on torque while rotating on bottom at 30 Klbf WOB

Figure 4-54 Percentage difference in torques at 25 and 30 Klbf WOB

In this case the most affected one is free rotating torque. But the behavior of on bottom torque is a bit different. We further take this with 35 Klbf WOB

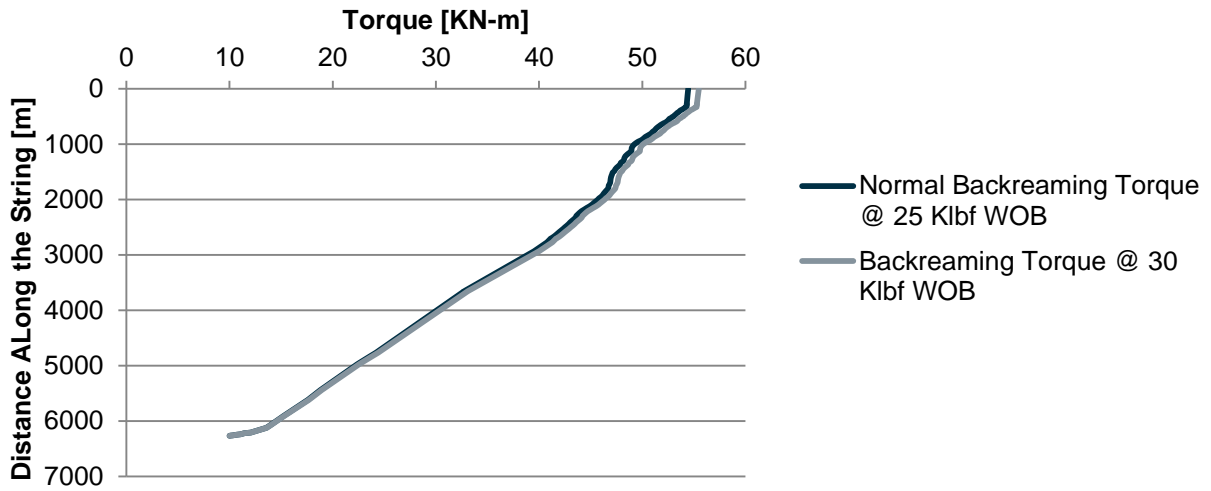**Figure 4-55 Effects of WOB on free rotating torque at 35 Klbf WOB**

Figure 4-56 Effect of WOB on torque while backreaming at 35 Klbf WOB

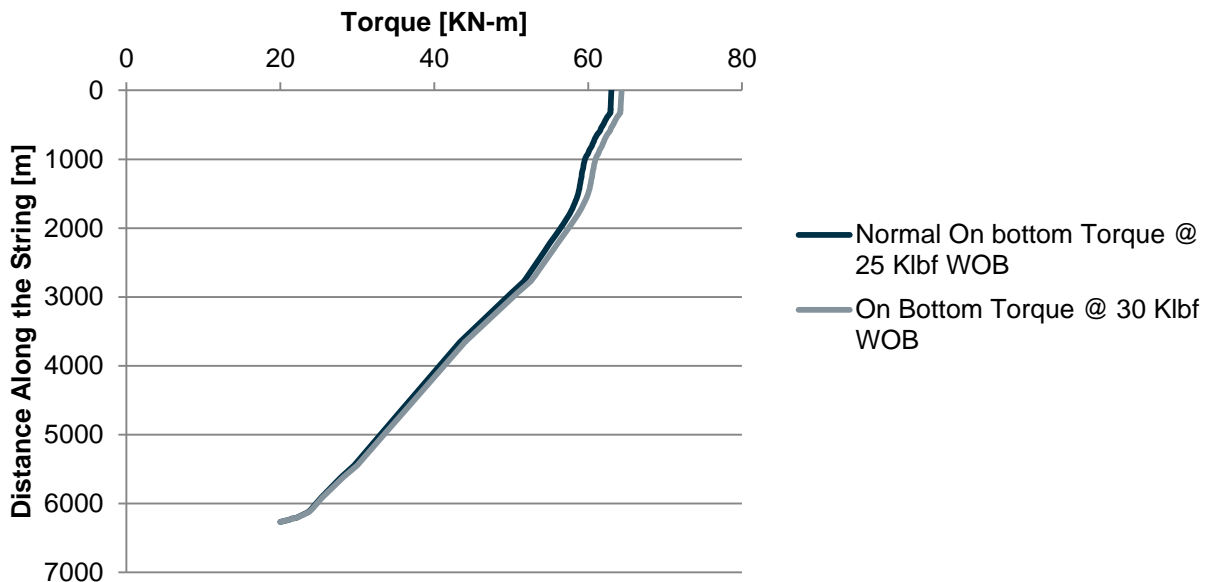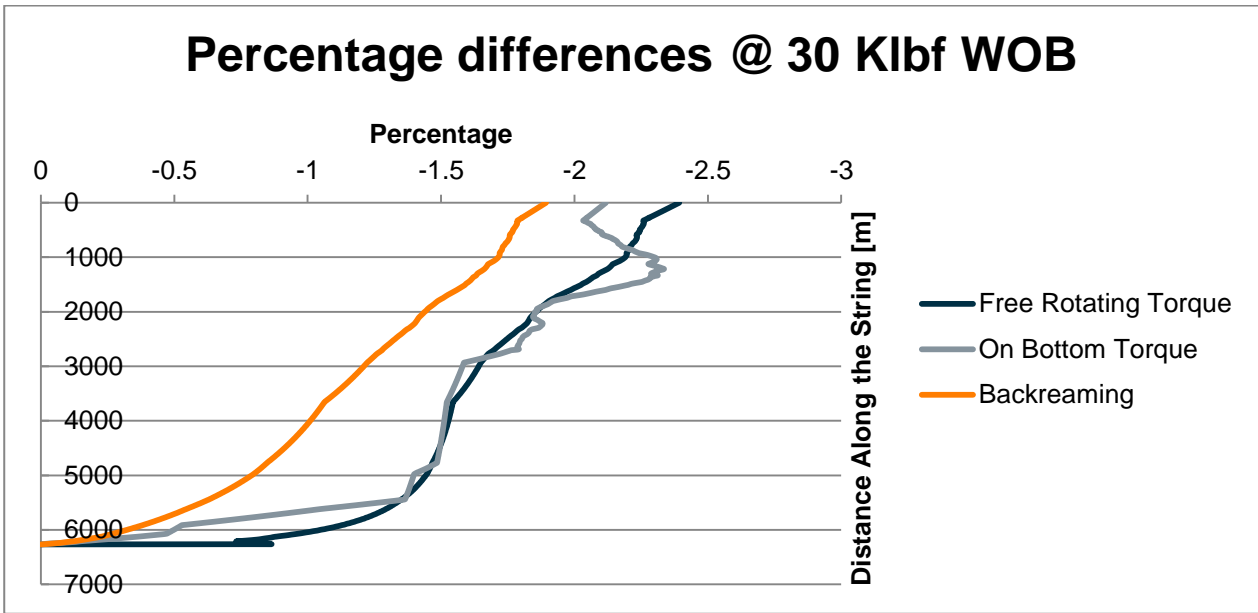**Figure 4-57 Effect of WOB on torque while rotating on bottom at 35 Klbf WOB**

Figure 4-58 Percentage difference in torques at 25 and 35 Klbf WOB

Figure 4-59 Effects of WOB on free rotating torque at 40 Klbf WOB

Figure 4-60 Effect of WOB on torque while backreaming at 40 Klbf WOB

Figure 4-62 Percentage difference in torques at 25 and 40 Klbf WOB
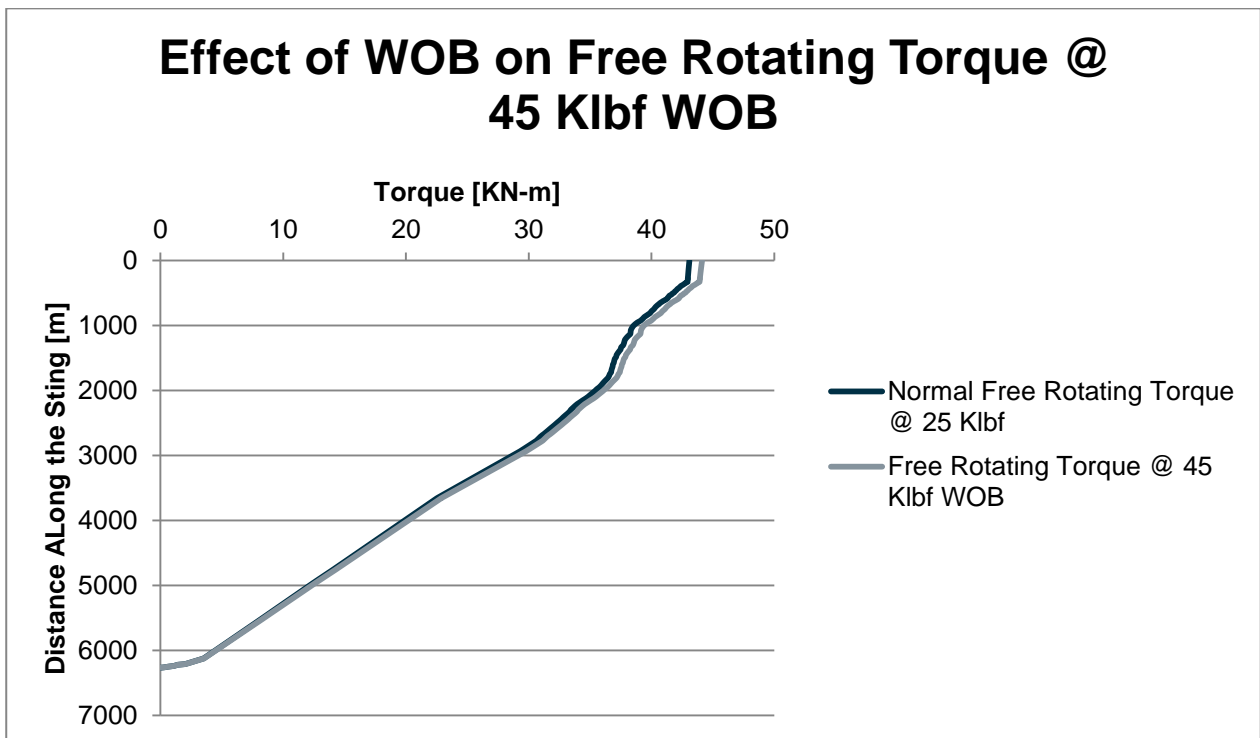
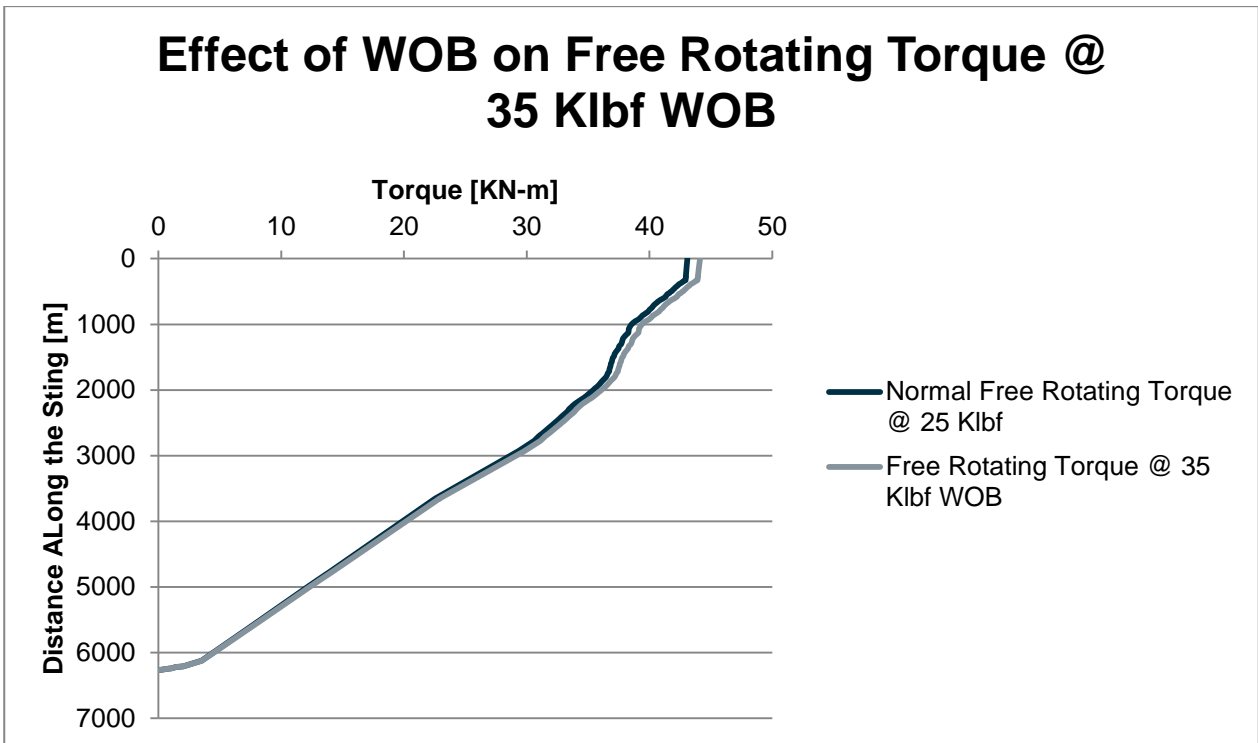

Figure 4-63 Effects of WOB on free rotating torque at 45 Klbf WOB

Effect of WOB on Torque while Backreaming @ 45 Klbf WOB

Torque [KN-m]

Normal Backreaming Torque @ 25 Klbf WOB

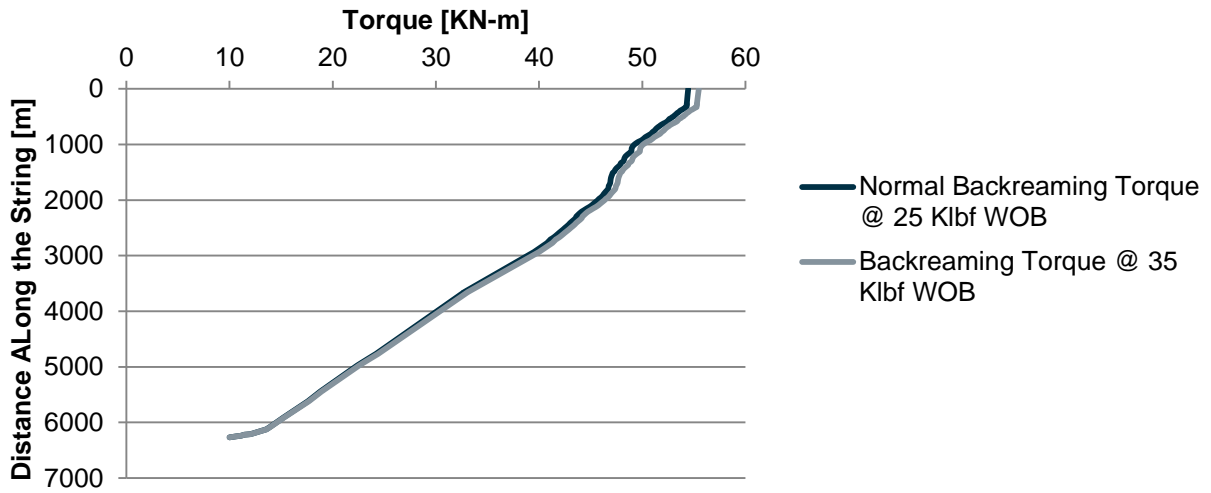Backreaming Torque @ 45 Klbf WOB

Distance ALong the String [m]
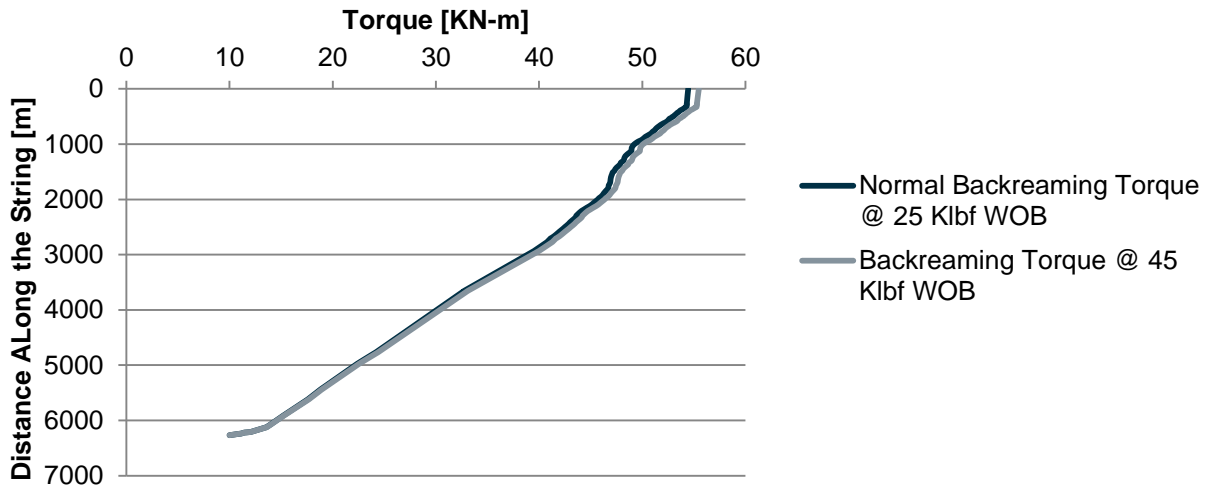
Figure 4-64 Effect of WOB on torque while backreaming at 45 Klbf WOB

Effect of WOB on Torque while Rotating on Bottom @ 45 Klbf WOB

Torque [KN-m]

Normal On bottom Torque @ 25 Klbf WOB

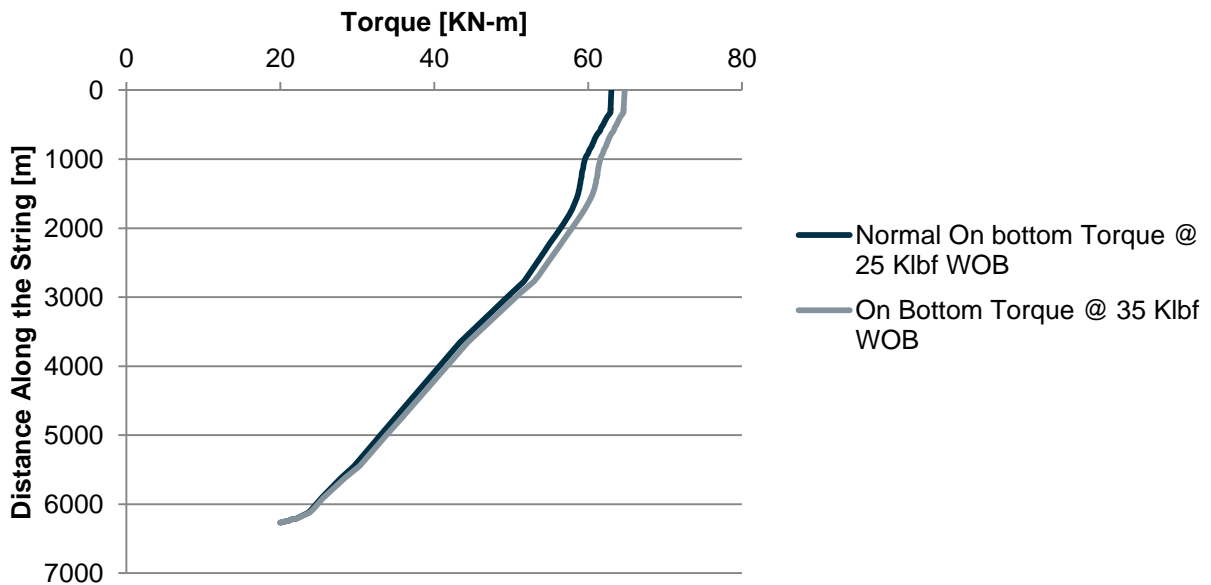On Bottom Torque @ 45 Klbf WOB

Distance ALong the String [m]
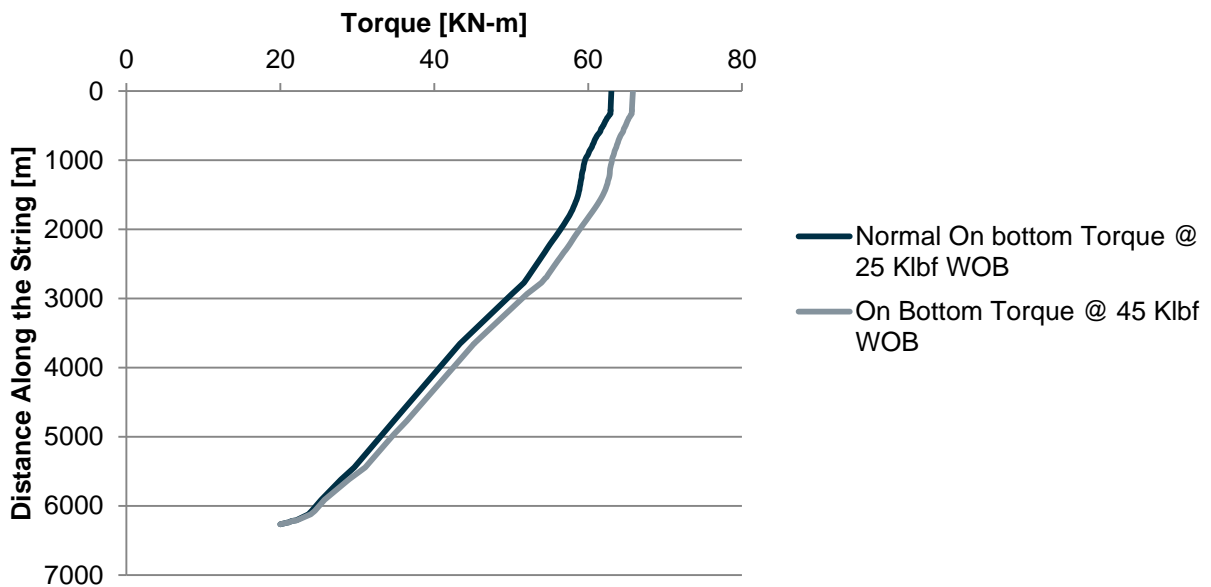
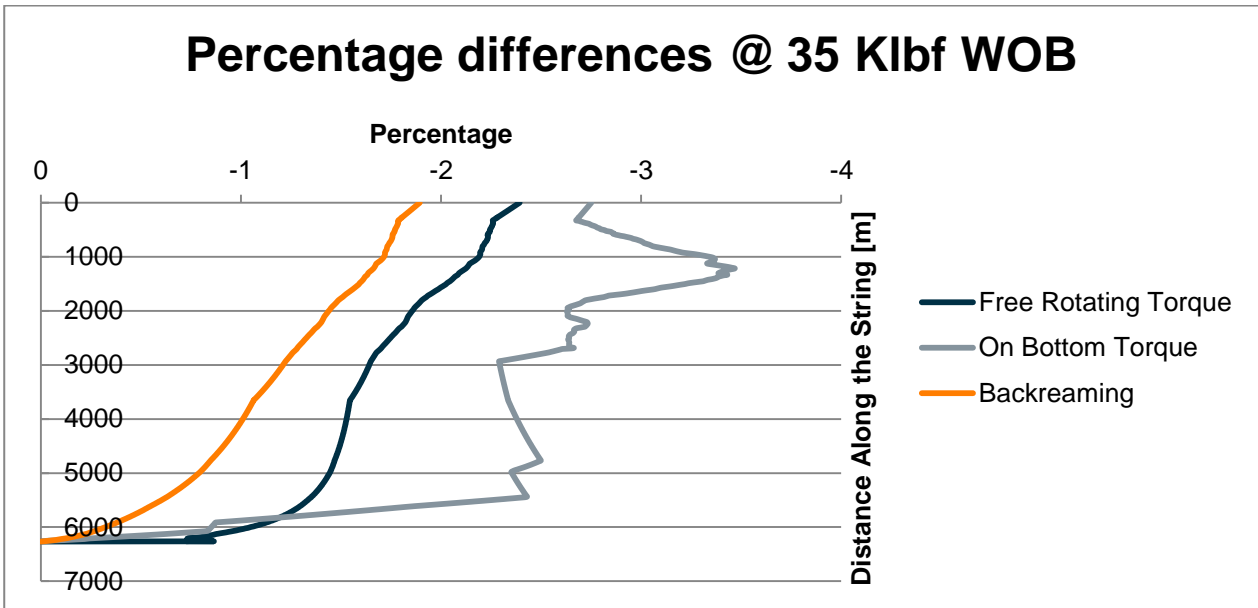**Figure 4-65 Effect of WOB on torque while rotating on bottom at 45 Klbf WOB**
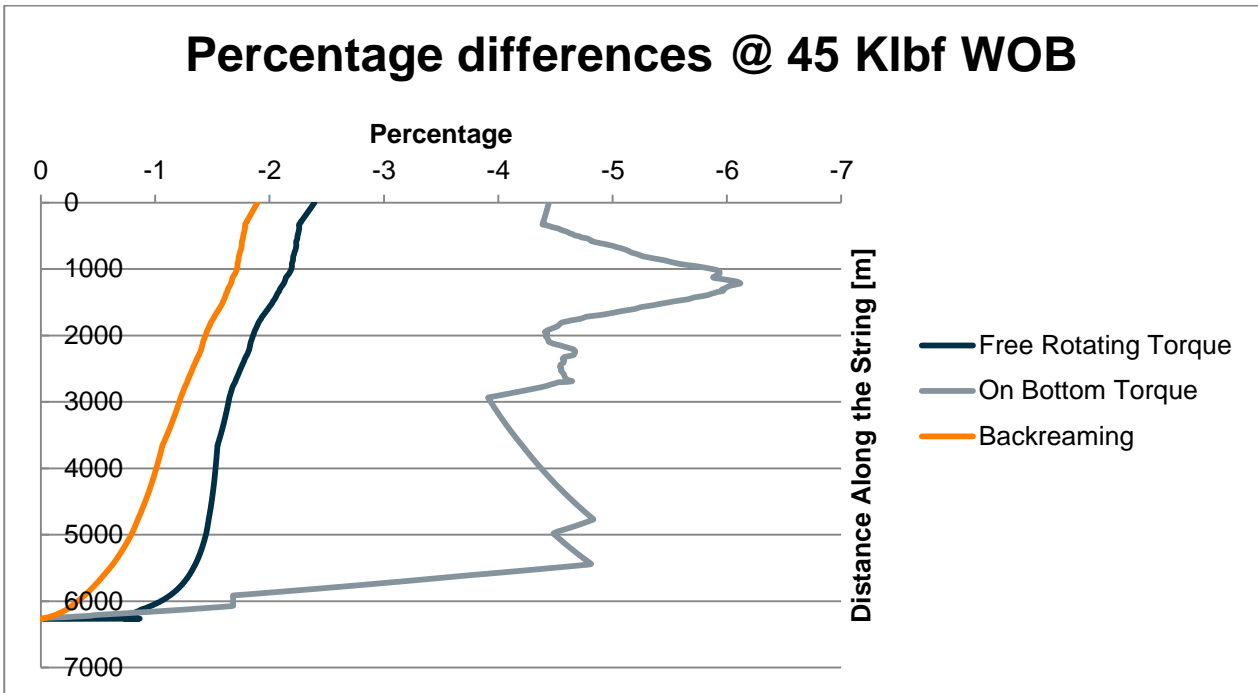
Figure 4-66 Percentage difference in torques at 25 and 45 Klbf WOB
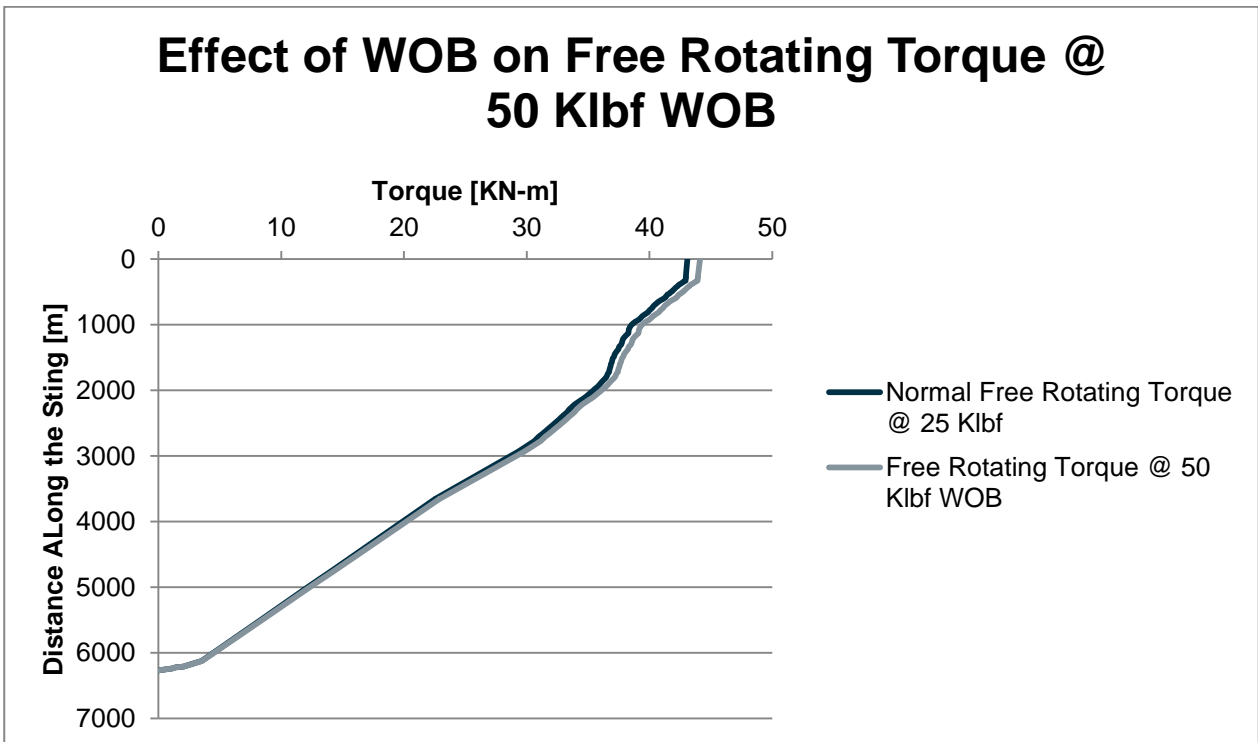
Figure 4-67 Effects of WOB on free rotating torque at 50 Klbf WOB

Effect of WOB on Torque while Backreaming @ 50 Klbf WOB

Torque [KN-m]
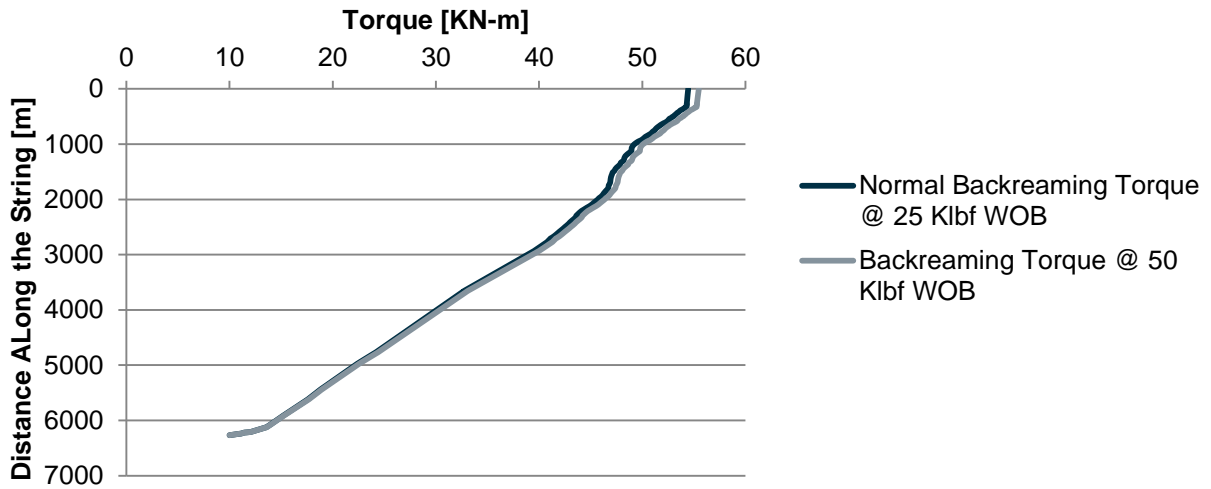
Figure 4-68 Effect of WOB on torque while backreaming at 50 Klbf WOB

Effect of WOB on Torque while Rotating on Bottom @ 50 Klbf WOB

Torque [KN-m]
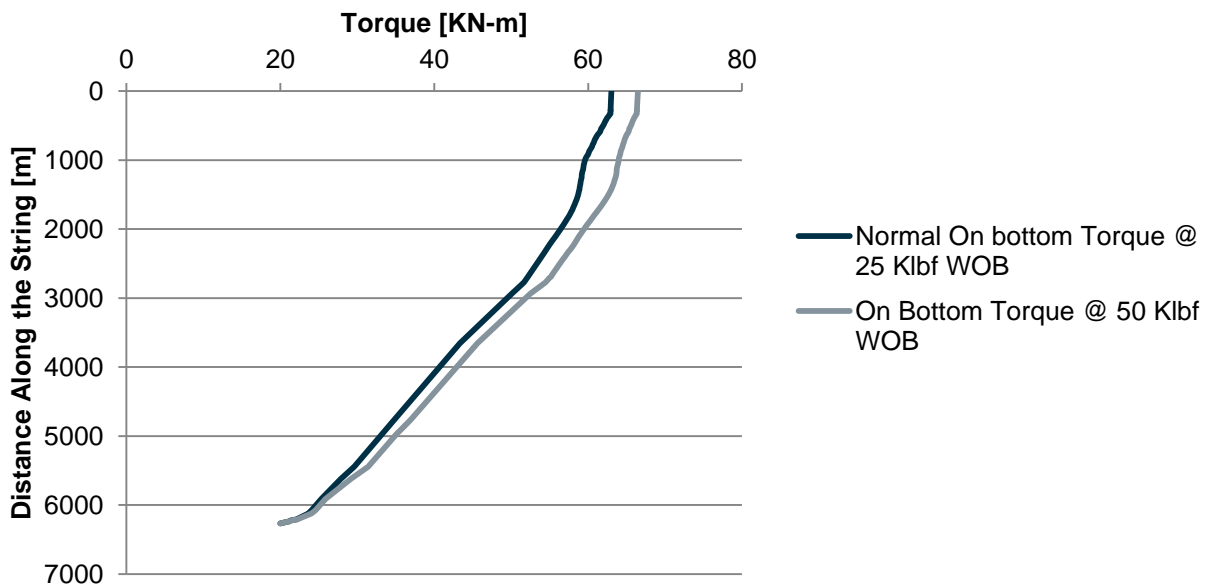
Figure 4-69 Effect of WOB on torque while rotating on bottom at 50 Klbf WOB

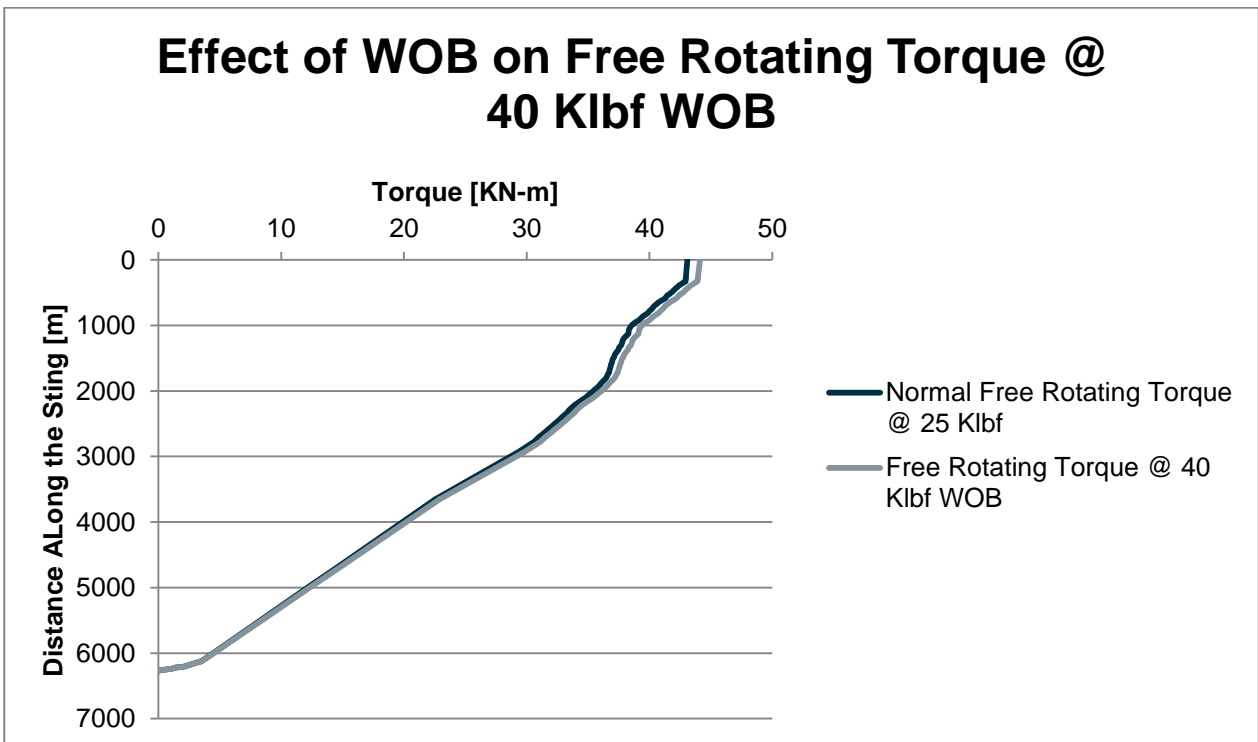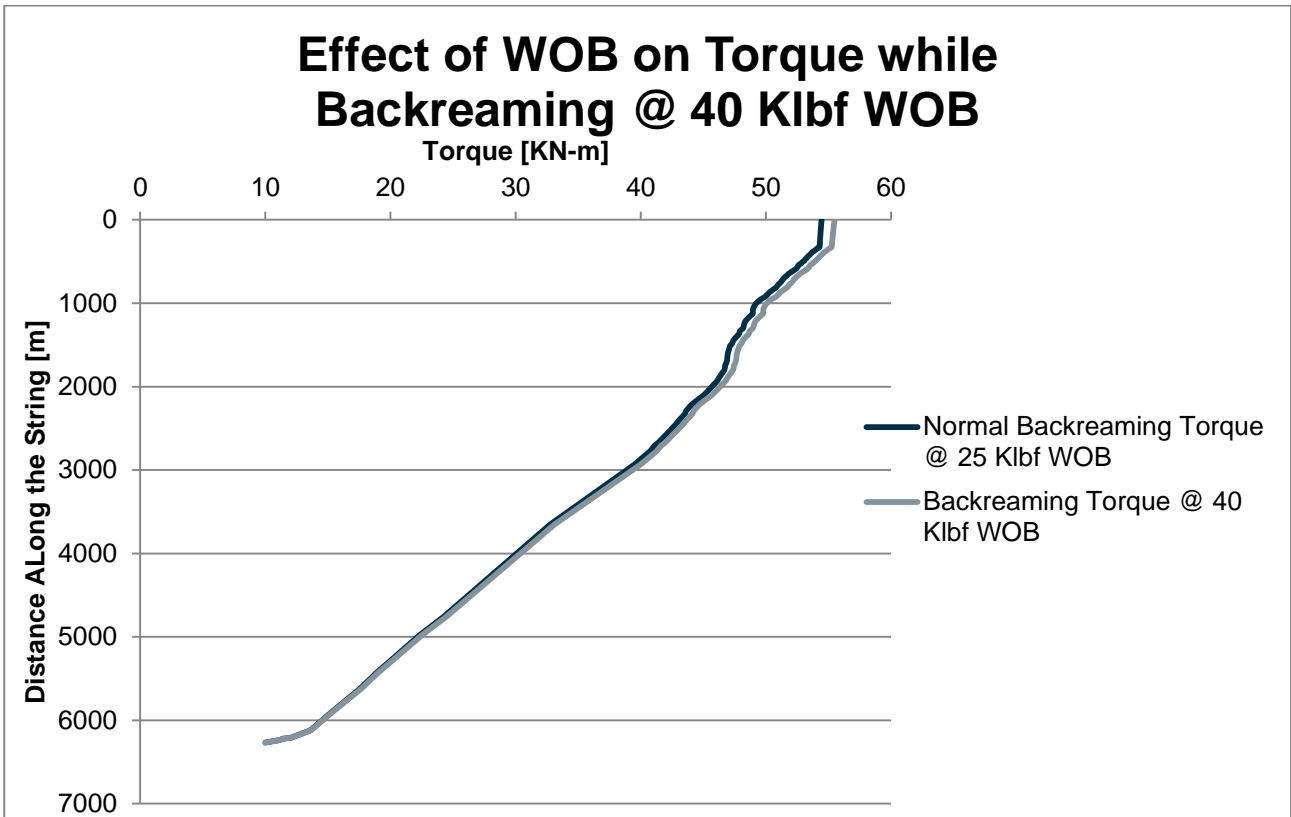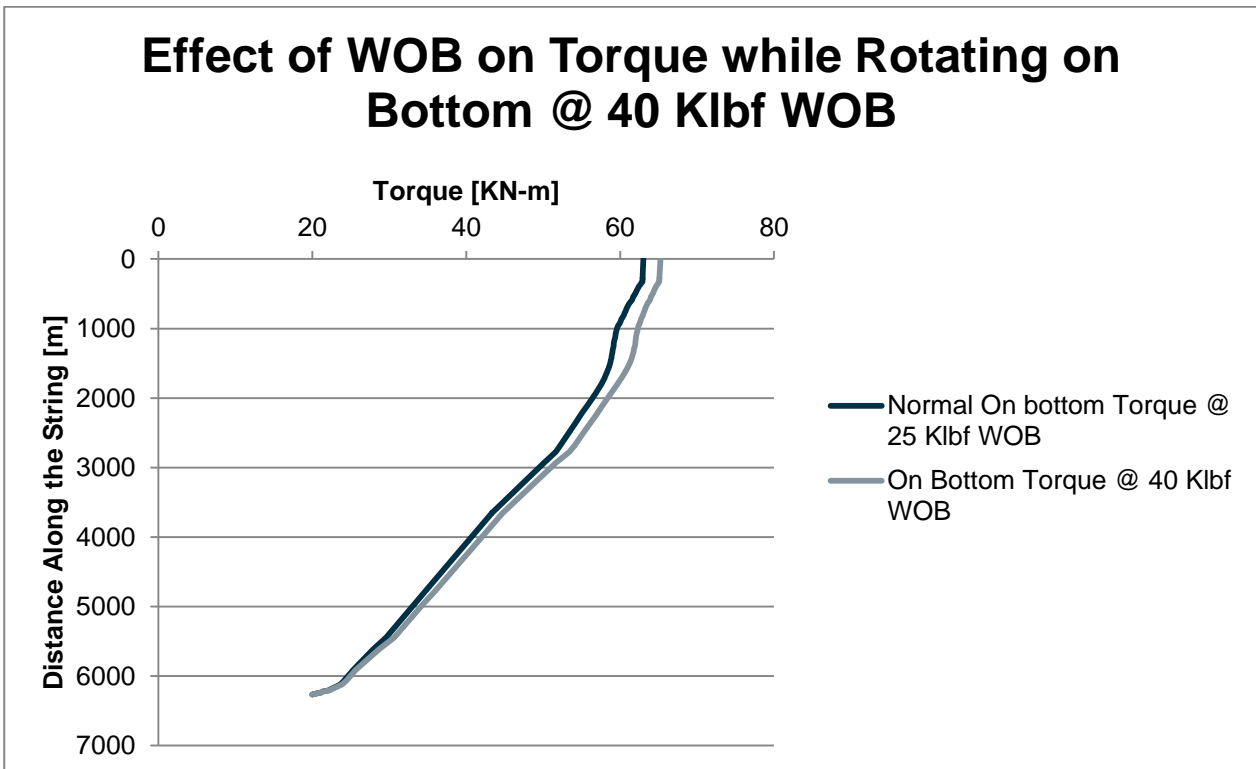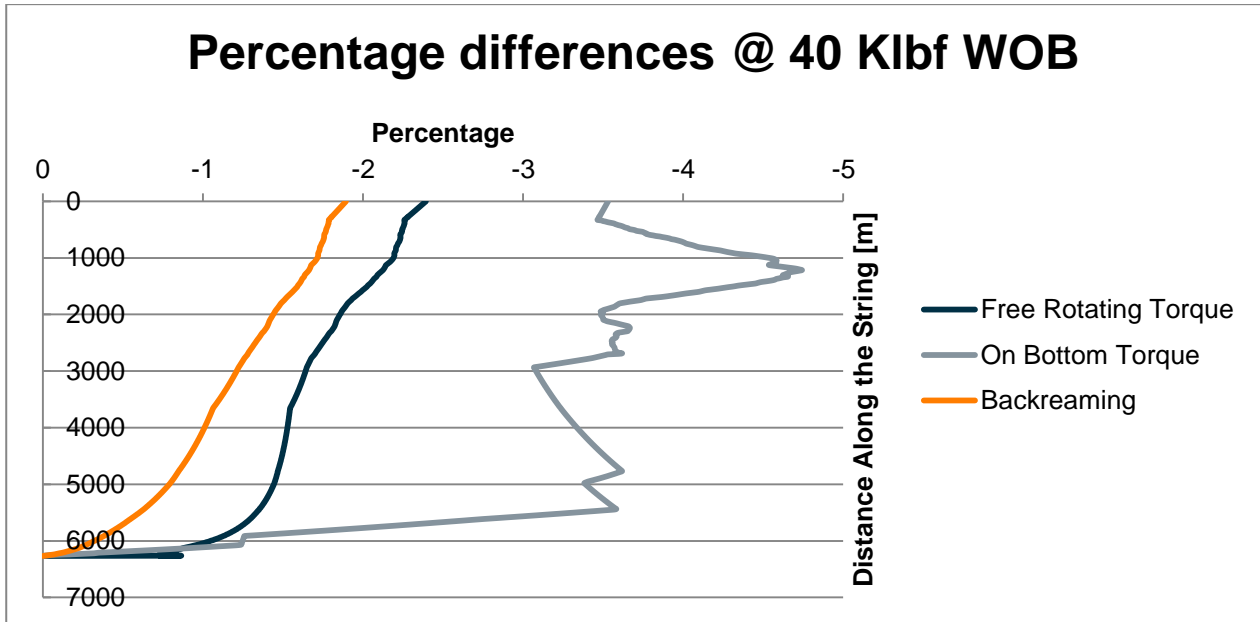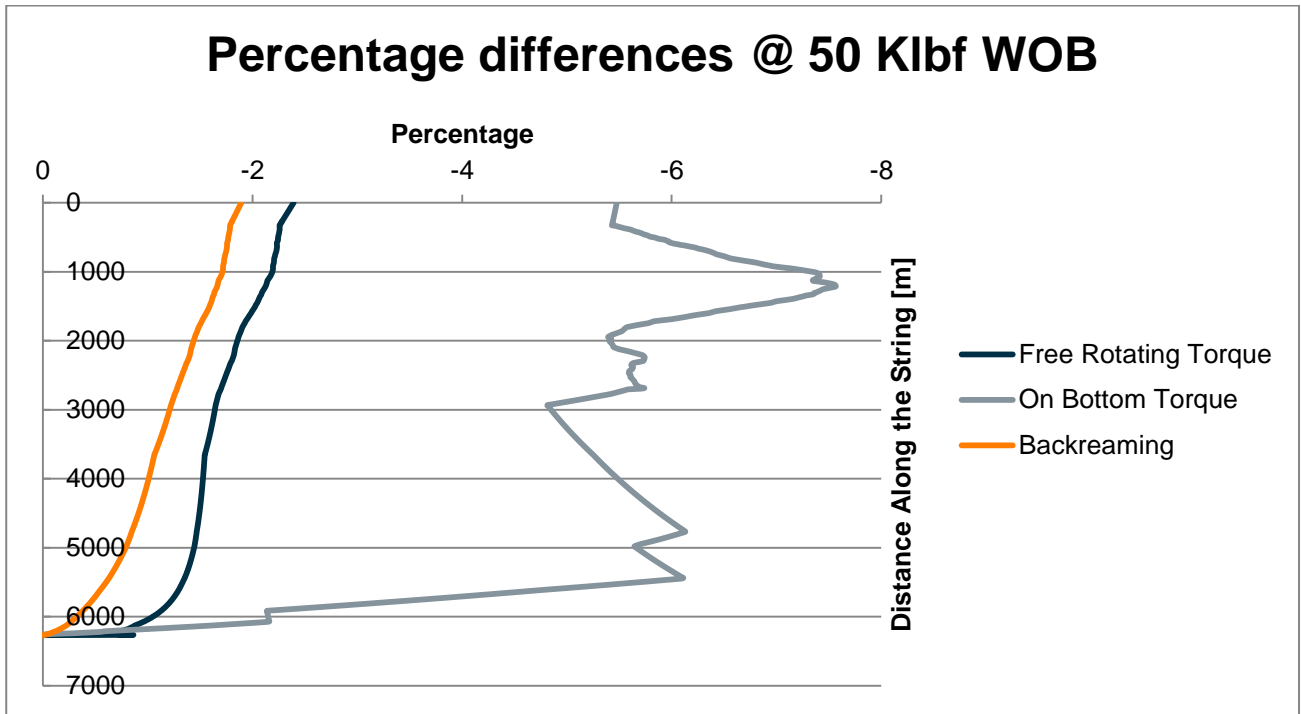**Figure 4-70 Percentage difference in torques at 25 and 30 Klbf WOB**

From Figure 4-51 to Figure 4-70 reveal that WOB is majorly affecting the torque while rotating on bottom. The reason is simple; when we apply more weight on bit while it is on bottom the additional force is required to rotate the bit due to the contact friction between rock and bit. Figure 4-71 to Figure 4-73 summarizes the effects of WOB on torque for various operations.
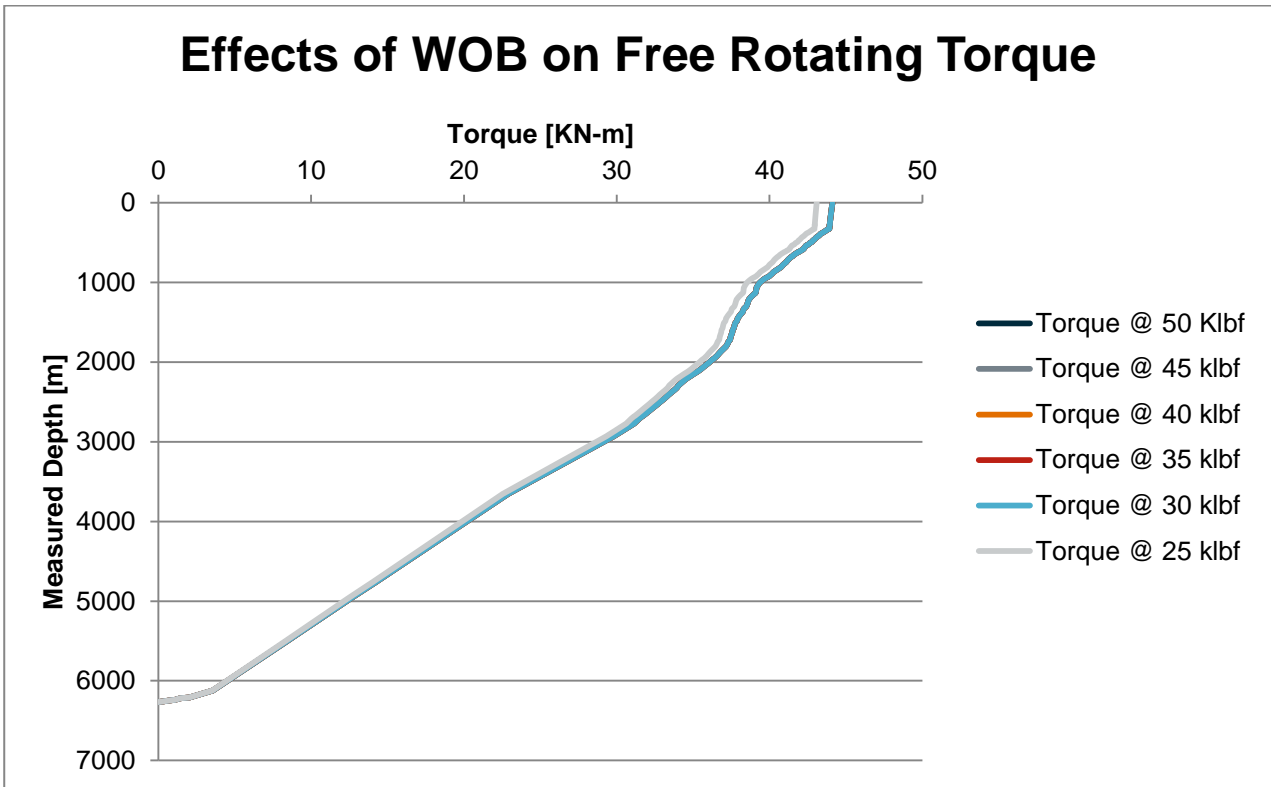
Figure 4-71 The overall effects of WOB on free rotating torque
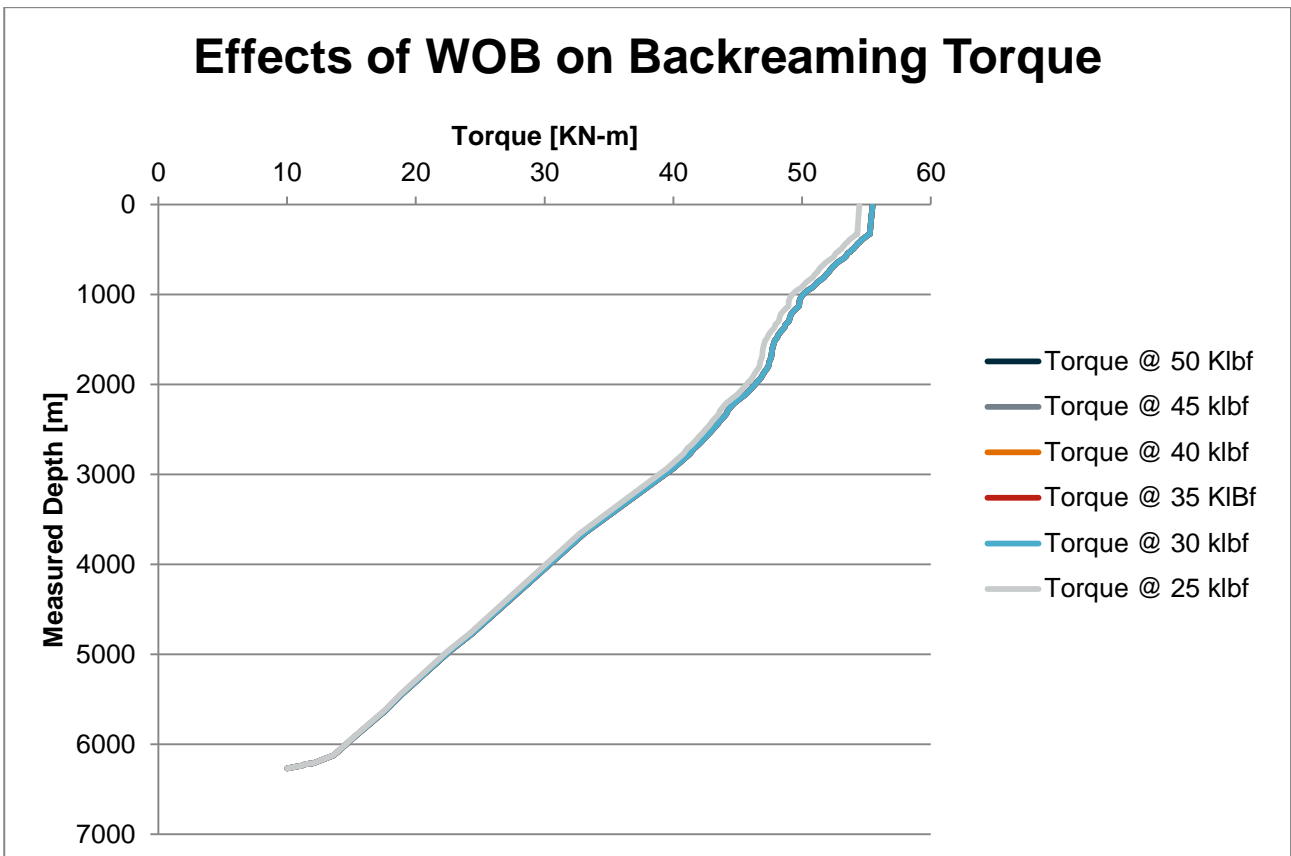
Effects of WOB on Torque, While Rotating on Bottom
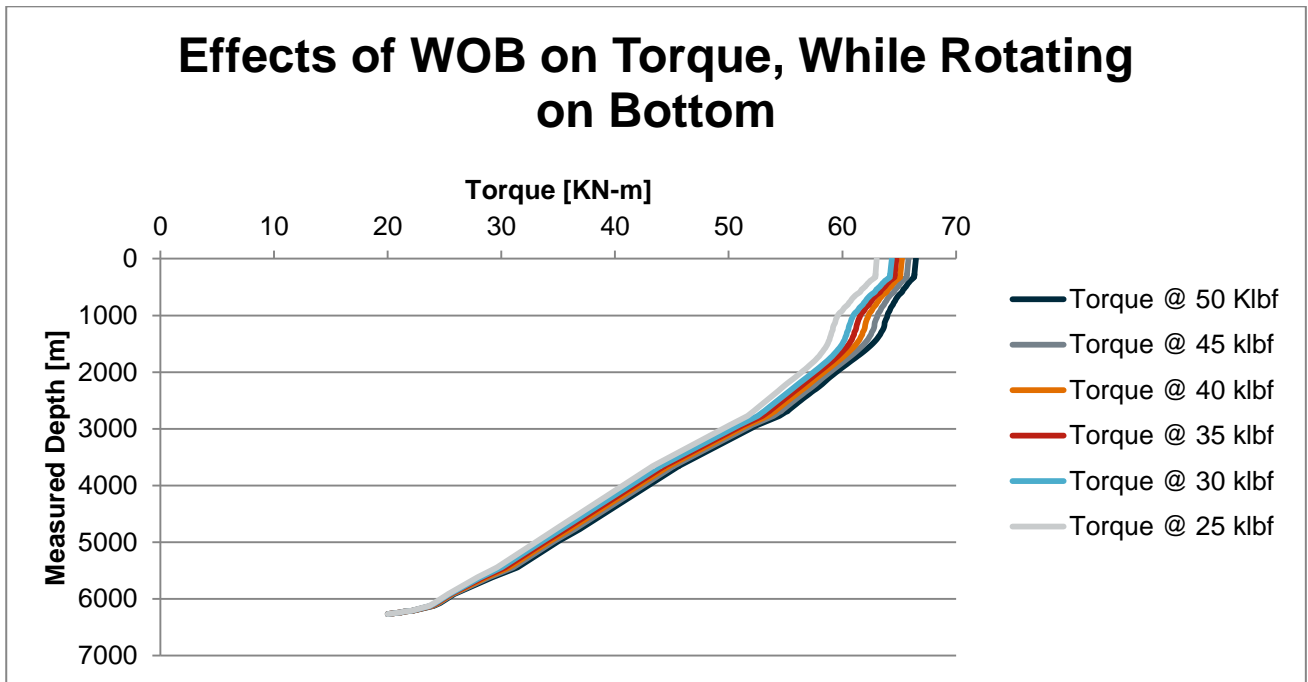
Figure 4-73 The overall effects of WOB on torque while rotating on bottom.

5 Conclusions & recommendations

In this chapter we will discuss the results the obtained by various analysis on torque and drag. We will try to give reasons of various behaviors and recommendations.

5.1 Hook load analysis

In section 4.2 we discussed the analysis of sheave friction and viscous drag forces on hook load. The effect of sheave friction is very obvious and in this analysis the maximum encountered effect is 17.6% while according to Luke, (1993)[11], this effect can be upto 19%. It is recommended to consider the effects of sheave friction must be considered while planning a well and during the torque and drag analysis and the weight of travelling block must be considered in order to accurately determine the hook load roadmap.

Viscous drag forces also came as an important factor which has considerable high effects on hook load especially when tripping in and in the hole of varying diameters. It can affect the hook load while tripping in up to 50 % as we encountered in our case for 500 GPM flow rate, but even without circulation this could be up to 25%. For tripping out it does not have much effect while circulating with higher flowrate. The main reason behind this effect is the total effective velocity. The effective velocity is total effective velocity considering the fluid velocity, string rotational velocity and tripping speed. It is recommended to use the robust available model for torque and drag analysis which can take care of various flow regimes together with combined velocities of string i.e. axial and rotational.

5.2 Torque analysis

In section 4.3 we discussed effects of viscous drag and weight on bit. We saw that the viscous drag has more effects on free rotating torque than on backreaming and on bottom torque. But the overall effects are not as much as were on hook load. But it is still wise to consider the effects of viscous drag while planning a well and establishing a torque and drag analysis.

We observe that WOB is mostly affecting torque while rotating on bottom but least on backreaming and free rotating torque, although the effects are not too big, but still it would be wise if we consider WOB while planning a well for torque analysis.

6 References

1. Johancsik, C.A., Friesen, D.B., Dawson, R., "Torque and Drag in Directional Wells – Prediction and Measurement", *Journal of Petroleum Technology,* June 1984.

2. Sheppard, M.C., Wick, C., Burgess, T., "Designing Well Paths To Reduce Drag and Torque", *SPE Drilling Engineering,* December 1987.

3. Maidla, E.E., Wojtanowicz, A.K. "Field Comparison of 2-D and 3-D Methods for Borehole Friction Evaluation in Directional Wells" SPE 16663 presented at *SPE Annual Technical Conference and Exhibition,* Dallas, Texas, September 1987.

4. Lesage, M., Falconer, I.G., Wick, C.J. "Evaluating Drilling Practice in Deviated Wells with Torque and Weight Data", *SPE Drilling Engineering*, September 1988.

5. Brett, J.F., Beckett, A.D., Holt, C.A., Smith, D.L. "Uses and Limitations of Drillstring Tension and Torque Models for Monitoring Hole Conditions", *SPE Drilling Engineering*, September 1989.

6. Lesso, W.G., Mullens, E., Daudey, J. "Developing a Platform Strategy and Predicting Torque Losses for Modelled Directional Wells in the Amauligak Field of the Beaufort Sea, Canada", SPE 19550 presented at the *Annual Technical Conference and Exhibition*, San Antonio, Texas, October 1989.

7. Aarrestad, T.V. "Effect of Steerable BHA on Drag and Torque in Wells", SPE 20929 presented at *Europec 90*, The Hague, Netherlands, October 1990.

8. Wilson, T.P., Yalcin, O. "Two Double Azimuth-Double S-Shaped Wells Planned and Drilled Using Torque and Drag Modelling" SPE/IADC 23848 presented at the *SPE/IADC Drilling Conference*, New Orleans, Louisiana, February 1992.

9. Alfsen, T.E., Blikra, H., Tjotta, H. "Pushing the Limits for Extended-Reach Drilling, New World Record Well from Platform Statfjord C, Well C2" SPE 26350 presented at the *SPE Annual Technical Conference and Exhibition*, Houston, October 1993.

10. Rae, G., Lesso, W.G., Sapijanskas, M.. "Understanding Torque and Drag: Best Practices and Lessons Learnt from the Captain Field's Extended Reach Wells", SPE/IADC 91854 presented at the *SPE/IADC Drilling Conference*, Amsterdam, Netherlands, February 2005.

11. Luke, G.R., Juvkam-Wold, H.C. "Determination of True Hook Load and Line Tension under Dynamic Conditions", *SPE Drilling & Completion,* December 1993.

12. Maidla, E.E., Wojtanowicz, A.K. "Field Method of Assessing Borehole Friction for Directional Well Casing", SPE 15696 presented at the *Middle East Oil Show*, Manama, Bahrain, March 1987

13. Aarrestad, T.V., Blikra, H., "Torque and Drag – Two Factors in Extended – Reach Drilling", *Journal of Petroleum Technology,* September 1994.

14. Aadnøy, B.S., Fabiri, V.T., Djuurhus, J., "Construction of Ultralong Wells Using a Catenary Well Profile", SPE/IADC 998890 presented at the *SPE/IADC Conference,* Miami, February 2006.

15. Aadnøy, B.S., Djuurhus, J., "Theory and Application of a New Generalized Model for Torque and Drag", SPE/IADC 114684 presented at *the IADC/SPE Asia Pacific Drilling Technology Conference and Exhibition*, Jakarta, Indonesia, August 2008.

16. All section 3.4 is based on the models that WellPlan is using and can be obtained by WellPlan help file.

17. Gjerstad, Kristian, "A Medium-Order Flow Model for Dynamic Pressure Surges in Tripping Operations". SPE/IADC 163465 presented at *the SPE/IADC Drilling Conference and Exhibition.* Amsterdam, The Netherlands, March 2013.

18. Alum Whittaker. "Theory and applications of drilling fluid hydraulics". Reidel, Dordrecht, 1985. Ogs utgitt: Boston: International Human Resource Development Corporation.

19. Adam T. Bourgoyne. "Applied drilling Engineering" SPE textbook series. Society of Petroleum Engineers. Richardson, TX, 1986 Vol 2.

20. Kristian Gjerstad and Rune W. Time. *Simplified explicit flow equations for Herschel-Bulkley fluids in couette-poiseuille flow,* 2013,

21. Samuel, G. R. (March 2004). The Effect of Hole Curvature on the Wellbore Pressure Loss Prediction for Highly Tortuous Ultra-Deep Wells. *IADC Drilling Conference.*

7 Appendix

7.1 Well Information

Hole MD		6 266,83 m	Hole TVD		2 011,19 m
Air Gap		0,00 m	Water Depth		0,00 m
Datum Description	Mean Sea Level		Well Type	Subsea	
Reference Point	RKB		Job Type / Description		

Table 7-1 General case information

7.1.1 Well trajectory
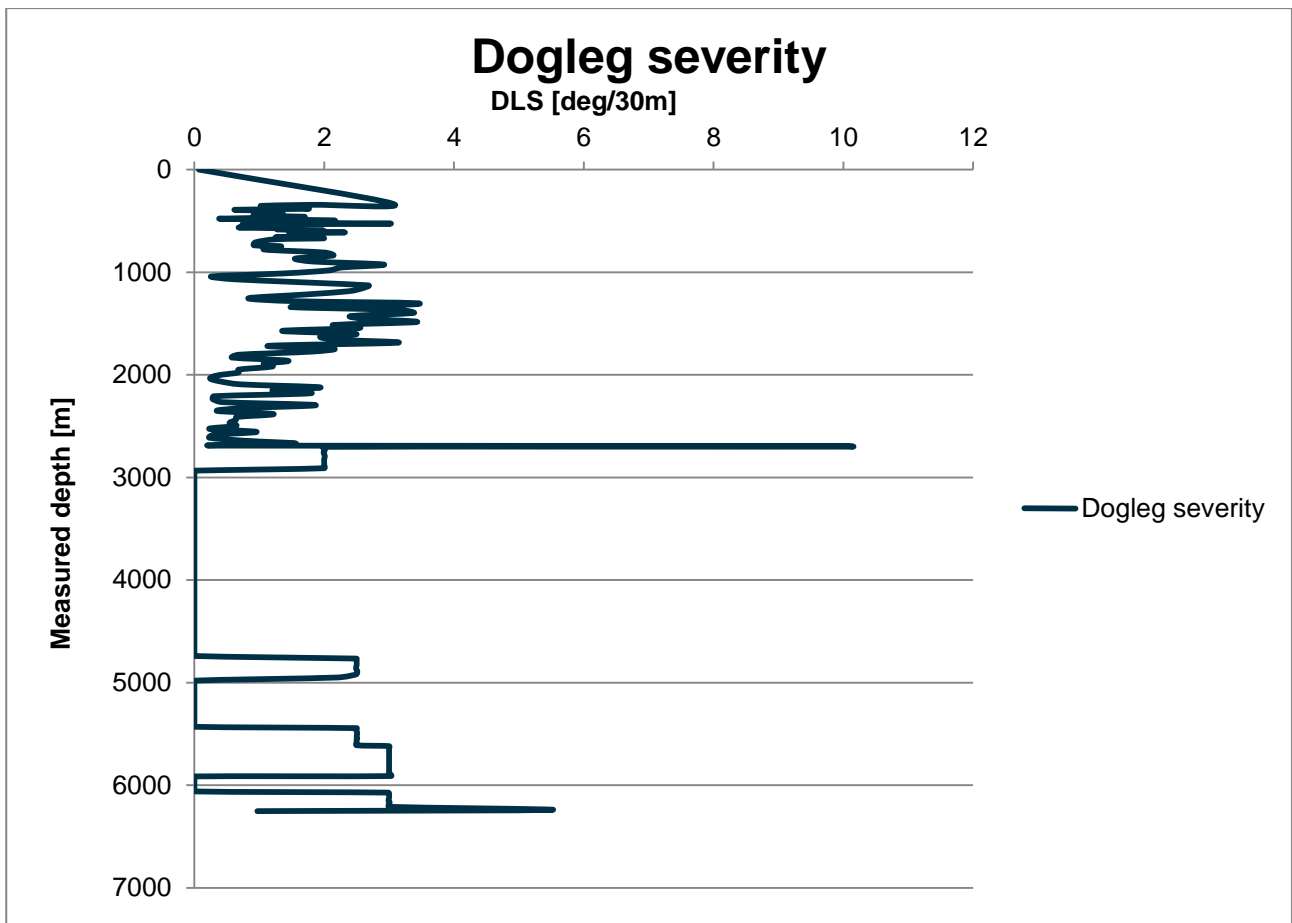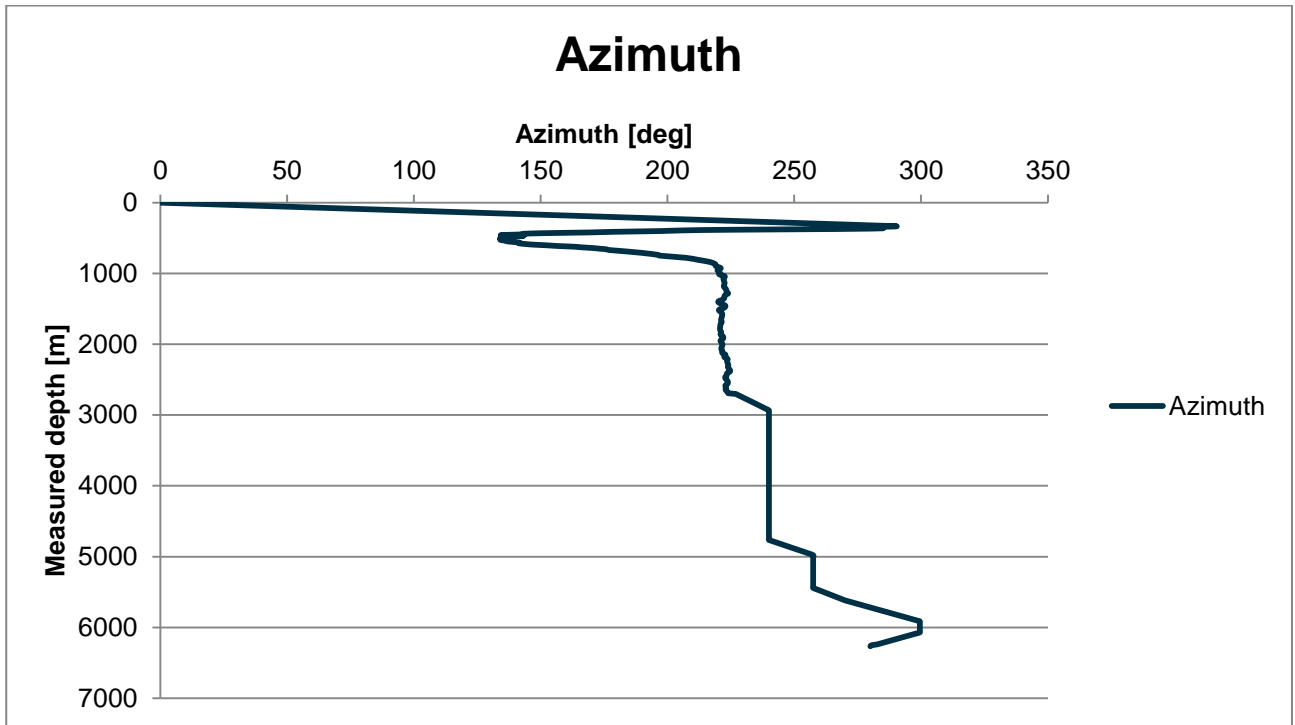

Figure 7-1 Dogleg severity

Azimuth

Figure 7-2 Azimuth

Profile
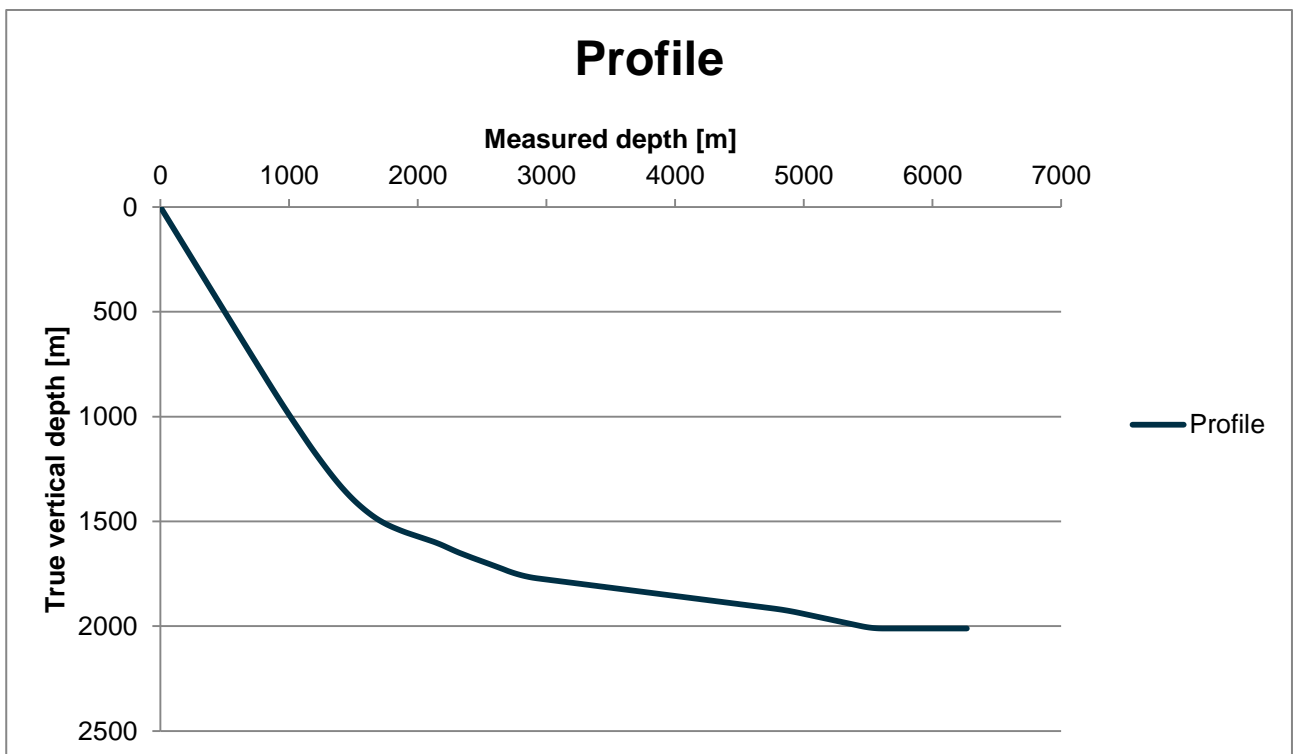
Figure 7-3 Vertical section
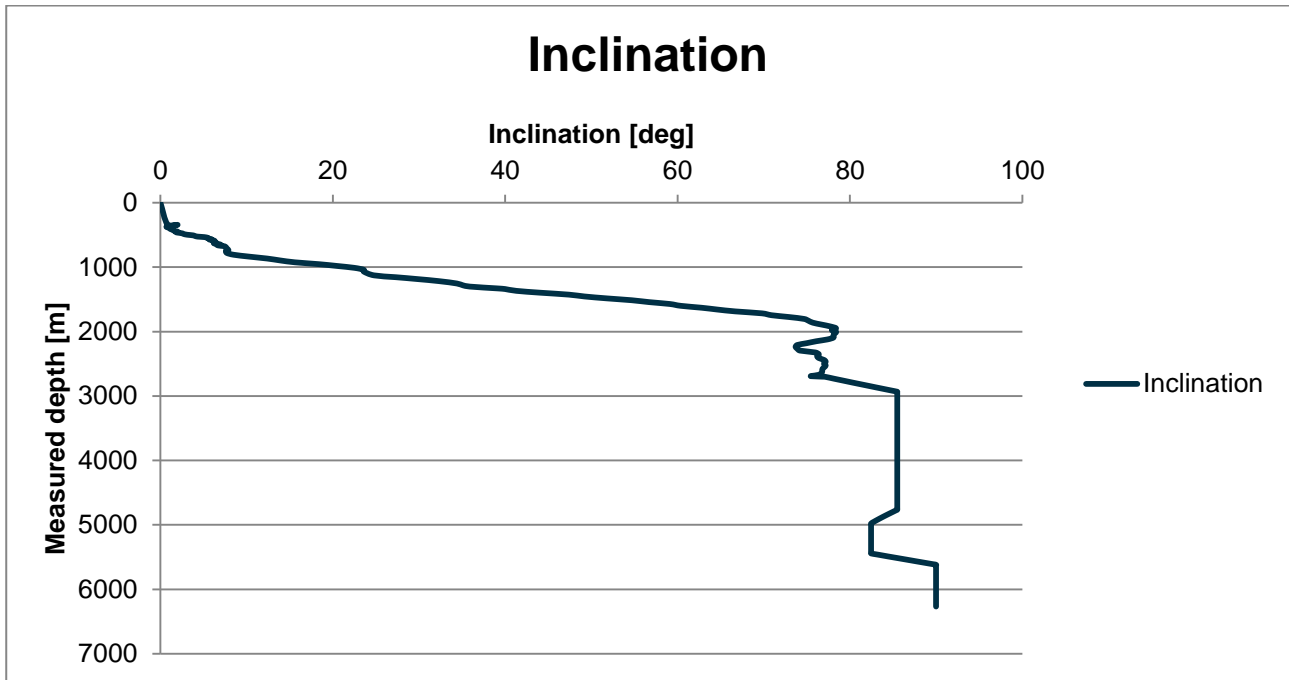
Inclination

Figure 7-4 Inclination

7.1.2 Hole section

Section Type	Section Depth (m)	Section Length (m)	Shoe Depth (m)	ID (in)	Drift (in)	Effective Hole Diameter (in)	Coefficient of Friction	Linear Capacity (bbl/ft)	Volume Excess (%)
Riser	26,00	26,000		17,750			0,20	0,3061	
Casing	2 773,00	2 747,000	2 773,00	13,375	13,375	13,375	0,20	0,1738	
Open Hole	6 266,83	3 493,830		12,250		12,250	0,30	0,1458	0,00

Table 7-2 Hole section information

7.1.3 Fluid rheology

Rheology model = Herschel – Bulkley

Temperature (°C)	Base Density (sg)	Ref. Fluid Properties	PV (MuInf) (cp)	n'	K' (lb*s^n/ft²)	YP (Tau0) (lbf/100ft²)	Fann Data	
							Speed (rpm)	Dial (°)
20,000	1,600	Yes	40,09	0,83	0,00283	8,602	600	91,00
							300	53,00
							200	42,00
							100	27,00
							60	21,00
							30	15,00
							6	10,00
							3	8,50

Table 7-3 Rheology data

7.2 Torque and drag setup

Measured Depth of Bit	6 266,83 m	Bending Stress Magnification	Yes
Traveling Assembly Weight	0,0 kip	Side Force Calculations	No
Enable Sheave Friction Correction	No	Viscous Torque and Drag	Yes
		Contact Force Normalization Length	9,45 m

Table 7-4 Operating parameters

Drilling	Use	WOB /Overpull (kip)	Torque at Bit (kN-m)
Rotating on Bottom	Yes	25,0	20,0000
Slide Drilling	Yes	25,0	20,0000
Backreaming	Yes	15,0	10,0000
Rotating off Bottom	Yes		
Tripping	Use	Speed (m/min)	RPM (rpm)
Tripping In	Yes	20,00	
Tripping Out	Yes	20,00	
Friction Factors	Hole Section Editor		

Table 7-5 Normal analysis data